Recycling plastic waste for 3D Printing filament by extrusion processing

António Saldanha Santos Barreiros Cardoso

Dissertation to Obtain the Master of Science Degree in

Industrial Engineering and Management

Examination Committee

Chairperson: Prof Miguel Simões Torres Preto

Supervisors: Prof Ana Isabel Cerqueira de Sousa Gouveia Carvalho

Prof Ana Clara Marques

Member of the Committee: Prof Moisés Luzia Gonçalves Pinto

September, 2021

Declaration

I declare that this document is an original work of my own authorship and that it fulfills all the requirements of the Code of Conduct and Good Practices of the Universidade de Lisboa.

Acknowledgments

First and foremost, I would like to thank my supervisors Prof. Ana Carvalho and Prof. Ana Clara Marques for all their support and for always being available for the doubts I had throughout this work. I am also extremely grateful to Prof. Beatriz Silva who performed important tests for my dissertation and clarifying many doubts that emerged with time.

I am very grateful to the Ph.D students that supported me during the experimentations and without whom I would certainly not be able to finish this work. Thank you David Duarte, Mário Vale, Mónica Loureiro and Ana Rosa. You were always available to help me and very supportive. There was not a single day that I felt alone in the labs and I will certainly not forget all the lunches we had together. I would also like to thank my colleagues Teresa Pereira and Beatriz Lopes for their company, guidance and for keeping me motivated especially during difficult times. Thank you, Beatriz, for always showing me the silver lining of the situations and teaching me (or attempting to...) to be more pragmatic.

I would like to mention all the professors that I have come across that had the biggest impact on my personal journey in Técnico and I will certainly not forget their names for a myriad of reasons: Prof. Pedro Girão, Prof. Cristina Câmara, Prof. Eloísa Grifo, Prof Eduardo Matos Almas, Prof. João Fernandes, Prof. Francisco Lima, Prof. Ana Carvalho, Prof. Augusto Moita Deus, Prof. António Ferraz and Prof. Paulo Carreira.

A final acknowledgment to my parents, Maria João and my closest friends who have always supported me tremendously and unconditionally over the last years. Any words would fall short over how important your support has been. Lastly, I would like to thank five persons who helped me overcome certain hardships and taught me how to deal with them: CC, VC, MH, MN and JPM.

Abstract

The excess of plastic waste and its mismanagement due to an ever-increasing production volume worldwide have led to a serious environmental crisis. Concurrently, additive manufacturing has gained considerable adoption from hobbyists up to industrial scale. The most widespread 3D printing (3DP) technology for plastics is Fused Deposition Modelling. The only raw material required is plastic filament. This presents a great potential for mitigating the waste management crisis: repurposing plastic waste into 3DP filament, bolstering circular economy. Polypropylene (PP) is one of the most produced plastics albeit little used in 3DP. In this context, this research aims to: (1) study filament extrusion processing, printability and characterisation of PP sourced from a waste management facility (rPP) and (2) compare the characteristics of rPP to those of commercial PP filament (vPP) to understand how to optimize filament processing. Initially, the material was separated by density and dried with varying parameters. This was followed by rheological, thermal and chemical characterisation of rPP and vPP. Filament extrusion was then tested to obtain optimal parameters followed by the same characterisation techniques. Tensile tests were performed with rPP and vPP for comparison. It was shown that rPP had higher content of inorganic additives (3.7% vs 0.2%) and melt flow rate (11.1 vs 4.5 g/10min at 200ºC) compared to vPP. Mechanically, rPP showed higher rigidity but the noteworthy difference was the strain at failure and strain ratio (ϵ_f / ϵ_y): 4.1% and 8.4 for rPP, 848% and 675 for vPP. Finally, rPP filament suitable for 3DP was not achieved.

Keywords: Extrusion, Recycled Plastics, rPP, Polypropylene, 3D Printing, Additive Manufacturing

Resumo

O galopante aumento da produção de plásticos nas últimas décadas resultou num problema global de gestão de resíduos e consequente crise ambiental. Concomitantemente, tem sido notória a evolução e adopção de tecnologias de fabrico aditivo para uso pessoal até larga escala industrial. A tecnologia de impressão 3D (3DP) com materiais plásticos mais comum é a chamada *FDM*. A única matéria prima necessária para a produção de qualquer produto é o filamento plástico. Assim, esta tecnologia representa grande potencial para a mitigação da crise de gestão de resíduos: transformação de resíduos plásticos em filamento de 3DP, fomentando a economia circular dos mesmos. Apesar do polipropileno (PP) ser um dos plásticos com maior produção global, o seu uso em 3DP é reduzido. Neste contexto, este trabalho tem como objectivos: estudar a extrusão, caracterização e potencial para impressão usando PP proveniente de uma empresa de tratamento de resíduos (rPP); comparar as características do rPP com as de filamento PP comercial (vPP) para melhorar o rPP.

O rPP foi separado por densidade. Seguiu-se a caracterização reológica, térmica e química de rPP e vPP. Procedeu-se à extrusão de rPP, caracterização do filamento obtido e ensaios de tracção. Verificou-se que rPP tem valores superiores de aditivos inorgânicos (3.7% vs 0.2%) e *melt flow rate* (11.1 vs 4.5g/10min, 200ºC). Constatou-se que rPP tem maior rigidez. A discrepância notável é a diferença na deformação de ruptura e rácio de deformações (ϵ_f/ϵ_y): 4.1%, 8.4 para rPP; 848%, 675 para vPP. Não se obteve filamento adequado a 3DP.

Palavras-Chave: Extrusão, Reciclagem Plásticos, rPP, Polipropileno, Impressão 3D, Manufacura Aditiva

Table of Contents

List of Figures

List of Tables

List of Abbreviations

3DP	3D Printing
ABS	Acrylonitrile Butadiene Styrene
AM	Additive Manufacturing
ASTM	American Society for Testing and Materials
Avg	Average Value
BJT	Binder Jetting
BPA	Bisphenol A
CAD	Computer-Aided Design
COTS	Commercial Off-The-Shelf
DED	Directed Energy Deposition
DIY	Do-It-Yourself
E	Young's Modulus
FDM	Fused Deposition Modelling
FFF	Fused Filament Fabrication
FTIR	Fourier-transform infrared spectroscopy
FTIR-ATR	Fourier-transform infrared spectroscopy with attenuated total reflectance
HDPE	High-Density Polyethylene
LDPE	Low-Density Polyethylene
MEX	Material Extrusion
MFR	Melt Flow Rate
MJT	Material Jetting
MP	Micro Particles
Mt	Million Metric Tonnes
N.A	Not Available
PA	Polyamide
PBF	Powder Bed Fusion
PBT	Polybutylene Terephthalate
PBTs	Persistent, Bioaccumulative and Toxic Substances
PC	Polycarbonate
PE	Polyethylene
PET	Polyethylene Terephthalate
PETG	Polyethylene Terephthalate Glycol
PLA	Polylactic Acid
PMMA	Polymethyl Methacrylate
POM	Polyoxymethylene
POPs	Persistent Organic Pollutants
PP	Polypropylene
PPE	Polyphenyl Ether
PS	Polysterene
PSU	Polysulfone
PVC	Polyvinyl Chloride
rHDPE	Recycled High-Density Polyethylene

RIC	Resin Identification Code
rPET	Recycled Polyethylene Terephthalate
rPP	Recycled Polypropylene
rPP(bulk)	Recycled PP as received from the waste treatment facility
rPP(cmp)	Recycled PP compounded filament (1 extrusion)
rPP(mix)	Recycled PP after separation in water
RT	Room Temperature
SEBS	Styrene Ethylene Butylene Styrene
SEBS-MA	Styrene Ethylene Butylene Styrene – Maleic Anhydride
SHL	Sheet Lamination
SPI	Society of Plastics Industry
Stdev	Standard Deviation
STL	Stereolithography
T_C	Crystallization Temperature
T_g	Glass Transition Temperature
TGA	Thermogravimetric Analysis
TM	Traditional Manufacturing
TS	Tensile Strength
U_r	Modulus of Resilience
U_t	Modulus of Toughness
UTS	Ultimate Tensile Strength
VPP	Vat Photopolymerization
vPP(3dp)	Commercial off-the-shelf PP Filament for 3D printing
ϵ_f	Strain at Failure
ϵ_y	Yield Strain
σ_y	Yield Strength

1 - Introduction

1.1 - Problem Motivation

This dissertation is motivated by the necessity of finding alternative ways of improving the plastic waste management problem.

Throughout the last decades the production, use and waste generation of plastic has increased sharply. It is expected that from 1950s up to 2050 the cumulative production of plastics will reach an appalling value of 26 000 million metric tonnes (Geyer, Jambeck, and Law 2017). The amount of plastic waste that ends in rivers, oceans and landfills has been sharply increasing due to the excessive use of the material. A considerable portion of this volume is due to single-use plastics with very short lifecycle, being mostly used in packaging (Barnes et al. 2009). The impacts of plastic pollution visibly affect the oceans, land, animals and greenhouse gases at increasing pace. The rise of 3D printing popularity and utilization across several domains, including commercial and industrial use, could play an important role on minimizing these effects. The amount of plastic waste has the potential to be reintroduced into the supply chains as recycled feedstock for 3D printers. Bearing this in mind, the problem to be addressed is how to turn plastic waste of a specific material into recycled filament to be used with 3D printers. This strategy has the potential to increase the value of plastic waste, reintroducing it in the economy and mitigating the disposal issue. Moreover, this can also contribute to reducing the costs of 3D printing raw materials that still pose an obstacle on the adoption of this technology. Research is still being done on improving the production of recycled filament using extrusion but further investigation is necessary. The most used commercial filaments in 3DP are made of polylactic acid (PLA), acrylonitrile butadiene styrene (ABS) and polyethylene terephthalate glycol-modified (PETG). In the domain of reprocessing plastic waste for 3DP filaments with extrusion, the most studied materials in the literature are, again, PLA, ABS and PETG. However, two other materials make for a very considerable percentage of all plastic waste and production worldwide: polyethylene (for this specific context high-density polyethylene, HDPE) and polypropylene (PP). In this regard, not only are these polymers seldom-used in 3DP but also the available studies on their repurposing by extrusion for 3DP filaments are scarce. This constitutes a literature gap and as such, this dissertation focuses on addressing the case of polypropylene. This work may provide information and data that can lead to an increased rate of adoption of filament recycling with enhanced quality and applicability. This sets the motivation to address the problem at stake.

1.2 - Objectives

The main objective of this work is to understand whether polypropylene sourced from waste treatment facilities can be repurposed for use in 3D printing. For such, optimisation of processes and characterisation of the material is performed to achieve adequate filament for printing. The research questions to be addressed in the experimentation were the following:

(1) What are the main characteristics (composition, chemical, thermal, rheological, mechanical) of PP flakes sourced from waste treatment facilities and of the subsequently produced filament by extrusion? What are the similarities and differences with those of 3DP PP filament?

(2) How can the processes by which rPP filament is obtained from heterogeneous bulk rPP flakes be improved in order to attain effective 3DP (FDM) printability?

The research questions are contextualised by Chapter 2 and the theoretical background is provided by the literature review in Chapter 3.

1.3 - Structure

This manuscript is structured in five main chapters which are preceded by an introduction and followed by the conclusions.

Chapter 2 provides the context and relevance of the problem to be addressed. An overview of plastic data regarding the evolution of production and other figures is initially presented. Then, the growing volume of plastic waste and the consequences of its mismanagement are discussed as well as the geographical distribution of plastic pollution, the implications on wildlife and the potential impact on public health. Chapter 2 ends with a topic that covers the definition of plastics, their classification and properties, the distribution of the use of each type of plastic and the existing recycling codes.

A literature review (state of the art) is presented in chapter 3. It is divided in five parts. The 3D printing and additive manufacturing are first addressed and the fused deposition modelling technique is explained. This is followed by a theoretical topic on the main principles of the extrusion process, widely used in plastics manufacturing. A review on the extrusion of recycled polymers to be used as 3D printing feedstock is carried out, focusing on three widely available materials, namely, polyethylene terephthalate, polypropylene and high-density polyethylene. Then, a review on the extrusion parameters used across the literature with recycled polymers and the main properties of the resulting filaments is made. The chapter closes by discussing the key aspects from the state of the art that will be crucial for the experimentation while also deciding on the material that will be the focus of the dissertation: recycled polypropylene.

In Chapter 4 the research methodology is explained. The chapter is organized in three subtopics: the research scope, materials and equipment and finally, the experimental procedures. In the first subtopic the two main research questions are addresse. Next, the materials and equipment are discussed. It includes the polymer materials being used, namely, the recycled polypropylene sourced from a waste management facility and commercial 3DP filament used for comparison. The equipment used on the experimentation can be categorized in the following way: processing, characterisation, measurement and software. A description of the main equipment and devices is provided accompanied by their respective illustrative images. The experimental procedure is then described in detail and a block diagram with the several processes and operations is provided as a complimentary visual summary. The procedure is organized in the following subtopics: pre-extrusion separation and drying, pre-extrusion characterisation, extrusion processing, post-extrusion characterisation, second extrusion

in mini extruder, mechanical testing. The chapter closes with a brief discussion of the changes to the initially planned methodology.

The results and discussion are presented in Chapter 5. It follows a similar structure to the previous chapter, albeit in a different order. After an overview, the subtopics are as follows: pre-extrusion separation and drying, pre-extrusion characterisation, extrusion processing, second extrusion in mini extruder, post-extrusion characterisation and mechanical testing. A discussion about the limitations identified in the experimental work and data analysis is provided in the end of the chapter.

2 - Current Plastics Hegemony

This chapter aims to provide the context for the project topic. It is structured in three sections. In section 2.1 the plastic market is explored. In section 2.2 an overview of the emergent plastic crisis is provided in which environmental issues arising from plastic pollution are discussed. Finally, section 2.3 covers the classification, uses and recycling standards of plastics.

2.1 – Overview of Plastic Data

Plastics have become a ubiquitous material over the past century. The first synthetic plastic was first produced in 1907. From the 1950s the global production rapidly grew and few materials surpass them (Ritchie and Roser 2018). In fact, in 1989 the production of plastics has outgrown the production of steel by volume (ISO Committee 2016) which is one of the most man-produced materials for construction industry.

Plastic can be generally defined as large organic compounds that can be obtained by polymerization. They can be moulded, extruded and processed into many shapes, films or fibres (ACC 2019). Although plastics have greatly varying characteristics most of them share the same set of global attributes (ACC 2019), namely, resistance to chemicals, thermal and electrical insulation, usually lightweight (low density) with wide range of strengths, different results can be obtained depending on the processing methods, ability to alter characteristics and broaden the set of applications through the use of additives which includes mimicking other materials' properties and lastly, most are made out of petroleum but some polymers are derived from renewable materials (e.g. polylactic acid).

Through the period 1950 and 2015 the sharp increase in global production of resins and fibres translates into a compound annual growth rate of 8.4% (Geyer, Jambeck, and Law 2017). In 2015 the total production was approximately 380 million metric tonnes (Mt). The cumulative total production over the same period is estimated to be close to 7800 Mt. If the additives that are usually present in a low percentage of resin polymers is also taken into consideration than the total cumulative production of resins alone accounts for 7300 Mt (Geyer, Jambeck, and Law 2017). If the current trend in production of primary plastics maintains than by 2050 the cumulative production of plastics (resins, fibres and additives) will reach a whopping value of 26 000 Mt (Geyer, Jambeck, and Law 2017). The data

analysed from 1950 to 2015 suggests that resin and fibre production curves follow polynomial time trends, second-order and third-order respectively (Geyer, Jambeck, and Law 2017). Recent data indicates that the total production of plastics (excluding polyethylene terephthalate fibres, polyamide-fibers and polyacril-fibers) in 2018 was 359 million tonnes worldwide with Europe accounting for 61.8 million tonnes (Plastics Europe 2019). In 2018, China alone produced 30% of world plastic production (excluding polyethylene terephthalate-fibers, polyamide-fibers and polyacril-fibers). The geographical disparity of production by regions is very considerable: 51% in Asia, 18% in NAFTA countries, 17% in Europe, 7% in Middle East and Africa, 4% in Latin America and lastly 3% in the Commonwealth of Independent States(ISO 2016). The plastics industry plays an important role in Europe. It includes raw material producers, converters, recyclers and plastics machinery manufacturers. It represents a direct employment of more than 1.6 million people working in nearly 60 000 companies with a turnover higher than 360 billion euros. Moreover, the plastics industry in Europe is ranked 7th in the list of industries with highest value-added contribution and a considerable multiplier effect of 2.4 in GDP and nearly 3 in jobs (Plastics Europe, 2019a). The distribution of plastic production by type application is illustrated in Table 1, which includes relative and absolute values. It is noteworthy that the main applications are packaging (30%), building and construction (17%), transportation (14%) and consumer and institutional products (10%).

Table 1: global plastics consumption distributed on different plastic applications (UNEP, 2018)

Application	Amount [tonnes]	Share [%]	Reference
Transportation - Other	4.75E+07	12%	(Geyer et al., 2017; Grand View Research, 2017)
Transportation - Tyres	7.07E+06	2%	(ETRMA, 2011; Geyer et al., 2017)
Packaging	1.15E+08	30%	(European Bioplastics, 2017; Geyer et al., 2017)
Building and Construction	6.41E+07	17%	(European Bioplastics, 2017; Geyer et al., 2017)
Electrical/Electronic	1.57E+07	4%	(European Bioplastics, 2017; Geyer et al., 2017)
Consumer & Institutional Products	4.06E+07	10%	(European Bioplastics, 2017; Geyer et al., 2017)
Industrial/Machinery	2.01E+06	0.5%	(Geyer et al., 2017)
Other	5.66E+07	15%	(European Bioplastics, 2017; Geyer et al., 2017)
Marine coatings	4.52E+05	0.1%	(Boucher and Friot, 2017)
Personal care products	2.54E+04	0.01%	(Boucher and Friot, 2017; Geyer et al., 2017; Gouin et al., 2015)
Road marking	5.88E+05	0.2%	(Boucher and Friot, 2017)
Textile sector - clothing	2.49E+07	6%	(Geyer et al., 2017; Grand View Research, 2017)
Textile sector - others	1.35E+07	3%	(Geyer et al., 2017; Grand View Research, 2017)

2.2 – The Emerging Plastic Crisis

As a consequence of the continuous rise in production of plastics and the excessive use of these materials several environmental issues have risen. Plastic materials are usually resistant and take decades or centuries to degrade when disposed (Le Guern 2020). The negative impacts arising from the excessive use and waste mismanagement have been seen in all environmental aspects: land, oceans, animals, humans and greenhouse gases to atmosphere. It was found that in 2019 the plastic

industry may contribute up to 850 million tons equivalent of carbon dioxide and if the trend of steady increase continues, by 2050 the emissions would rise to 56 billion tonnes, which comprises 14% of the carbon budget of the planet (CIEL 2019). As for land pollution it is noteworthy that it is estimated that microplastic pollution on land can be 4 to 23 times higher than in marine environments (UNEP 2018). Furthermore, it is estimated that around one third of all the plastic waste ends in either soils or freshwater. Since most plastics keep disintegrating into smaller and smaller particles (microparticles and nanoparticles with sizes below 5 millimetres and below 0.1 micrometres, respectively) they become present in the entire food chain (Machado et al. 2018). Another important vector of distribution of microplastics is sewage. Frequently, sewage sludge is used as fertilizer which leads to the deposition of thousands of tonnes of microplastics in soils every year and these are able to reach tap water (UNEP 2018). As a consequence, the soil fauna is also affected having considerable impact on earthworms and soil condition (Machado et al. 2018). Moreover, toxic particles can also pass from the soil to groundwater or other water sources. In a study of microplastic pollution in tap water, it was found that out of 159 samples analysed from six regions, 83% contained plastic particles. The United States samples proved to be the most polluted with a contamination rate of 94% and the least polluted were the European countries (U.K, Germany and France) tested with a contamination rate of 72%. The particles were mostly fibres, accounting for 99.7% (Kosuth, Mason, and Tyree 2017). The plastic pollution on the oceans has been an ever more target of public awareness campaigns. According to estimates, every year approximately 3% of the global annual plastic waste goes to the oceans (Jambeck et al. 2015); back in 2010 this accounted for nearly 8 million tonnes of plastic waste (Ritchie and Roser 2018). It has been reported that 5 countries alone dump more plastic into the seas than all other countries combined: China, Indonesia, Philippines, Thailand and Vietnam. These account for 55% to 60% of all the plastic waste entering in the oceans (OC 2015). A considerable amount of the litter accumulates in the ocean gyres – large vortexes into which the litter flows through currents. These gyres are the equivalent to enormous dumpsters in concentrated regions of the oceans. The majority of the ocean plastic pollution comes from land-based sources which are estimated to contribute nearly 80% of total waste (Hammer, Kraak, and Parsons 2012). The remaining 20% account for marine sources, such as fishing fleets with fishing nets and lines (Ritchie and Roser 2018). Some of the main routes through which plastics end up in the ocean are the river systems that carry waste from deeper inland. A study on this issue estimated that nearly 67% of global annual river input is caused by the top 20 polluting rivers and in geographical terms the concentration is mostly in Asia, which alone accounts for 86% of the total river plastic inputs to the ocean. Just the river Yangtze sources approximately 330 000 tonnes of plastic waste to the ocean (Lebreton et al. 2018). This geographical disparity is best illustrated through the following figures 1 and 2 that show the distribution of river plastic waste sourcing for the top rivers and regions.

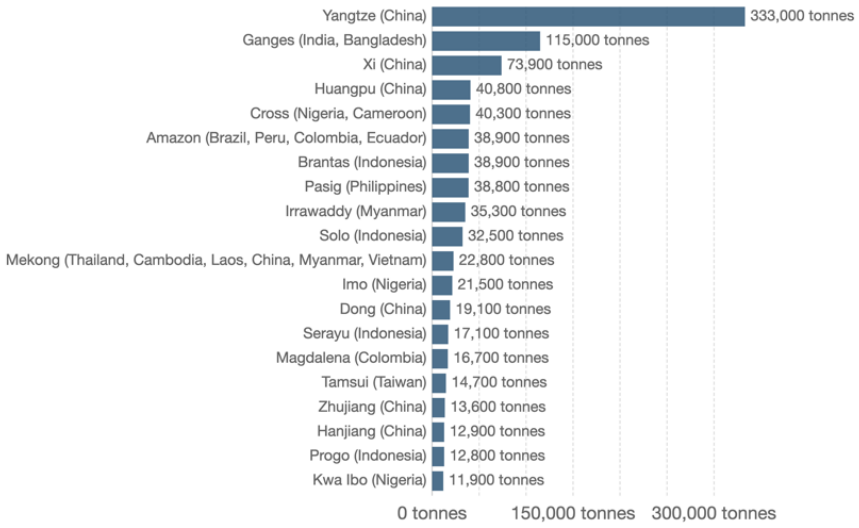

Figure 1: Plastic ocean input from the top 20 rivers with location and estimated input in tonnes (adapted from Ritchie and Roser 2018)

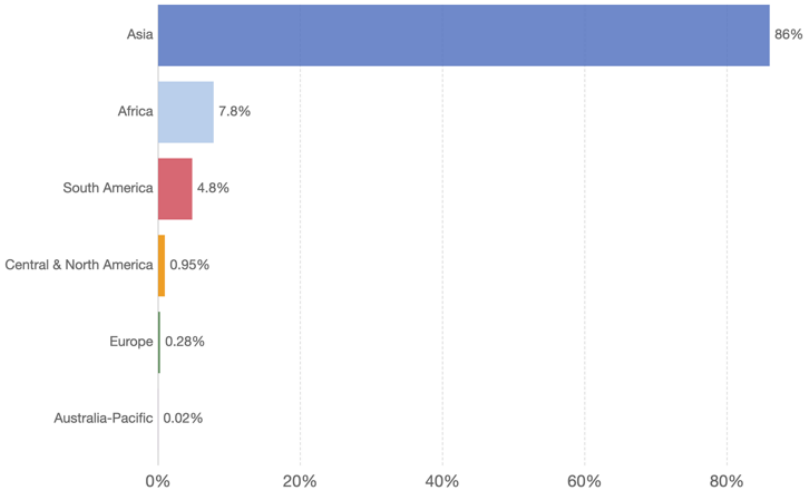

Figure 2: Global share of river plastic input to the ocean by region, data from 2015 (adapted from Ritchie and Roser 2018)

Another concern that has risen is the volume of landfills in which plastic accumulates and is only protected by a containment layer that is often prone to break, causing leakage of toxic chemicals into the soil. A considerable amount of plastic waste that ends up in landfills is originated from the single-use plastics, which are mostly used in packaging (Barnes et al. 2009). A factor that is vital in this case is whether the landfill is located in developed countries or in developing countries. In the former landfills are well-managed and regulated while in the latter the landfills are usually done in poor conditions, in open landfills causing a much higher impact on the surrounding environment (Ritchie and Roser 2018). Effects of plastic pollution on animals are already chilling. These can be categorized into entanglement, ingestion and interaction (Law 2017). These depend on the characteristics of the plastic waste such as size, shape and chemical characteristics. Figure 3 describes through a flow chart the inputs of plastics into the marine environment. The lower level of the chart represents direct sources and blue colour

represents maritime activities while red indicate land activities and purple indicates the source is either maritime or land.

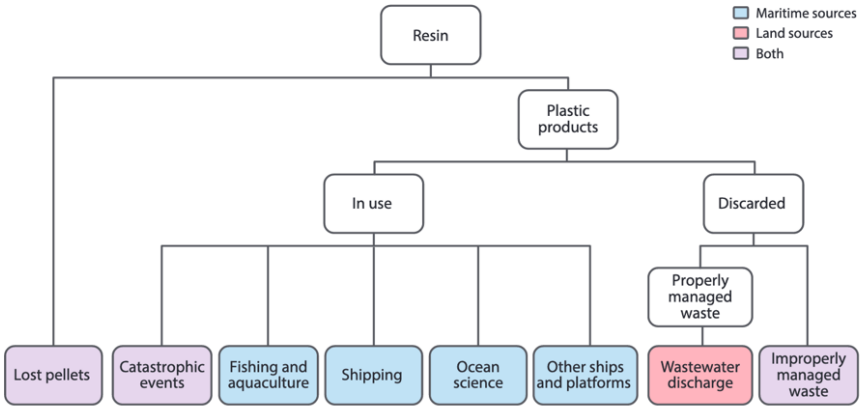

Figure 3: Flow chart describing inputs of plastics into the marine environment (adapted from Law 2017)

The entanglement involves “the entrapping, encircling or constricting of marine animals by plastic debris” (Ritchie and Roser 2018). It occurs mostly with turtles, seals, whales and seabirds and usually it involves waste from maritime activities such as fishing with the disposal of fishing gear, nets and plastic rope. Another material that has great impact on this category is plastic waste from packaging. Some consequences can go from suffocating or drowning to death by starvation. The ingestion effect is one of the most unsettling. Large and small plastic waste both play an important role. Some of the most impacted animals are sea turtles which frequently ingest plastic bags due to mistaking them with jelly fish. Birds also often mistake plastic waste with food leading to internal damage of digestive system. Reports on incidents with whales have appeared with dead whales appearing on beaches found with large amounts of plastic waste inside their stomachs. An article by The Guardian (2018) reported that a whale died with direct cause being ingestion of more than 80 plastic bags. Toxic chemicals – also called persistent bioaccumulative and toxic substances (PBTs) - flow throughout the food chain. Some of these include polychlorinated biphenyls, bisphenol A, phthalates and polybrominated diphenyls (flame retardant present in plastics), which cause changes in metabolism, enzyme activity, developmental defects, hepatic stress, cancer, and others; some of the plastic materials involved are Polyvinyl chloride (PVC), low-density polyethylene (LDPE) and polyethylene (PE) (Rochman et al. 2013). The bioaccumulation in animals poses a significant threat with absorption of contaminants through contact with debris. This will be addressed further on regarding the potential negative effects on humans (at the end of the food chain) which have been recently much investigated. The third category, interaction, concerns physical consequences of plastic debris colliding with animals, damage coral reef, interference with substrate due to reduced light penetration and constraining oxygen exchanges between organisms (Ritchie and Roser 2018). The impact of microplastics on humans which are at the top of the food chain has research ongoing but little evidence exists. The plastic waste that is most concerning is the micro and nano (between 0.1 μm and 1 mm and lower than 0.1 μm, respectively) particles that could be ingested, inhaled or absorbed through skin. One study reported on the presence of microplastics on

table salt in Spain, namely, PET, PE and PP fibres where the amount of micro particles (MP) was in the range of 50 to 280 in all samples (Iñiguez, Conesa, and Fullana 2017). The authors warn of the importance of investigating the risks of transmission of such microplastics along the food chain since plastic debris have been shown to be prone for sorption of persistent organic pollutants (POPs) (Iñiguez, Conesa, and Fullana 2017). The most clinically significant chemicals so far are bisphenol A (BPA) and phthalates (present in PVC), both having similar effects. BPA can cause problems in fertility, reproduction, changes in thyroid and growth hormone levels and in sex hormones (Denoncourt et al. 2015).

2.3 – Plastics classification, properties and standards

As we have previously seen the term plastics refers to synthetic polymers. At this point it is important to clearly define what polymers are. They can be defined as “long chain, giant organic molecules assembled from many smaller molecules called monomers. Polymers consist of many repeating monomer units in long chains, sometimes with branching or cross-linking between the chains (…) A chemical reaction forming polymers from monomers is called polymerization, of which there are many types. A common name for many synthetic polymer materials is plastic, which comes from the Greek word plastikos, suitable for moulding or shaping” (Ophardt and Morsch 2015). These materials are very versatile and are considered easy to manufacture and bear low costs. They also have good resistance to chemicals and environments. They can further be enhanced and altered easily for other purposes through the use of additives in their composition. Some important additives include fillers, colorants, retardants, stabilizers, plasticizers, lubricants and blowing agents. As a consequence, many products made of a certain synthetic polymer frequently have small percentages of additives that must be considered when being disposed of or recycled. There are several ways to classify polymers in general terms. Some of the most used classifications are based on five categories according to: structure, source, properties, polymerization processes and uses. The category *properties* is one of the most commonly used and comprises: thermoplastics, elastomers and thermosets. From these three categories the most common are thermoplastics and thermosets. The first term refers to plastics that when heated they become softer or melted allowing to shape them and upon cooling they become harder as they solidify. Moreover, they can be heated and cooled multiple times. This characteristic is especially important since it allows mechanical recycling and easy processing (Plastics Europe (2) 2019). Some examples of thermoplastics include the widely used polypropylene (PP), polyvinylchloride (PVC), polysterene (PS), acrylonitrile butadiene styrene (ABS) among many others. Thermosets differ from thermoplastics in crucial aspect: once formed it cannot be remelted since heating will only lead to decomposition of the material. Thus, its hardening is not reversible. Bakelite, the first synthetic polymer to be produced, is a well-known thermoset. Other common thermosets are the polyurethanes and polyester resins. These materials can undergo various processing methods to produce plastic products. The four main methods are extrusion, injection moulding, blow moulding and rotational moulding. In this research extrusion will be widely covered further on since it will be used in experimental context. Thermoplastics are the majority of use cases and as such, it is important to be familiarized with how this

category further divides. The main categories in thermoplastics are the amorphous plastics, semi-crystalline plastics and the imide materials (these can have properties of both the amorphous and semi-crystalline plastics) (IAPD M2 2015). Both can be subdivided into high performance (or special), engineering and commodity plastics. In figure 4 we can see a scheme that shows the key characteristics of each of the listed categories and examples of polymers for all cases.

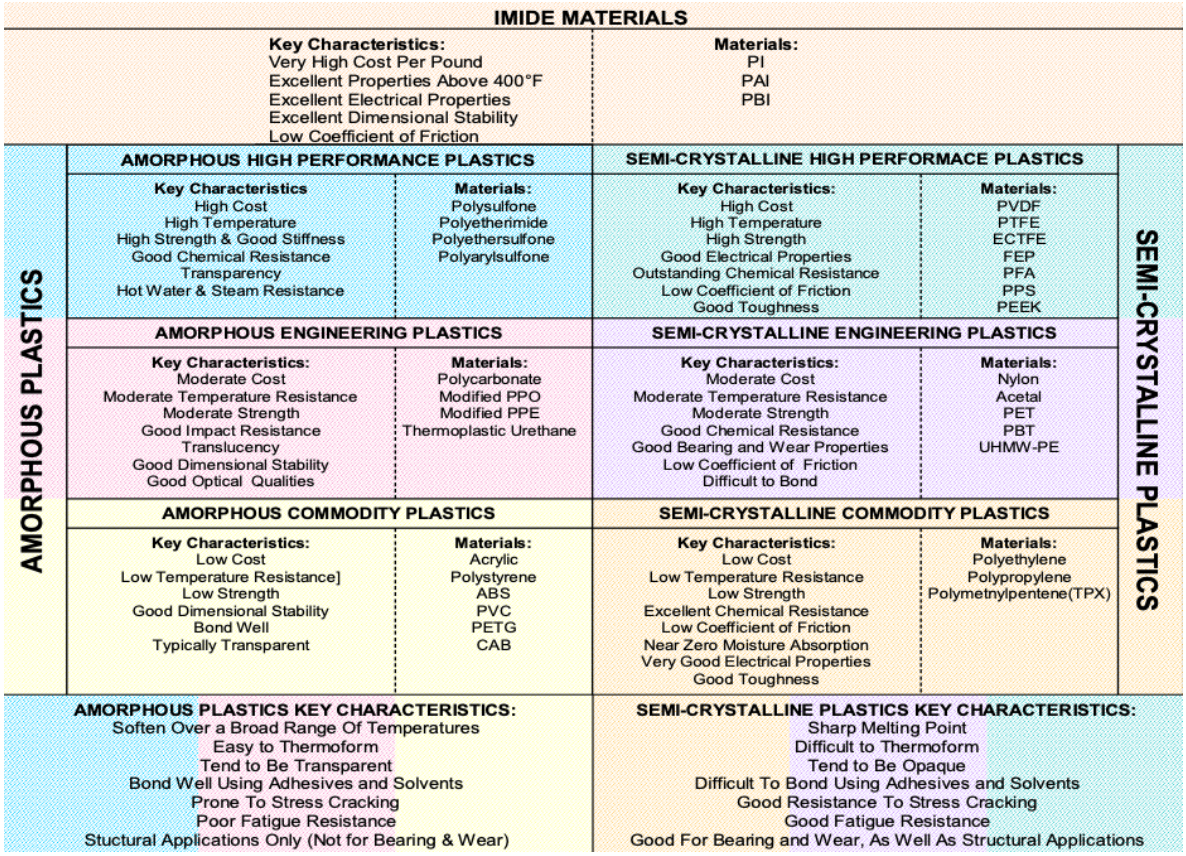

Figure 4: Scheme by The International Association of Plastic Distributors which systematises the main categories of thermoplastics as well as key characteristics and relevant polymers (adapted from IAPD M2 2015)

The commodities' plastics are more affordable and produced in large scale. These include polyethylene (PE), polypropylene (PP), polystyrene (PS), polyvinyl chloride (PVC) and acrylonitrile butadiene styrene (ABS). The engineering plastics are used in cases where certain properties are required such as good structural and thermal properties. The most relevant plastics are polyamide (PA), polyoxymethylene (POM), polycarbonate (PC), polyethylene terephthalate (PET), polyphenyl ether (PPE) and polybutylene terephthalate (PBT). The high performant or special plastics are those that excel in a specific property for which no other plastic type matches and plastics that are mechanically resistant at high temperatures. These are not commonly known as they are used in very specific use-cases. Plastics such as polymethyl methacrylate (PMMA, high transparency), Teflon (resistant to temperature) and polysulfone (PSU - mechanical resistance at high temperatures) are examples of this category (AIMPLAS 2019). At this point, it is important to assess how the market share is distributed according to the plastic materials. The three categories of thermoplastics can be ordered by market share. Globally, the commodities plastics (or standard) represent nearly 90% of market share, engineering plastics nearly 10% and high-

performance plastics less than 1% (ISO 2016). The distribution of the most common plastics of these categories is well represented Figure 5 which shows the market share for standard and engineering plastics worldwide in 2015. The PET on standard plastics refers to bottle grade PET while in engineering plastics category it refers to injection grade PET. On Figure 6 the market share for the most used plastics in Europe is presented with more recent data from 2018. Although there is a gap of 3 years between the data it can be seen that the market shares are quite different in Europe compared to worldwide.

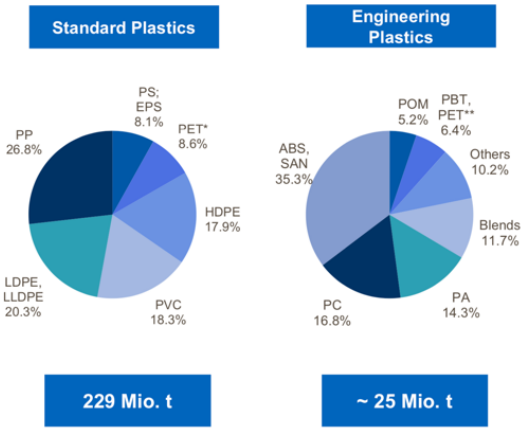

Figure 5: The global thermoplastics demand by types in 2015 is shown (adapted from (ISO Committee 2016)

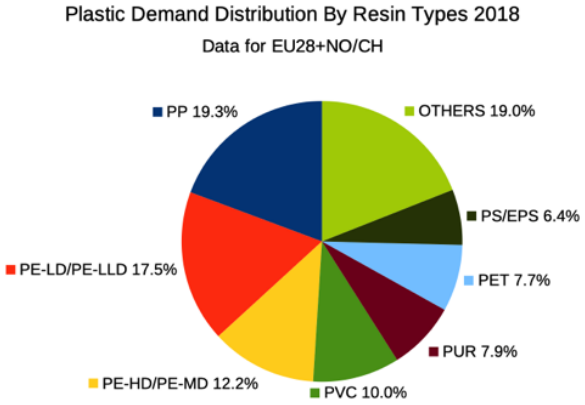

Figure 6: market share for the most used plastics in Europe (adapted from (Plastics Europe (3) 2019)

In the 1980s with the adoption of recycling programs in many states across the United States of America the need to have a consistent system of identification of plastics arose. This would allow to facilitate recycling of used consumer plastics. At the time, in 1988, the Society of Plastics Industry (SPI) developed the Resin Identification Code (RIC) with the intent of having a national system to aid recycling facilities in sorting and separating resins according to categories. Many organizations that were implementing recycling programs adopted the code to ease the sorting operations to ensure that each type of material could maintain its value so that it could be reused afterwards. This requires quality control on the sorting process so that the recycled material is homogeneous. In 2008 the administration of the RIC standard shifted to the American Society for Testing and Materials (ASTM) which later revised the symbols used. Upon shifting the administration, the new standard became ASTM D7611 which stands for Standard Practice for Coding Plastic Manufactured Articles for Resin Identification (D20 Committee 2019). Figure 7A shows how a plastic resin of a manufactured item is identified. It has 3 elements: an equilateral triangle, an integer (resin identification number) and below, an abbreviated term for the polymer.

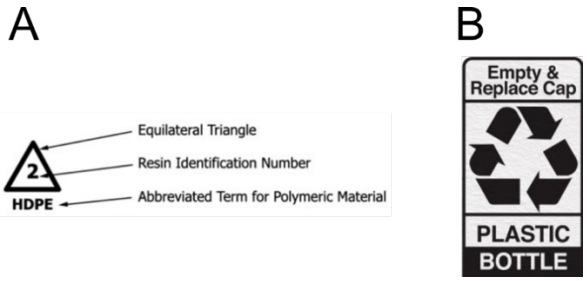

Figure 7: A) Example of a Resin Identification Marker for the polymer HDPE (adapted from D20 Committee 2019). B) Example of a label using How2Recycle system (adapted from (How2Recycle 2020).

It should be noted that the RICs are not recycle codes but rather an aid to recycling (D20 Committee 2019). Furthermore, when a given product has a RIC inscribed it does not mean that it is recyclable or that there are systems to process it locally. Another label system emerged also in the U.S – How2Recycle created by the Sustainable Packaging Coalition. Instead of indicating the material a certain product is made of, it indicates one of the following labels: widely recycled, limited, not yet recycled or store drop-off (How2Recycle 2020). Each label refers to the percentage of the country that can recycle the said product. This system also aims to get consumers to approach local authorities to ask the type of plastics the local recycling facilities can process. This system labelling can be better understood through Figure 7B that depicts an example and will be explained afterwards. The label is composed of 4 elements. At the top it states how to prepare the material for recycling (in this case, Empty & Replace Cap), the second element indicates how widely it is recycled in the country (in the example it translates to Widely Recycled), the third element refers the type of material (plastic) and the bottom element indicates which parts of the packaging needs to be recycled according to previous elements (a bottle in this case).There are also multi-component labels that includes several parts of a package. The idea of this system is to communicate effectively and concisely information that enables one to understand how recyclable a given product is and how it should be treated when sent for collection. For Europe a different system is used. The European Commission defined a list of resin identification codes, which includes plastics, batteries, paper, metals, organic material, glass and composites. This list closely resembles ASTM RIC. Other systems exist such as the Chinese codes defined by the Standardization Administration of the People's Republic of China (SAC) that attributes a number (code) to a specific material with codes from 1 to 140(SAC GB16288-2008 2008; GB 18455-2001 2001). In Table 2-3 a summary of the plastics covered by RIC according to ASTM is provided, which includes the 7 categories and a list of plastic materials, main properties, product examples and common uses.

Table 2: Summary of the 7 categories of thermoplastics PET, HDPE and PVC using the RIC system: material, properties and use-case examples of both new and recycled material (adapted from ACC 2019)

Resin Codes	**Plastic Type**	**Main Properties**	**Common Uses**	**Products Made with Recycled Content**
1 PET	Polyethylene Terephthalate (PET, PETE)	• Clear and smooth surfaces • Good barrier to O2, H2O, CO2 • High impact and shatter resistance • Excellent resistance to most solvents* • Capability for hot-filling* • Softens at 80ºC**	- Plastic bottles (soft drinks, water, juice, beer) - Food jars - Ovenable film and microwavable food trays* - Outside of packaging: textiles, monofilament, carpet, films, engineering moldings*	- Fibers (carpet, fleece jackets, tote bags)* - Containers (food and beverages) - Film
2 HDPE	High Density Polyethylene	- Excellent resistance to most solvents* - Polyethylene form of higher tensile strength - Relatively stiff material with useful temperature capabilities* - Hard to semi-flexible - Softens at 75ºC**	- Bottles for milk, water, juice, cosmetics, shampoo, dish and laundry detergents and household cleaners* - Bags for groceries and retail purchases* - Outside of packaging: injection molding applications, extruded pipe and conduit, wire and cable covering*	- Bottles for non-food items (shampoo, conditioner, liquid laundry detergent, motor oil, antifreeze)* - Plastic lumber (outdoor decking, fencing and picnic tables)* - Pipe, floor tiles, buckets, crates, flower pots, recycling bins*
3 PVC	Polyvinyl Chloride	- High impact strength, brilliant clarity, excellent processing performance* - Resistance to grease, oil and chemicals* - Softens at 80ºC**	- Rigid packaging applications (e.g. blister packs, clamshells)* - Flexible packaging uses (e.g. bags for bedding and medical, shrink wrap, deli and meet wrap and tamper resistance)* - Outside of packaging: rigid applications such as pipe, window frames, fencing, decking, railing* - Flexible applications: medical products (blood bags, medical tubing), wire and cable insulation, carpet backing*	- Pipe, decking, fencing, gutters, carpet backing, floor tiles and mats, resilient flooring, mud flaps, trays, electrical boxes, cables, traffic cones, garden hose, mobile home skirting - Packaging, film and sheet, loose-leaf binders*

Table 3: Summary (continued) of the 7 categories of thermoplastics LDPE, PP, PS and others using the RIC system: material, properties and use-case examples of both new and recycled material (adapted from ACC 2019)

Resin Codes	**Plastic Type**	**Main Properties**	**Common Uses**	**Products Made with Recycled Content**
4 LDPE	Low Density Polyethylene (includes Linear LDPE – LLDPE)	Excellent resistance to acids, bases and vegetable oils Toughness, flexibility and relative transparency (good combination of properties for packaging applications requiring heat-sealing) Softens at 70ºC	Bags Shrink wrap, stretch film Coatings Container lids Toys Squeezable bottles Outside of packaging: injection moulding applications, adhesives and sealants, wire and cable coverings	Shipping envelopes, garbage can liners, floor tile, panelling, furniture, compost bins, trash cans
5 PP	Polypropylene	Strong, hard but flexible High melting point Low moisture vapour transmission	Containers for yogurt, margarine meals, Bottles for medicine,	Automobile applications (battery cases,

		Inertness towards acids, alkalis and most solvents Softens at 140ºC	Outside of packaging: fibers, appliances and consumer products, durable applications such as automotive and carpeting	signal lights, battery cables, etc Garden rakes, storage bins, shipping pallets, trays
6 *PS*	Polystyrene (rigid or foam) (iwhen combined with rubber: High Impact PS – HIPS)	Excellent moisture barrier for short shelf life products* Excellent optical clarity in general purpose form Significant stiffness in both foamed and rigid forms Low density and high stiffness in foamed applications* Low thermal conductivity and excellent insulation properties in foamed form* Affected by fat, acids and solvents Softens at 95ºC	Food service items (cups, plates, bowls, etc) with foamed or non-foamed PS Protective foam packaging Compact disc cases Outside of packaging: agricultural trays, electronic housings, cable spools, building insulation, medical products and toys	Thermal insulation, light switch plates, desk trays Foamed foodservice applications (e.g. egg shell cartons) Plastic mouldings Expanding polystyrene (EPS) foam protective packaging
7 *Other*	Package contains a resin not listed above or it is made of more than one resin in a multi-layer combination e.g. nylon (PA), acrylonitrile butadiene styrene (ABS), polycarbonate (PC)	Properties depend on the specific plastic or combination of plastics	Bottles Oven-baking bags, barrier layers and custom packaging	Bottles and plastics lumber applications

2.4 – Problem Characterization

In the preceding sections the current environmental crisis arising from the rapidly growing production rate of plastic materials, their waste mismanagement and focus on disposable plastic products has been extensively discussed. Over the last years companies and researchers have been exploring new methods to tackle the seemingly insurmountable challenge of the accumulating plastic waste. Recycling/treatment facilities are still lacking considering the amount of waste generated and disposed of every year. At the same time, additive manufacturing and 3D printing have been rising considerably in popularity and adoption. The embracement of AM goes from hobbyists with affordable 3D printers to universities carrying research on it and leading technology companies that already produce high-performance parts. An example of the latter is Boeing's new wide-body passenger jet, with each jet engine of the plane having around 300 additively manufactured components (Metal AM 2020). The rapid growth of 3D printing technologies that employ plastic materials as feedstock are of particular interest. Filament spools are still relatively expensive and their production further aggravates the environmental crisis. However, the large amounts of plastic waste readily available and the increasing use of plastic 3DP can be combined together to tackle the current crisis. By reprocessing plastic waste into recycled filament, the lifecycle of materials would increase and higher-value goods could be produced and marketed. One way of achieving this is to combine together the sorting, cleaning and shredding of plastic waste with an extrusion process in order to obtain recycled filament that can be

used as feedstock for 3DP. This could also provide cheaper raw materials for printers. There are many challenges in this process integration. The processing greatly varies according to the chosen polymer. Many of the polymers that constitute the majority of plastic waste are not yet much used in 3DP, namely, PET, PP and HDPE. Moreover, the sourcing usually involves an heterogenous mix of materials whose exact composition is unknown, different material grades are used and usually with additives present which further increase the process complexity. Hence, this project aims to establish the theoretical background and an in-depth review of the current literature on production of recycled filament by extrusion. Emphasis will be put on specific cases of PET, PP and HDPE. The project thus sets the starting point for the dissertation that will be comprised of experimental work regarding the extrusion process of a specific polymer to develop recycled filament. The literature review that follows on chapter 3 is particularly important to understand the current limitations of the process and proven approaches to overcome the associated challenges.

2.5 – Conclusions

Throughout the last decades a rampant increase in the production of plastic materials has occurred. Their production by volume has even outgrown the production of steel by volume, which is one the most produced materials for economic activity. The attractiveness of plastics comes from the fact that they are generally lightweight, resistant to chemicals, good insulators, provide a wide range of strengths and set of applications can be further extended by mixing additives. The data analysed from 1950 to 2015 suggests that the production curves of resins and fibres follow polynomial time trends of second-order and third-order, respectively. Over the last years an environmental crisis as emerged due to the continuously higher production rates of plastics, their excessive use and the disastrous waste mismanagement. The negative impacts have been seen across several domains: land, oceans, wildlife, greenhouse gases and human life. It is estimated that approximately one third the plastic waste ends in soils and freshwater. Some of the toxic chemicals related to plastics that are entering the food chains can affect metabolism, fertility, thyroid hormone levels and sex hormones in humans.

Plastics are commonly classified into three categories based on their properties. They can be divided into thermoplastics, elastomers and thermosets. Some of the plastics produced in largest scale include PET, PP, PS, PVC and ABS. As an aid to recycling, the SPI has developed the Resin Identification Code so that a common standard could be used at the national level. Another important label system has been created by the Sustainable packaging Coalition called How2Recycle. A review is then carried out on the main properties and use-cases of the most common plastics. The problem to be addressed with the current project is then characterized in-depth on section 2.4.

3 - State of the Art

This chapter is divided in four sections. It starts with an introduction to 3D printing and a theoretical exposition on important concepts of polymer extrusion. Further on, a review is carried out on the recent literature concerning the extrusion of recycled filament for 3DP using plastic waste.

In section 3.1 3D printing and additive manufacturing are introduced and their disruptive nature on manufacturing and industries is discussed. Moreover, section 3.1.1 focuses on fused deposition modelling which is the 3D printing technology that will be used in this research. Section 3.2 is dedicated to the theoretical background of the extrusion process. An introduction to the process is presented in section 3.2.1 and in the section 3.2.2 the single screw extrusion process is discussed since it will be used for the experimentation later on. In section 3.3 a literature review on the extrusion of recycled polymers to use as 3D printing feedstock is presented and it is divided into rPET, rPP, rHDPE and finally an overview of the process feasibility. Lastly, in section 3.4 the available information on the literature concerning extrusion parameters and recycled filament properties is reviewed. The chapter ends with the main conclusions drawn from the literature review and focus on some key points regarding experimentation methods and techniques that will be useful on the experimental study.

3.1 – 3D Printing and Additive Manufacturing

The terms 3D Printing and Additive Manufacturing (AM) are often used interchangeably as if they were synonyms, they are technically used in different contexts. The terminology and general principles of additive manufacturing have been standardized in a cooperation of ISO and ASTM to establish common standards to facilitate communication and collaboration worldwide. According to the relevant standard from ISO/ASTM (AM Terminology 2015), AM is "*the process of joining materials to make parts from 3D model data, usually layer upon layer, as opposed to subtractive manufacturing and formative manufacturing technologies*". Oppositely, subtractive manufacturing (CM, 2016) refers to construct an object by cutting material from a block of material successively (e.g. using computer numerical control machines or CNC). Formative manufacturing, on the other hand, refers to constructing an object more commonly by the use of injection moulding (melted plastic injected into a mould with the shape of the item). The international standard previously referenced defines 3D Printing as "*the fabrication of objects through the deposition of a material using a print head, nozzle, or another printer technology"* and also refers *"term often used in a non-technical context synonymously with additive manufacturing"* and sometimes associated with low-end machines (AM Terminology 2015). However, other sources distinguish both terms differently. This is the case of Ben-Ner and Siemsen (2017) who use both terms as synonyms. Pechter (2019) refers both terms overlap in certain domains but that AM is used in the context of enterprise and supply chain in the sense of manufacturing process. Moreover, 3DP is more related to the equipment, printing technologies and specific processes involved or as the author says, more in the sense of "*factory floor*". Thus, AM can be seen as the big picture. Another common view is that additive manufacturing is the industrial version of 3D Printing (Turbide 2015). Lastly, in the context of an operation being at the core of a given manufacturing process, 3D

Printing can be seen as *"the operation at the heart of additive manufacturing"* (Zelinski 2017). Even though there are numerous AM technologies they all follow a generalized process chain. This can be seen as a sequence of several steps that distinguish the different operations. This concept is illustrated in Figure 9.

Figure 8: Additive manufacturing process chain (adapted from Terner, 2015).

In the international standard created and managed by ASTM/ISO seven process categories were defined as a basis for easiness of communication world-wide. The categories and their acronyms are defined as: binder jetting (BJT), directed energy deposition (DED), material extrusion (MEX), material jetting (MJT), powder bed fusion (PBF), sheet lamination (SHL) and vat photopolymerization (VPP)(AM Terminology 2015). There are numerous technologies available in additive manufacturing and these can be clustered according to the power source they use (e.g. heat, electron beam), the material type (e.g. polymer, metal) and the material physical form (e.g. liquid, powder) (Terner 2015). In Table 4 several AM technologies are presented and organized according to the ISO/ASTM nomenclature:

Table 4: AM technologies organized by ISO/ASTM categories

BJT	DED	MEX	MJT	PBF	SHL	VPP
Three-Dimensional Printing (3DP)	Laser Engineered Net Shaping (LENS)	Fused Deposition Modelling (FDM)	Multi-Jet Modeling (MJM)	Selective Laser Sintering (SLS)	Laminated Object Manufacturing (LOM)	Stereolithography (SL)
	Directed Light Fabrication (DLF)	Fused Filament Fabrication (FFF)		Selective Laser Melting (SLM)	Ultrasonic Additive Manufacturing (UAM)	Digital Light Processing (DLP)
	Directed Metal Deposition (DMD)			Electron Beam Melting (EBM)	Sheet Metal Clamping	
	Electron Beam Freeform Fabrication (EBF)			Infrared Beam Melting (EBM)		
				Infrared Selective Sintering		

Additive manufacturing has the potential to bring huge disruptions through an industrial revolution. The traditional manufacturing (TM) greatly differs from AM across several domains. A side by side comparison between both methods is summarized in Table 5 below.

Table 5: Traditional vs Additive manufacturing (adapted from Ben-Ner and Siemsen 2017)

TM	Domain	AM
Unitary cost lowers substantially with economies of scale but large quantities are required	Production cost	Unitary cost is scarcely dependent on volume of production
Parts design constrained by feasibility with available production methods	Design freedom	Shapes that were previously difficult to obtain (e.g. hollowness, etc) are now achievable with no added cost relative to common shapes

Specialized tools cost shared and divided by production volume	Tools and moulds	No costly specialized tools are required whose cost would be distributed along production volume
Higher transportation lead times	Delivery speed of order	Faster delivery times due to decentralized production leading to shorter supply chains
Dedicated equipment for certain products which means that high production volume is required to justify utilization rates	Capacity utilization	Given the flexibility of the equipment the capacity utilization required is achieved across several products instead of being dependent on high volume of a single specialized items
Expansion requires large investments that often delay capacity adjustments	Capacity expansion	Expansion can be obtained by increments with lower costs associated thus providing flexibility in capacity needs
Product specific learning may be involved	Learning curve	Does not require product specific learning, only machine specific that applies to wide range of products
Statistical aggregation is complex and predictions can thus be inaccurate	Forecasting	Higher accuracy since aggregation occurs at raw material level instead of product mix level
Large number of parts and raw materials	Bill of materials	Low parts count since most parts are integrated in the printing process
A large number of suppliers and high part count on purchase	Purchasing	Simplified purchasing portfolio since needs come down to list of raw materials
Complex transportation of both parts and finished goods	Transportation	Less transportation (parts and final goods) as a consequence of localized production, aggregate demand of raw materials
TM relies on subtractive processes which entails more waste	Material usage	Additive nature of process results in considerable reduction of material waste and energy consumption as opposed to formative and subtractive processes
Branding requires large investments to improve global image and trust	Marketing	Local networks awareness reducing investment in branding
Complex supply chains; production is centralized and for complex products the assembly lines and factories become very expensive and with low flexibility	Supply chain and assembly	Very simplified supply chains and elimination of complex and rigid assembly lines on factories; production takes place closer to customer

Additive manufacturing technology has the potential to benefit a broad array of industries, some which are already adopting this new paradigm. It has been discussed that two main categories of applications arise: rapid prototyping and component manufacturing (Bogue 2013). The former brings cost and time reductions in manufacturing prototypes across the several stages of innovation; the latter mainly related to industries that work which parts that are required in low quantities but with complex specifications and small error tolerances. It is the case of aircraft engines which have been innovating considerably in the incorporation of AM parts. The industries that are being affected by this technology include aerospace, automotive, healthcare and medical tools, retail, machine tool production among many others. Attaran (2017) provides a brief analysis of which industries and applications are impacted by the recent developments of AM. Applications such as prototyping, component manufacturing and structure weight reduction are bringing considerable changes to the aerospace and automotive sectors. Regarding the healthcare industry AM is bringing changes with the fabrication of custom implants (hearing aids and prosthetics) and fabrication of human tissue and organs. More specifically in dentistry some of the AM applications include the production of customized orthodontic devices, tailored teeth and dental crowns among other. In the architectural and construction industries the impact of AM is also visible through the fast generation of scale models and even the printing of houses with adapted cement materials which many companies are pursuing in order to tackle the lack of affordable house solutions in underdeveloped countries. On the retail industry 3D printed consumer goods are emerging in the

markets but 3DP is impacting especially the rapid prototyping of goods with decreased time to shelf rates and lowered costs and time of innovation.

It is known that AM is a disruptive technology with wide impact on many industries but it is still in its infancy (Attaran 2017). In order to implement it with great impact and growth some obstacles must be tackled first. One considerable obstacle is the size restrictions posed by the type of 3D printers to be used. Printers can only produce parts that are smaller than their casing and as such the size of the object to produce can be greatly limited. If no large enough printer is available the parts would be produced in segments requiring assembly time. Even if large printers are used a much bigger dedicated space Is required and advantage gains would decrease noticeably. Production time is another challenge to consider: AM is considerably slower when compared with traditional manufacturing in mass production. The production output is lower so until printer technology improves in this aspect the conventional manufacturing will still prevail for mass production. However, even with the slower output rates the AM will probably succeed in mass customization. The cost of quality printing equipment is considerably high but it is expected that prices will decrease with the many technological advances rapidly occurring and the increase in the numbers of manufacturers entering in the market. The Chinese government intends to be the largest player in the sector of 3DP. Although quality plastic filament is not cheap its prices have been decreasing continuously and progress on testing used plastics for filament will further bring it down. One domain that might become concerning is regulation. Usually regulation does not keep up with technology advancements and as such issues will arise. Certification of products might be an issue as well as the ability to trace products to their origin. Another example is the past availability of blueprints in the internet to produce plastic handguns (Bogue 2013) that would bypassed most security mechanisms. Thus, there might be government intervention to bring restrictions on the uses (Attaran 2017).

3.1.1 – Fused Deposition Modelling (FDM)

Among the AM techniques previously discussed, material extrusion is one of the most commonly used. In fact, (FDM) is one of the most popular techniques both for end-use and industrial use. It was patented in 1989 by the co-founder of Stratasys (Crump 1992) and commercially available in the beginning of the 1990s. This technique is the one used on the 3D printers that are going to be used on this research. The review paper on FDM by Sheoran and Kumar (2020) provides some guidance on FDM technique, a collection of findings regarding parameters and optimizations on past research and some conclusions regarding current state. In FDM a filament of thermoplastic material is continuously supplied (using a spool) and enters the heating element inside a liquefying head where it is heated into a semi-liquid phase. Then, it goes through the extrusion nozzle and is extruded on the printing bed (Sheoran and Kumar 2020) One important characteristic is that the semi-liquid filament being deposited in the bed does not solidify immediately so that it fuses with the existing layer before solidifying into a layer-stacked part in ambient temperature. This technique is relatively simple and enables high-speed and low-cost printing (Sheoran and Kumar 2020). These advantages contributed to its high popularity. However, some disadvantages must be considered. Firstly, FDM is process parameter-dependent mechanical

properties thus resulting in anisotropy. Secondly, the technique frequently leads to poor surface finishing which may lead to the necessity of post-processing. Lastly, FDM is limited to the use of thermoplastic polymers given that the thermoplasticity is the property that lies at the heart of FDM without which 3D printing the material would not be possible (Sheoran and Kumar 2020). The typical setup apparatus of FDM and the main parts is exemplified in Figure 9.

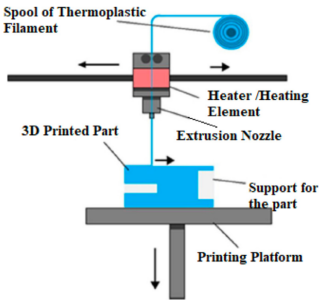

Figure 9: Setup apparatus of FDM process (adapted from Dizon et al. 2018)

As it was mentioned, the quality and mechanical properties of the printed parts are highly dependent on the parameters used. These have been extensively studied. The generic process variables or inputs are: layer thickness, raster angle, air gap, raster width, build orientation, number of contours, contour width, printing speed, infill pattern, infill density etc (Sheoran and Kumar 2020). The authors provide a set of process parameters that are more used and variables that affect them which are summarized in Table 6.

Table 6: FDM process parameters (adapted from Sheoran and Kumar 2020).

(1)	Layer thickness	Measured along the z-direction (or vertical direction of machine). Usually lesser than extruder nozzle diameter and mostly dependent on material and extruder nozzle tip diameter.
(2)	Build orientation	How the part is oriented within build platform relative to X, Y or Z direction of the machine and the angle at which the part would be printed.
(3)	Raster angle / Raster orientation	Angle with respect to X direction of build platform, raster angle pattern measured relative to X-axis and usually in interval [0º, 90º]
(4)	Air gap	Distance between 2 adjacent tool paths (rasters) on a single layer of the printed part.
(5)	Extrusion Temperature	Temperature to which material is heated inside the nozzle.
(6)	Print Speed	Speed of nozzle tip along the XY plane while depositing material.
(7)	Infill Pattern	Pattern in which material is deposited for the internal structure of part. Common patterns: diamond, cross, honeycomb and linear. Honeycomb has a higher mechanical load resisting capacity.
(8)	Infill density / Interior infill percentage	Inside structure can be sparse and of varying infill patterns, sizes and shapes and thus infill density refers to the solidity degree of structure.
(9)	Nozzle Diameter	Diameter of nozzle tip.
(10)	Raster Width	Width of the beads deposited along extruder tool path. Depends mainly on (9).
(11)	Number of Contours	Number of solid outer layers surrounding internal infill pattern
(12)	Contour Width	Thickness of the outer layers (contour) surrounding internal structure.
(13)	Contour to Contour Air Gap	Distance or air gap between the solid outer layers (contours).

The authors conclude on the critical findings and the domains which require further research. Firstly, given that only thermoplastics can be employed on FDM some of the most used polymers researched are polylactic acid (PLA) and ABS. Secondly, the several process parameters have been studied much more thoroughly than others, namely, the raster angle, layer thickness, build orientation and raster width

as opposed to interior infill pattern, infill density, temperature of extrusion and number of contours for instance. Thirdly, the most part of optimization is made for a single output variable or multiple-output variables that are optimized one at a time and not simultaneously. Because of this, the authors suggest that research must be carried out for multi-objective optimization, i.e., optimize multiple output variables simultaneously (Sheoran and Kumar 2020). Lastly, the optimization techniques are mostly based on statistical techniques and a multi-disciplinary research is advised employing image processing, machine learning and deep learning. Some physical constraints of the machines pose obstacles to optimization techniques: layer thickness and extruder nozzle tip diameter. The former is usually a fixed value on a machine and specific standard values are commonly used and as such, it is not possible to test a large continuous interval with minimum and maximum. The latter is typically fixed and according to standard values, thus, intermediate values cannot be taken into account in optimization analysis. Moreover, the fixed extruder nozzle tip constraints the raster width parameter. It is noteworthy that software constraints also have impact on the physical parameters number of solid contours which limited by the slicing software. Sheoran and Kumar (2020) reviewed FDM process parameters optimization analysis for several materials. The parameters considered are the air gap (A_G), layer thickness (L_T), raster angle (R_A), raster width (R_W), build orientation (B_O), print velocity (V_P), support material (Mat_{Sup}), support material density (ρ_{Sup}), infill pattern (IP), contour width (C_W), number of contours (N_C), interior infill density (ρ_{int}), nozzle temperature (T_N).

3.2 – Extrusion

3.2.1 – Introducing the Extrusion Process

Extrusion is the process of pushing a material through an orifice. This process is widely used in the manufacturing industry. Common examples include: metals, clays, ceramics, foodstuffs (e.g. noodles and sausages), among many others. Nowadays, it is widely used in the plastics recycling industry as it allows polymer reshaping for thermoplastics.

In the polymer processing industry, the extruder is one the most important machine tool. The extruder contains an opening in its end through which the material is forced - the extruder die. The extruded product, after passing through the extruder die, is called the extrudate. Materials can be extruded in the molten state or in the solid state. In the case of thermoplastics these are generally processed in the molten state. As it was previously discussed in Chapter 2 thermoplastics can be heated and cooled successively without changing the chemical properties. Hence, the changes are reversible as opposing to thermosets that after being heated cannot return to their initial state upon cooling.

Extruders in the polymer industry come in many different designs. One way of categorizing them is distinguishing between two major types of extruders with respect to the mode of operation: continuous or discontinuous. Continuous extruders are capable of developing a sustained, steady-state continuous flow of material. Discontinuous extruders deliver the product in an intermittent fashion. Continuous extruders are the most universally used. These can be further divided into two sub-categories: single-screw and multi-screw extruders. The single-screw extruder is the most commonly used in the polymer extrusion process. Its main advantages are: low cost, straightforward design, ruggedness and reliability,

and a favourable performance/cost ratio (Rauwendaal 2014). Since in the laboratory work the extrusion will be performed with a single-screw machine, this will be the type analysed further on.

3.2.2 – Single Screw Extrusion

In this sub-topic the single-screw extruder will be thoroughly analysed covering the equipment parts, how it works and variables regarding the process. Figure 10 illustrates how a single-screw extruder is usually designed with all the components discriminated.

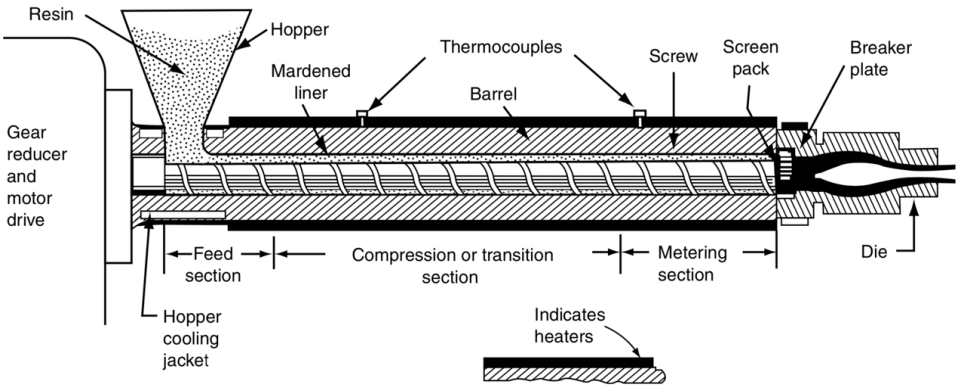

Figure 10: Scheme of a single-stage single-screw extruder with components and sections (Chanda and Roy 2007, 2–23).

The single-screw extruder can also be classified as plasticating or melt-fed depending on whether the polymer is fed in a solid or melt state. The plasticating single stage (i.e. only one compression section) is the one that will be considered along the review. A single stage extruder is made of three geometrically different sections as illustrated in Figure 12: feed section (near hopper and where material is in solid state), the compression section and the metering section (where the material is in molten state). There is a large variety of screw geometries. A typical screw is made of flights of varying height with channels in-between along which the melted material moves. In the first section the screw flights are deep as opposed to the metering section where they are shallow. Along the screw channel the flights height diminishes which leads to an increasing compression of the material inside. This is a crucial geometric aspect in the screw, and it is shown in Figure 12 below.

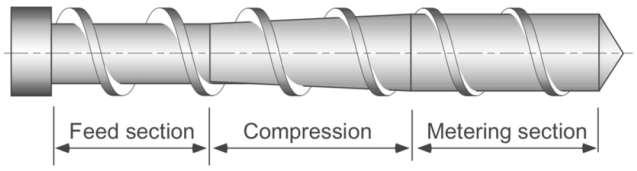

Figure 11: Common screw geometry profile (Rauwendaal 2014, 31).

Two properties to generally classify an extruder are the diameter of the extruder barrel and the length to diameter ratio (L/D). A common extruder usually has a ratio between 20 and 30 (Rauwendaal 2014). For thermoplastic materials the higher L/D ratios are more appropriate while for elastomers lower ratios are preferable. The main intent of the extrusion process is to convert a softened material into a certain form. The process starts with the feeding operation in which the plastic material is deposited in

the hopper in granular (pellets for instance) or powdered form. The rotating screw then makes the material move forward through the barrel. As the material goes from the feed section to the compression (also referred as transition) section the pressure increases which coupled with the heat from external heating system and the friction of the viscous flow causes the plastic material to turn into a molten stream (Chanda and Roy 2007). The majority of the heating occurs due to the friction and shearing action inside the barrel but initial external heating is required for melting process. Given the generation of heat from the process it is common to have a cooling system to maintain the appropriate temperatures. Without a correct cooling, the subsequent overheating degrades the polymer. The molten stream then reaches the highest pressure right before entering in the die. Upon reaching the end of the metering section, the molten material goes through the screen pack. This part consists in "a number of fine mesh gauzes supported on a breaker plate" (Chanda and Roy 2007). The screen pack is located right next to the screw. Its purpose is to filter out impurities and lumps that did not melt correctly and make the flow into a straight path. After that, the molten material is pumped into the die driven by the pressure force. The shape of the extrudate exiting the die depends on the die's geometry (cross-sectional shape): a round orifice will result in a pipe shaped extrudate, a square orifice will result in a square profile, among many other die geometries. It is noteworthy that the pressure inside the die, commonly referred as diehead pressure, is dependent on the die itself and the flow process inside of it, the temperature of the polymer melt and its rheological properties (Rauwendaal 2014). Hence, with everything else constant the diehead pressure is not dependent on the extruder itself, depends exclusively on the die. As the material is extruded it is necessary to lower its temperature, at least below glass transition temperature (T_g). Some common methods for doing so are: diving it in a water tank, spray water, air cooling at room temperature, air cooling with fans, among others (Chanda and Roy 2007). Depending on the polymer being handled the screw sections have different optimal lengths. It depends on factors such as the type of molecular structure and the melt rate. For polymers that melt slowly it is more appropriate to have a compression section with a length comprising almost the entire screw. This is usually the case of amorphous polymers such as PVC. Since with crystalline polymers, e.g. Nylon, the melting occurs more abruptly it is more appropriate to have a short compression section. For polymers melting gradually, e.g. LDPE, sections can have similar lengths (Groover 2013, 303).

It is important to note that the extruding shaping process is related to two essential properties of polymers: viscosity and viscoelasticity. Viscosity can be defined as "a fluid property that relates the shear stress experienced during flow of the fluid to the rate of the shear" (Groover 2013, 299). For certain simple fluids, called Newtonian fluids the viscosity (η) is constant at a given temperature so it does not change with the shear rate. In this case, the viscosity is the constant of proportionality between shear stress and shear rate:

$$\tau = \eta \cdot \dot{\gamma} \tag{1}$$

Where τ is the shear stress (Pa), η is the coefficient of shear viscosity ($N \cdot s/m^2$) and $\dot{\gamma}$ is the shear rate (s^{-1}). Polymer melts though, have a different behaviour. Their viscosity decreases with the shear rate which translates into the fluid becoming thinner when subject to higher rates of shear. Thus, polymer melt does not behave as a Newtonian fluid. The behaviour is called shear thinning or pseudoplasticity. An approximate model for the polymer melt is

$$\tau = k \cdot (\dot{\gamma})^n \quad (2)$$

Where *k* is the viscosity coefficient (constant) and *n* is the flow behaviour index (for $n = 1$ we would have a Newtonian fluid; for polymer melts we have $n < 1$)(Groover 2013, 299–300).

The viscoelasticity is responsible for an important phenomenon that occurs during extrusion operation: die swell. Once the polymer melt exits the die it expands. As the polymer passes through the metering section to the die the cross section decreases abruptly and the compressive stresses acting on the melt flow do not relax in the short die length. Hence, when the melt flow exits the die physical constraint is removed and the unrelaxed stresses due to section geometry differences (metering section – die – exit) cause the material to expand (Groover 2013, 300). In cases where it may prove problematic it is possible to attenuate the phenomenon by using a die with higher channel length to reduce swelling.

A simple mathematical model to describe the melt flow through the extruder is discussed in Groover (2013). The authors Lafleur and Vergnes (2014) provide a more detailed analysis on models describing the extrusion process.

3.3 – Extrusion of Recycled Polymers for 3D Printing Feedstock

In this section the most relevant papers and researches on the extrusion of recycled polymers to produce filament for 3DP are reviewed. ABS and PLA are the most used polymers in 3DP and they are well optimized and tested across the literature. There is large abundance of PP, HDPE and PET waste which translates into a highly available source of materials and these polymers have not been much used in 3DP. Therefore, this set of polymers will be the main focus of the review that follows next. Sections 3.3.1, 3.3.2 and 3.3.3 will be dedicated to rPET, rPP and rHDPE respectively. On section 3.3.4 an overview on the feasibility of extrusion and printing with the recycled materials is presented. After the complete review one of these polymers will be selected when drawing the conclusions to be the focus of the experimental part of the research.

3.3.1 – Review of rPET Filament Extrusion for 3DP Use

In the study of Lehrer and Scanlon (2017) the goal was to determine the feasibility of extruding recyclable plastic into usable filament to create a sustainable technology for 3D printing. The method for testing was to design a costume extruder with a lid to reduce moisture on plastics, larger power supply for higher temperature output and 1.75 mm die size. An initial validation for the extrusion process was performed by establishing a baseline with PETG pellets at 190ºC with a die at 1.80 mm. This was compared with the blend of recyclable PET bottles 50% + PETG 50% at a 245ºC with the same die size. The major results show an overall successful PETG print resulting in a filament with 1.55 mm diameter. PET plastic 50%+ PETG 50% was successfully extruded when the temperature was increased to 245ºC compared to 190ºC for only PETG for the same filament result. A drying process before extrusion to reduce moisture was implemented. Viscosity of PET bottles was the most important parameter for the production of filament, hence the incorporation of 50% PETG in the PET bottle mix.

In the work of Mutiva, Byiringiro, and Muchiri (2018) a positive comparison was shown between recycled PET and virgin PET, ABS and PLA as 3D printing filaments. In their work, they used PET water bottles as a substitute for standard 3D printing filaments. The PET bottles were washed and the labels removed, then shredded and dried. The filament was produced using a Brabender Twin Screw DSE 20 model with six temperature zones. These were divided into feed zone heating, compression zone heating, pumping zone heating and the die. Cold-air gun, water-bath, and table blower were used as cooling methods during extrusion optimization. An electric spooling device served as a puller for the filament during production while the filament was wrapped around a plastic profile tube. A 3D printing dummy test was developed in CAD and converted to STL file for the 3D printing comparison test. The comparison between the recycled PET and virgin PET was based on the tensile performed. The results show that recycled PET have comparable properties to the standard 3D printing filaments and thus can be used as a more sustainable substitute feedstock. Also, the puller speed was shown to be critical during extrusion and influence drastically the quality of the filament. Not only that, but the distance between the puller and the die and the cooling method during extrusion are also important factors for the recycled PET filament quality.

The final paper analysed regarding PET is from Zander, Gillan, and Lambeth (2018). The objective was to perform a study of the potential applications of PET as a new FFF feedstock material. This work involved the use of PET sourced from plastic bottles, soda bottles and salad containers. The authors proceeded with removing labels and rinsing with soap and water followed by an ethanol rinse and left the containers to dry at room temperature. These were later shredded into pieces and dried under vacuum at 120ºC. The shredded polymer was fed into a Thermo Scientific Process 11 Parallel Twin-screw extruder. The extruder had 8 temperature control zones. The feed port was set to 200ºC followed by a 240ºC zone, then 5 zones at 260ºC and finally the die at 240ºC. All this process is set with a screw speed at 100 rpm. The extrudate was collected over a conveyor belt cooled with nitrogen at 20ºC and then wound on a spooler. The same method was performed on recyclable PET and commercial off the shelf PET (COTS-PET). The produced filament was dried at room temperature under vacuum and tested on a Taz 6 FFF printer. Later, the 3D printed samples were chemically and thermally characterized, with additional rheological and mechanical tests. The paper presented an extended characterization of the different materials. The most important results show that different PET items' produce identical feedstock and their chemical characteristics are almost identical, hence different PETs can be mixed with no issue. The drying of the recycled PET leads to an increase in the polymer viscosity. The recycled PET also showed similar elongation to failure, tensile strength and robustness compared to commercial ABS filaments, confirming PETs potential applications for FFF feedstock. Table 7 summarizes the results from the mechanical tests performed with samples produced with printed commercial PET, injection moulded recycled PET, die-cut from containers and printed recycled PET. From the Fourier-transform infrared spectroscopy (FTIR) chemical analysis, all COTS-PET, PET and rPET show identical spectra. Hence, no degradation and no relevant impurities or additives were found in the recycled PET. For the thermal stability, a residual mass of 11% was calculated which is indicative of some additives or fillers present in the rPET. Major differences were identified in the viscosity of COTS PET and rPET which shows a higher molecular weight for the COTS-PET than the rPET. Similar

behaviour was found for the mechanical testing between rPET and PET which are also similar to the PC-ABS. The most relevant issue is the crystallinity of rPET, thus a controlled process temperature and additives to the rPET mix need to be constantly checked to maintain rPET quality.

Table 7: Summary data for the mechanical testing performed on die-cut from bottles, injection moulded rPET, printed rPET and printed COTS PET (Zander, Gillan, and Lambeth 2018).

	Printed COTS PET	*Injection Moulded rPET*	*Die-Cut*	*Printed rPET*
TS [MPa]	28 ± 9	68 ± 1	102 ± 19.3	35.1 ± 8
E [MPa]	2000	2994 ± 801	1837 ± 259	2112 ± 196
ε^f *[%]*	2.5	3.2	59	3.5

3.3.2 – Review of rPP Filament Extrusion for 3DP Use

Iunolainen (2017) performed a research in order to assess the suitability of rPP to produce filament for 3DP. The main objectives were to experimentally test the production of filament from rPP, study the mechanical and flow properties of the material and finally to measure MFR values of commercial ABS and PLA filaments to compare with rPP. The methods were divided into extrusion, MFR measurement and production of dumbbell test specimens by injection moulding followed by tensile testing. For the experiments the equipment used were a KFM Eco Ex extruder, a Mitaten plastometer (MFR measurement), and ENGEL injection moulding machine and a testometric material testing machine for tensile tests. The extruder had 6 temperature zones and several cooling systems were tested, namely, cold-air gun and cooling water bath with an heating element and thermostat. A pulling device was also employed. For the optimization of the extrusion 3 experiment setting were carried out. In the first experiment the cooling method used was the cold air gun (pressurized) and the temperatures were the same as for the virgin PP. In the second experiment the cooling method was changed to heated water bath using a heating element and thermostat. The temperatures were raised as an attempt to obtain a smoother filament surface since there were swelled areas caused by parts that did not melt completely. In the third experiment the temperature of the cooling bath was increased to try to obtain better filament roundness and the material used to clean the extruder prior to the experimentation was changed from Asaclean purging compound to virgin PP (brand Sabic, violet). To control the dimensions of the filament produced the diameter was measured twice at one point in intervals of 1 m with a digital calliper. The melt flow index was measured for virgin PP (Sabic), rPP (provided by a recycling company), rPP filament sample, COTS ABS and PLA according to ISO 1133:2005. The tensile testing was performed using dumbbell test specimens obtained from injection moulding with rPP and virgin PP pellets. The properties measured were tensile strength, elongation at yield and Young's Modulus according to ASTM Standard D638. Three test specimens of each material were run on the testometric machine. Regarding the results, the most successful experiment was the third, which showed the best results in terms of filament quality. However, the resulting filament was still unsuitable for use in a 3D printer due to surface flaws and diameter variations. The temperatures used were 210-215-215-225-225 ºC (zones 5 to 1 respectively), the extrusion speed was 25 rpm and the water bath was heated to

50 ºC. The filament surface was less rough but there were considerable diameter variations and the shape was more elliptical than round shaped. The MFR obtained was, in increasing value, virgin PP, rPP and rPP filament (7.2, 14.4 and 16.4 g/10min respectively). The stress at yield, Young's modulus and strain at yield were higher for the virgin PP.

In another research on rPP, Domingues et al. (2017) have established a solution for the management of used waste recovered from tires and used PP plastics. Using a blend of 60% tire waste granulate and 40% rPP the authors were able to generate components with added value such as urban furniture through 3DP. For such a prototype of a 3D printer was adapted in-house, composed of a robotic arm, modified extruder and heated print bed. It provides the chance to produce much bigger parts compared to the common 3D printers (Robot Yaskawa Motoman HP20F). The blend used was made of polymeric matrices from rPP and tire waste in micronized state. A twin-screw extruder was used for the polymer processing. The resulting processed material was characterized with tensile tests and thermal analysis after printing six specimens of PP/Tires blend. The printing was done with an heated base at 120 ºC and extrusion nozzle at 198 ºC. The tensile test was performed according to ISO 527-4 with an Instron 4505 test machine. The thermal analysis conducted included differential scanning calorimetry (DSC) and thermogravimetric analysis (TGA) with a heating of range 30-250 ºC followed by cooling. The properties assessed were heat of fusion, melting temperature and crystallization temperature. The results from the tensile testing showed that the ultimate tensile strength was 6 MPa with a corresponding deformation of 0.03 (3%). From the thermal analysis it was concluded that when comparing PP with the blend PP/Tire the former had a lower crystallization temperature (T_C 107 ºC vs 116 ºC) thus showing that the presence of tire waste lead to an increase of T_C. According to Domingues et al. (2017) knowing the melting point is important in order to optimize the printing parameters. The PP/Tire blend showed a marginally higher melting point compared to PP (161 ºC vs 157 ºC). For PP/Tire the thermal analysis showed two different peaks. The first is associated with the beginning of melting of one of the blend constituents and the second leads to the polymer fusion at higher temperature value. The authors demonstrated that it is possible to do 3DP of large parts using a blend of tires and PP plastic waste. The blend ratio still needs to be optimized and further investigated. They intend to study in future work the use of curable resins as binder material for the blend so that when applying UV lights stronger bonds can be achieved during printing.

3.3.3 –Review of rHDPE Filament Extrusion for 3DP Use

Regarding HDPE the first analysis was performed on the dissertation by Hamod (2015). Its objectives were to investigate the recycling process of rHDPE to produce filaments for 3D printing, compare it with standard 3D printing filaments (ABS and PLA) and virgin HDPE. Moreover, it was intended to perform a complete assessment of the rHDPE material properties. The methods involved gathering HDPE materials from shampoo bottles, detergent containers, cleaning agent bottles and milk jars. The separation was performed by colour. Afterwards, a washing process was applied to remove any contamination and labels. After the cleaning step, the plastics were shredded and dried. The shredded bits were turned into pellets using an extruder. Melt flow index was calculated for the materials

involved as well as tensile tests. The main results from this research were that recycled HDPE tests are similar to PLA concerning melt flow, yield strain, melt temperature and extruding temperature. Some difference, however, was noted for the tensile strength and Young's modulus. Throughout the experiment, the puller speed greatly influenced the filament quality. Other influencing factors were the extruding temperature, the distance between the die and the pulling device and finally the cooling method. Overall, the recycled HDPE was deemed comparable to PLA as 3D printing filaments.

In a dissertation by Angatkina (2018) the objective was to explore the feasibility of producing high quality recycled HDPE filaments. A comparison was made between rHDPE and a reference HDPE material with tensile tests to analyse their mechanical properties. Both rHDPE and HDPE were provided in pellets and fed into the extruder hopper. No pre-drying was performed. At the end of the extruder, a cold air gun was set up to cool down and support extrudate in the air followed by a water bath and a pulling unit with a cooling device. It was important to have an adequate water temperature for a slow cooling process of the filament. After the filament was extruded, the porosity and impurities were inspected with an optical microscope. MFR tests were conducted according to ISO 1133:2005 and finally tensile tests were performed according to the ASTM D638-67T standard. To finalize, a 3D printing test was performed comparing both rHDPE and HDPE. From all the tests done, there were some positive and negative results. Regarding the extrusion, the material flow often stopped and no cause for the issue was found. The filament roundness was non-uniform and inconsistent on its diameter. Some impurities were found in the rHDPE filament surface. MFR tests showed similar results between HDPE and rHDPE. It was shown that both recycled and pristine HDPE filaments produced comparable printing quality with similar Young's moduli. Moreover, the recycled material exhibited higher yield strength and better ductility. Thus, despite some extrusion complications, it was asserted that recycled HDPE has a potential for feedstock material to be used in FDM.

Lastly, the paper by Chong et al. (2017) addressed the potential of the recycled HDPE for 3DP. This study evaluates, in terms of physical characterization, the feasibility of using rHDPE relative to ABS. Additionally, a comparison between rHDPE pellets (higher material grade) and rHDPE flakes (locally processed) was addressed in this work. HDPE exists in most forms of containers such as detergent containers, shampoo bottles, household bottles and milk bottles. These materials were soaked at 60ºC in water, followed by manual removal of the labels and glue. Afterwards, the materials were dried in an oven at 100ºC. This was followed by a shredding procedure and then dried. A single-screw Filastruder Kit was used to extrude the material, with a 3 mm die and optimal temperature around 180-190ºC. The materials were characterised by diameter consistency, extrusion rate (filament length produced during a given time period), differential scanning calorimetry, thermogravimetric analysis, Fourier transform infrared spectroscopy, Raman spectroscopy and water absorption. For the diameter consistency, the rHDPE(pellets) yielded the best result. From the FTIR, additional small peaks were detected for the rHDPE(flakes) spectra caused by existent contamination. The pellets show no additional peak, due to the pellets being of higher grade and sourced from a company, with quality control and thus have improved cleaning standards. Also, sunlight exposure has shown great degradation for the rHDPE (both) but not the case with ABS. From the Raman Spectroscopy analysis, rHDPE(flakes) show higher intensity levels, most likely due to its higher crystallinity. Regarding the

thermal properties, rHDPE(flakes) show greater weight loss compared to rHDPE(pellets) which showed the least weight loss. For the water absorption test, filaments rHDPE(flakes) showed the least water absorption. Regarding the surface morphology, ABS(pellets) led to the smoothest surface and both rHDPE(pellets) and rHDPE(flakes) led to cracks in the extrudate. Overall, the rHDPE(flakes) is the least preferred candidate as 3D printing feedstock compared to the rHDPE(pellets) and ABS. However, the rHDPE(pellets) is an equal candidate for 3D printing as the ABS. To make the rHDPE(flakes) better an improved cleaning process needs to be implemented before the extrusion process.

3.3.4 – Overview on the Feasibility of Filament Extrusion for 3D Printing

The aim of the research is to extrude plastic filament for subsequent 3DP with recourse to plastic waste of controlled sources. A summary of the feasibility of extrusion and subsequent use for 3DP is presented in Table 8 for the set of polymers previously reviewed (rPET, rPP and rHDPE).

Table 8: Review on extruding and printing feasibility of a selection of abundant materials (adapted from Lehrer and Scanlon 2017; Mutiva, Byiringiro, and Muchiri 2018; Zander, Gillan, and Lambeth 2018; Domingues et al. 2017; Iunolainen 2017; Baechler, DeVuono, and Pearce 2013; Hamod 2015; Chong et al. 2017; Angatkina 2018; Zander et al. 2019)

Polymer	Author	Material Source	Extruder Type	Extruder Feasibility	Printing Feasibility
rPET/ PETG blend (50/50)	Lehrer and Scanlon (2017)	PET-G pellets PET water bottles	Custom built	Successful	N.A
rPET	Mutiva et al. (2018)	PET water bottles	Twin screw	Successful	Suitable
rPET	Zander, Gillan and Lambeth (2018)	PET water bottles	Parallel twin screw (conveying mode)	Successful	Suitable
rPP Blend	Domingues et al. (2017)	60% Granulated tire waste and 40% rPP	Twin screw	Successful	Suitable
rPP	Iunolainen (2017)	rPP pellets provided by recycling company	N.A	Unfeasible	Unfeasible
rHDPE	Baechler et al. (2013)	Heavier pieces from detergent/ shampoo containers	Custom (RecycleBot)	Successful	Suitable
rHDPE	Hamod (2015)	Collected domestic products (shampoo bottles, detergent containers, milk jars)	N.A	Successful	3DP not performed
rHDPE	Chong et al. (2017)	Containers/bottles of detergent, shampoo, milk	Single-screw	Successful	Possible, low quality
rHDPE	Angatkina (2018)	Municipal Solid Waste	Single-screw	Possible but very inconsistent	Possible
rPET/rPP/rPS blends with/without compatibilizers	Zander et al. (2019)	Recycle bins (rPET salad, yogurt rPP containers, rPS petri dishes)	Twin-screw	Successful	Successful

3.4 – Review of Extrusion Parameters and Properties of Recycled Filaments

Several authors use materials from different sources which introduces a considerable variability. As an example, Hamod (2015) recycled milk jars together with shampoo bottles and detergent containers. However, since milk jars are food containers there are many quality and material requirements that must be met for such use. As such, it is expected to have different additives and material grades when compared with the other containers used. This can have impact on the mechanical and chemical properties of the resulting recycled filament. The source of materials, the pre-processing of them, the extruder parameters and the cooling methods greatly impact the results. Bearing this in mind a complete review on process parameters and the mechanical and rheological properties of the recycled filaments obtained has been carried out and summarized in Tables 9-11. Most of the authors of the studies perform the experiments by starting with the processing of controlled material, usually a virgin polymer or in some cases recycled polymer from controlled source (usually obtained from recycling companies). The results obtained are considered the baseline which will be compared to the results obtained from the extruded filament originated from the mixed sources. This allows to compare the melt flow index of virgin and recycled polymers as well as the mechanical properties of test specimens made from the baseline material and the recycled material for comparison. The polymers included are PET, PP, HDPE and blends. This consolidates all information regarding melt flow index, pre-processing conditions, extrusion temperatures and screw speed, cooling methods, type of pooling, tensile strength, elastic modulus, strain at yield and key factors impacting the filament quality according to each author. The fields marked with an asterisk (*) refer to the optimal parameters as tested by the respective authors. For the materials marked with (1) the mechanical properties were assessed on injection moulding test specimens and not in 3D printed specimens.

Table 9: Review on extruder parameters, mechanical properties and rheological properties of recycled PET filaments (Mutiva, Byiringiro, and Muchiri 2018; Zander, Gillan, and Lambeth 2018)

	PET (baseline)	**rPET**	**PET (baseline)**	**rPET**
MFI [g/10min]	3.37	2.85	N.A	N.A
Pre Processing	NA	Drying	Drying	Drying
D_d [mm]	N.A	N.A	2.5	2.5
T_{extr}* [ºC]	N.A	255	200 (1) 240 (2) 260 (3-7) 240 (die)	200 (1) 240 (2) 260 (3-7) 240 (die)
v_{extr}* [rpm]	N.A	15	100	100
Cooling Method*	N.A	RT	N.A	Nitrogen-cooled conveyor belt RT Water cooled
Pooling* [V]	N.A	8.4	Custom	Custom
d [mm]	N.A	N.A	N.A	2.60 ± 0.3
d target [mm]	N.A	1.75 ± 0.02	2.5 – 3.0	2.5 – 3.0
TS [MPa]	17.7	35.7	28 ± 9	35.1 ± 8

E [MPa]	971	1200	2000	2112 ± 196
Strain at Yield [%]	16.12	16.12	2.5	3.5
Author	Mutiva et al. (2018)	Mutiva et al. (2018)	Zander, Gillan and Lambeth (2018)	Zander, Gillan and Lambeth (2018)
Key Factors in Filament Quality	N.A	Puller speed Distance die-puller Cooling method	N.A	Reprocessing may cause degradation by hydrolysis in melt and chain scission Cooling method (water) Appropriate drying Use of Conveyor belt

Table 10: Review on extruder parameters, mechanical properties and rheological properties of recycled HDPE filaments (Hamod 2015; Angatkina 2018)

	HDPE(1) (baseline)	**rHDPE(1)**	**HDPE (baseline)**	**rHDPE**
MFI [g/10min]	3.37	2.85	0.324	0.336
Pre Processing	N.A	Washing Drying Pre-extrusion	None	None
D_d [mm]	2	2	3	3
T_{extr}* [ºC]	190	175	180 (1-2) 190 (3) 195 (4) 200 (Die)	180 (1-2) 190 (3) 195 (4) 200 (Die)
v_{extr}* [rpm]	20	15	20	20
Cooling Method*	RT	RT	Water bath (50ºC) and RT (0.75m, 1m)	Water bath (50ºC) and RT (0.75m, 1m)
Pooling* [V]	21	8.4	N.A	Custom
d [mm]	1.75 ± 0.02	1.75 ± 0.02	1.76	1.66
d target [mm]	1.75 ± 0.02	1.75 ± 0.02	1.75 ± 0.05	1.75 ± 0.05
TS [MPa]	25.45	25.59	7.4	10.36
E [MPa]	446.37	428.38	336	385
Strain at Yield [%]	16.12	16.12	3	5.50
Author	Hamod (2015)	Hamod (2015)	Angatkina (2018)	Angatkina (2018)
Key Factors in Filament Quality	N.A	Puller speed Fine tuning of extruding temperature Distance between die and puller RT cooling	N.A	Water bath cooling (50ºC) for shape and diameter (ensure slow cooling) No suitable parameters found (Author refers critical issues of unknown causes (material stoppage, filament geometry)

Table 11: Review on extruder parameters, mechanical properties and rheological properties of recycled filaments (Chong et al. 2017; Iunolainen 2017; Zander et al. 2019)

	rHDPE(p) (baseline)	**rHDPE**	**PP(1) (baseline)**	**rPP(1)**	**rPET, rPP, rPS blends (SEBS/SEBS-MA)**
MFI [g/10min]	N.A	N.A	N.A	16.4	N.A
Pre Processing	None	Cleaning (warm water for label, glue), drying	None	None	Cleaning with water and ethanol, dried

		(100ºC), shredding, drying (50ºC)			Vaccum rying overnight (rPET 120ºC; rPP at RT) rPS grounded to powder
D_d [mm]	3	3	N.A	N.A	2.5
T_{extr}* [ºC]	180-190	180-190	N.A	210 (1) 215 (2) 215 (3) 225 (4) 225 (5)	140 (1) 170 (2) 260 (3-7) 245 (die)
v_{extr}* [rpm]	N.A	N.A	N.A	25	100 (first extrusion, uniformity) 25 (second extrusion, filament)
Cooling Method*	N.A	N.A	N.A	Water bath (50ºC)	Conveyor belt RT
Pooling* [V]	N.A	N.A	N.A	N.A	Custom
d [mm]	2.93 ± 0.22	3.17 ± 0.30	N.A	N.A	N.A
d target [mm]	2.80 ± 0.20	2.80 ± 0.20	1.75	1.75	N.A
TS [MPa]	N.A	N.A	31.65	25.18	[17.2, 35.1]
E [MPa]	N.A	N.A	677.1	594.32	N.A
Strain at Yield [%]	N.A	N.A	10.81	9.83	[0.007, 0.4]
Author	Chong et al. (2017)	Chong et al. (2017)	Iunolainen (2017)	Iunolainen (2017)	Zander et al. (2019)
Key Factors in Filament Quality	N.A	Drying prior to extrusion Hypotheses raised on pelletizing and using additives to counter feedstock issues Feedstock source quality control	N.A	Clean extruder with virgin PP material prior to recycling experiment Warm water bath	compatibilizers increased viscosity, improved bonding between phases and performance window of materials

3.5 – Conclusions

In the first sections of the State of the Art the scope of the research was approached. The first topic of discussion was the technology disruption caused by 3DP in the context of AM and its impact in several industries across a myriad of domains that involve rapid prototyping and part manufacturing. Further on, the FDM printing technology was introduced and discussed since it will be the 3DP technique used with the filaments. The next topic introduced was the extruding process of polymers in which the principles of the technique are addressed and the specific case of single screw extruder is analysed in more detail, from the components to the mechanism and melt process along the barrel. The importance and role of viscosity and viscoelasticity is discussed since these are relevant properties of polymers for the extruding shaping process. In the third section an extensive review was made regarding the use of recycled plastics, namely, PET, PP and HDPE, to produce filaments for 3D printers. This information is complemented with a review and systematization of the extrusion process parameters and tested properties of recycled filaments from all the available papers considered.

Based on the previous reviews it is possible to assess which polymers are currently feasible solutions to be extruded and subsequently used for 3DP. It was shown that rPET can be successfully extruded and in the cases where no blend was used a twin-screw extruder was always employed. The blend of PET/PETG was also shown be feasible by successfully extruding the material although no printing was tested with the filament. All research that involved rPET used water bottles which allows for a higher quality source control, leading to a less heterogenous mixture when the material is recycled and with more similar plastic grades and composition (Lehrer and Scanlon 2017; Mutiva, Byiringiro, and Muchiri 2018; Zander, Gillan, and Lambeth 2018). Regarding rPP the results available were less favourable. In the research by Iunolainen (2017) the extrusion proved to be unsuccessful and the filament obtained could not be used in a 3D printer. The material used was rPP pellets provided by a recycling company. However, tensile tests were performed to specimens produced with injection moulding. Some of the factors that proved to be important and are noteworthy are the heated water bath as cooling method and the extruder cleaning with virgin PP prior to using rPP. Another study tested the use of rPP blended with tire waste (Domingues et al. 2017). A twin-screw extruder was used and the extrusion was successful. Based on the results from extrusion and data provided by the author it seems printing is suitable even though it was not carried out. Lastly, regarding rHDPE, more data is available and the extrusion is more studied. The material sources used across the authors in literature is very similar and includes containers of shampoo, detergent and milk and in one case, municipal solid waste. In the studies where information of extrusion method is provided the equipment used was single screw (Chong et al. 2017; Angatkina 2018). Three out of four rHDPE studies report that extrusion was successful and is feasible while one reported that extrusion might be possible but the results were very inconsistent. Furthermore, the 3DP using the recycled filament showed poor quality in one of the two studies that effectively tested printing. Water bath showed good results as cooling method.

Overall, some methods proved to be important across most of the studies reviewed. These include the pre-processing of sorting, washing, drying prior to extrusion and in some cases pelletizing (one cycle of extrusion to obtain more homogenous pellets). Relevant tests performed to assess the quality of the recycled materials and benchmark them against virgin materials include mechanical tests (determining yield point, ultimate tensile strength, Young's modulus, strain at yield or failure) and thermal and chemical analysis such as MFI measurement, FTIR, TGA, DSC and dynamic-mechanical analysis (DMA). This information is especially important for the design of the experiment that will follow. With the review undertaken it is clear that this topic constitutes a gap in the available literature. Moreover, it is possible to conclude that rPP is the polymer less investigated and with greater variability of results. As such, this is the basis to sustain the decision of focusing solely in rPP for the experimental part of the investigation to fill in the literature gap that it constitutes.

4 - Methodology

4.1 Research Scope

Chapter 3 provides the theoretical background sustaining this research. An exploratory review of literature was carried out in order to identify the current state of the employment of reused plastics as feedstock to produce 3DP filament and subsequent use in FDM printers. It was found that a literature gap exists regarding rPP reuse for 3DP. This polymer is one of the main constituents of plastic waste generated yearly over the past decades. As such, PP is the material selected for the evaluation and experimentation on this research. Accordingly, this thesis is developed within the purpose of applied research with an analytical study by nature and following a quantitative and exploratory method.

Important issues to assess include the characterization of the material before and after extrusion, possibility of improving the recycled material properties prior to processing, determining the best combination of variables in extrusion, how to control diameter of the resulting filament, among others.

Two research questions are at the core of this research. The first one is descriptive and comparative and the second is action based:

(1) What are the main characteristics (composition, chemical, thermal, rheological, mechanical) of PP flakes sourced from waste treatment facilities and of the subsequently produced filament by extrusion? What are the similarities and differences with those of 3DP PP filament?

(2) How can the processes by which rPP filament is obtained from heterogeneous bulk rPP flakes be improved in order to attain effective 3DP (FDM) printability?

Figure 12 provides an overview of the research. In the next chapters each process depicted will be expanded into the operations performed throughout the experimentation with detailed descriptions. The research boundary starts with the entrance of the PP material under study in the laboratory of CERENA Research Centre. The PP was obtained from a recycling facility that receives plastic waste and subsequently separates by type of polymer and grinds the materials into flakes. After the material was received it was then processed and characterised prior to the extrusion process. The second stage was the optimization of the extrusion of rPP with selected variables. The third stage comprised the characterisation (thermal, chemical, mechanical) of the filament obtained and its comparison with virgin PP filament for 3DP, vPP(3DP), available in 3DP related stores.

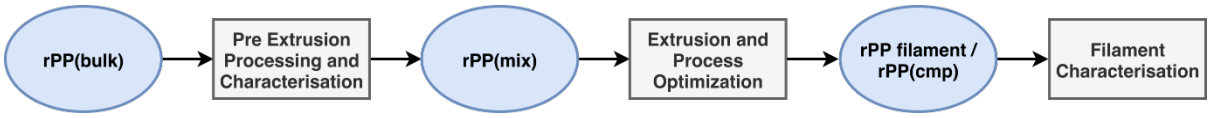

Figure 12: Overview of the research.

4.2 Materials and Equipment

The main material used is the recycled PP that was provided by the recycling company, namely, Lipor. This company specializes in municipal waste treatment and recovery and serves eight

municipalities in the district of Oporto. The material provided is henceforth labelled as rPP(bulk). This is due to the fact that there is no certainty of the exact composition of the flakes provided in bulk. As it can be seen in Figure 13A, the material is extremely heterogeneous (flake size, colours, composition) and as such it can contain other polymers.

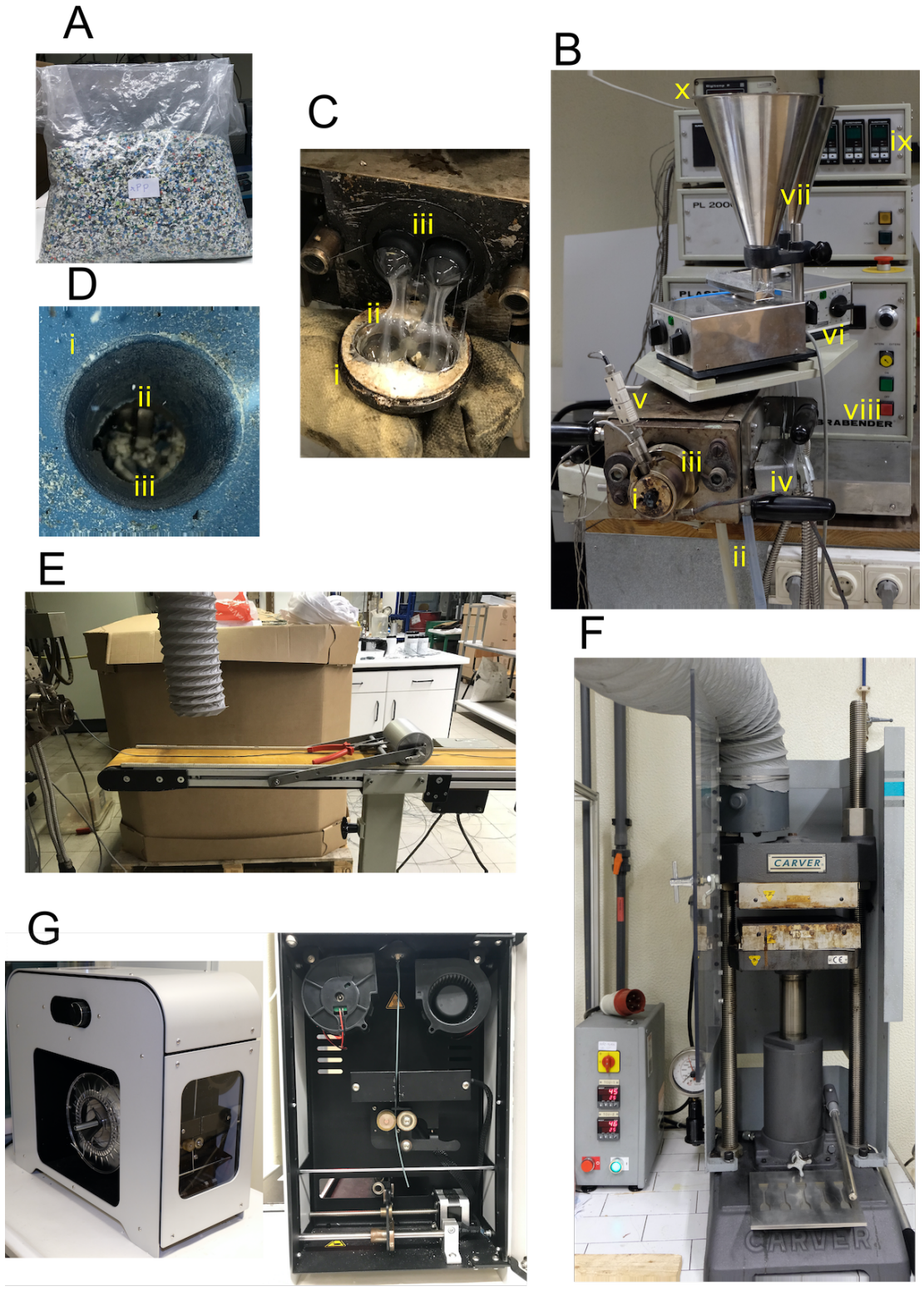

Figure 13: A) rPP material provided by LIPOR for research in CERENA, IST. B) Twin-screw extruder. C) Extruder screws and die once the main plate is taken out. D) Feeding zone of the twin-screw extruder. E) Conveyor belt used with extruder. F) Hot press and mould to create test specimens with polymer pellets. G) Mini extruder 3devo Composer.

The 3DP virgin filament used, vPP(3DP), sometimes designated COTS filament, was purchased from the Portuguese online store of RepRap (RepRap PT 2021) a company devoted to 3D printing and related equipment. It is referenced in the online shop as *PP (Polipropileno) RepRap PT – 1.75mm 500gr Natural.* The supplier did not have a technical data sheet but was able to provide the following properties: melt flow rate 8g/10min (230ºC, 2.16Kg), flexural modulus of 400 MPa and density of 0.92 g/cm^3. Another widely used material was the silicone H plastic mould release agent (produced by Henriquímica, Produtos Químicos Lda). Moreover, cutting instruments, pans, sieves and glass trays (to use in ovens) were also frequently used.

The equipment used can be divided into four categories: processing, material characterization, measuring and software. The complete list of equipment by category is presented in table 12 below:

Table 12: List of most important equipment used in the laboratory work.

Equipment Category	Equipment
Processing	Twin screw extruder Brabender DSK 42/7
	Conveyor belt
	Pelletizer
	Oven
	Hot press and mould
	Mini extruder 3devo
Characterisation	Plastometer
	Thermal scale (Karl-Fischer test)
	FTIR-ATR
	TGA
	Microscope with digital head
	Instron universal test machine
Measurement	Scale Shimadzu
	Scale Metler Toledo
	Camera
	Digital caliper and micrometer
Software	QtiPlot
	Microsoft Office
	Python3, Anaconda, Spyder

In processing the most important equipment was the twin-screw extruder. The model used was a Brabender DSK 42/7 Co-Rotating Twin Screw Extruder with a data processing Plasti-Corder PL2000 module with Eurotherm temperature controller. This extruder is depicted in Figure 13B above. In *B* the main elements of the equipment are identified with letters from *i* to *x* by order of appearance in terms of depth of field. Most of these elements were described in chapter 2, Figure 10, for a single-screw extruder. In *Bi* we have the die which in this case is characterized by circular geometry. The breaker plate is inside and such not shown in the figure. In *Bii* the two tubes belong to the refrigerating system. It is an open-loop circuit with water entering from wall, passing through the motor and other elements to maintain functioning temperature below the limit and exits into a sink. Whenever the extruder is operated the circulating system is the first thing to turn on to ensure the integrity of the equipment. In *Biii* we have the plate which connects the screws to the die and breaker plate. It is possible to remove it to access the screws' ends for cleaning operations among others. For such, at least two persons are required due to the weight of the components and high temperatures involved so that safety measures are always followed. In *C* the inside of element *Biii* (after taking it out) is shown and the screws are easily identifiable.

In element *Biv* the heating system is shown which provides the required energy to maintain the screw zones (1 to 4) at the set-up temperature values of operation which are chosen according to the polymer being used. In element *Bv* it can be seen the thermopar/thermocouple temperature sensor connected to the die to provide temperature readings and data to the temperature control module (it uses a feedback loop in order to control the temperatures in the system). The temperature value can be read in figure element *x*. In *vi* we have the vibration module which controls the rate of material fed to the extruder through the hopper (only barely visible in the picture, blue line). The stronger the vibration, the higher the feeding rate of material. This is extremely useful since the feeding zone should never be completely filled with pellets and the feeding rate is an important control variable. In *vii* we have the feeding cones where the pellets are placed and through the vibration of module *vi* they go into the hopper (not shown) which is connected to the extruder feeding zone. In *viii* we have the screws motor control module. In *ix* the temperature control module is shown and each screen with buttons is used to control the temperature of the individual screw zones (up to eight different zones if required).
In Figure 13C the interior of die is shown in *i* as well as the counter-current screws in *iii*. The polymer being used is visible in *ii*. In this particular moment it was PET. In Figure 13D the hopper and extruder feeding zone are shown (zoomed in). In *i* it is the hopper, *ii* is the initial region of one of the screws pushing the pellets forward (pressure exerted by the flights of the screw) and in *iii* the polymer pellets that were fed (in this case it is rPP). Another critical equipment that is of mandatory use with the extruder is the motorized conveyor belt which pulls the filament from the die (Figure 13E). Other equipment that was crucial for processing include the pelletizer, the oven, the hot press with mould and the mini extruder. The pelletizer is used to turn polymer filament into pellets (the filament is fed to the device and with a rotating blade driven by a motor the filament is cut into small pellets that are deposited in a plastic bag). The oven was used to dry the polymer after the separation in water and to control the polymer water content. The hot press was used to fabricate tensile specimens with the extruded rPP filament. The model used was a Carver M-2089 25 ton-force with heated plate 30ºC-500ºC capacity. The hot press and mould are shown below in Figure 13F. A small, compact extruder was also used to make filament when only small samples were available for processing and testing. The mini extruder used was a 3devo Composer and is shown in Figure 13G. The model is shown on the left side of the figure. On the right side the front of the extruder is depicted with the panel opened. This allows to see the main elements working.

For material characterization the available equipment allowed for the determination of chemical composition, moisture contents, thermal behavior analysis, rheological properties, imaging and mechanical analysis. For chemical analysis a PerkinElmer Spotlight 200i FTIR (Figure 14A) with Attenuated Total Reflectance (ATR) was used. This allowed to obtain the infra-red spectra of several material samples in order to compare them and assess molecular bonding elements with the peaks shown. For thermal stability and degradation analysis the equipment used was a Hitachi STA7200 Thermal Analysis System (Figure 14B).

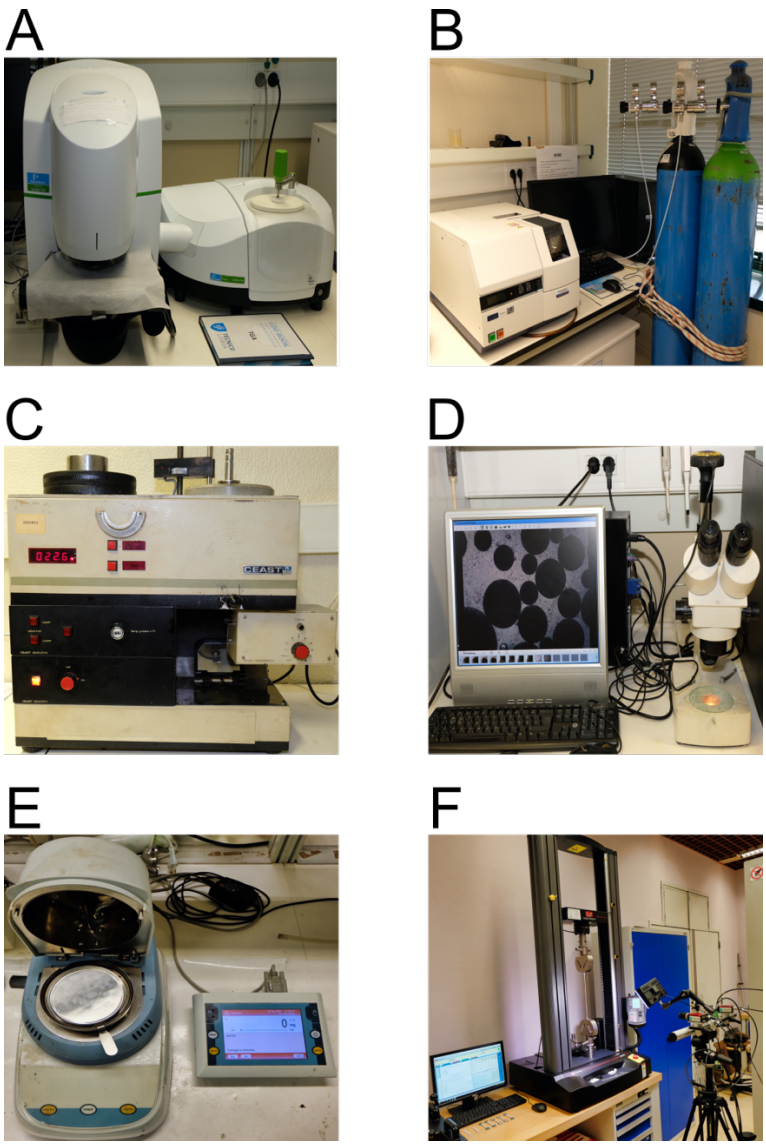

Figure 14: A) FTIR-ATR microscope; B) Thermal Analysis System for TGA. C) Plastometer used for the melt flow rate determination. D) Optical microscope. E) Thermal scale. F) Instron test frame equipment for the tensile tests.

In order to obtain the melt flow rate of samples a plastometer CEAST 6540/010/011 was used extensively (Figure 14C). This equipment is extremely important for characterization. Its main elements are the barrel, piston and heating system. The pellets are placed inside the heated barrel and afterwards the piston goes into the barrel with a pre-determined weight on top. This weight causes the piston to go down, pushing the pellets which melt along the path and go through a small die. For every fixed time period the filament is cut and weighted in a scale. Based on the weight per time interval, the MFR is determined and indicates the fluidity of the polymer. A microscope with digital adapter was also used to characterize samples (Figure 14D). In order to characterize the moisture content of several samples (an important parameter to have under control for extrusion and printing) a thermal scale was used (Karl-Fischer analysis; Figure 14E). Lastly, another crucial equipment for characterization is the Instron test frame used for the stress-strain mechanical tests of tensile specimens (Figure 14F). The equipment used was an Instron 5966K9184 with Max Load 10 kN and the extensometer system was Digital Image

Correlation (DIC) by Dantec Dynamics. Regarding the measurement category the following devices are included: precision scales, digital calliper, digital micrometre and photography equipment. The scales used were a Mettler Toledo PB3002 and a Shimadzu AUY220 (precision scale). A Mitutoyo calliper was used in the Hands-On Polymer and in the mechanical lab an Insize Digital Spherical Anvil Tube micrometre was used along with a Mahr Type 16 ER digital calliper. For registering images during the tensile tests and other situations both an iPhone 7 and a Fujifilm XT-2 were used.

Lastly, regarding the software category several programs were used. For writing and data logging and analysis Microsoft office 2016 Mac edition was extensively used. For data analysis and scientific graphing QtiPlot (ver. 1.0.0-rc14 64bit) was used. Finally, some small scripts in Python 3 (ver. 3.8.5) were used to process and clean data using Anaconda scientific platform (ver. 1.10.0) and Spyder IDE (ver. 4.1.5).

4.3 Experimental Procedure

4.3.1 Overview

Topic 4.3 details the experimental procedure and is organized in six subtopics. Each subtopic relates to a specific process that is easy to isolate in terms of block diagrams. A diagram with an overview of the processes is presented in Figure 15 below:

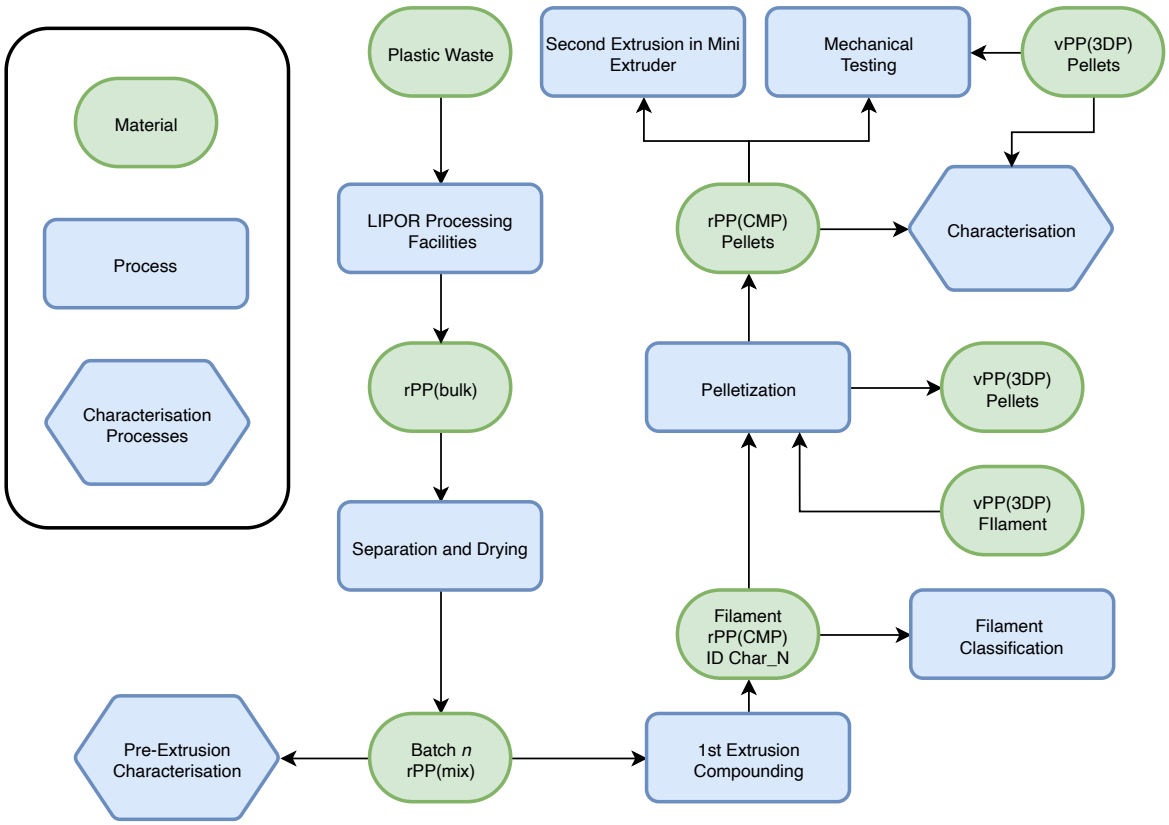

Figure 15: Overview block diagram of the processes and materials in the experimentation phase.

In the diagram block of Figure 15 the processes and PP materials are identified in blue and green respectively. Accordingly, the six subtopics are: Pre-extrusion Separation and Drying (4.3.2), Pre-Extrusion Characterisation (4.3.3), Extrusion Processing (Compounding) (4.3.4), Second Extrusion in Mini Extruder (4.3.5), Post-Extrusion Characterisation (4.3.6) and Mechanical Testing (4.3.7). It is important to note that throughout the methodology different labelling names are used for the same material depending on the processing phase it undergoes. The waste-derived polypropylene material delivered by the recycling and treatment facility is labelled as rPP(bulk): a very heterogenous mixture of flakes obtained from a great variety of sources and products with different and uncertain composition, material grades, additives, fillers and manufacturing processes. This constitutes the raw material for the research, received as is and defines the beginning of experimental research boundary. After the separation and drying process, the material is labelled as rPP(mix): cleaned, one separation step excluding all flakes that do not meet certain properties. After the first extrusion (that acts as compounding) the material obtained is rPP(cmp) filament and if pelletized it then becomes rPP(cmp) pellets. It has a homogeneous colour and aspect when visually inspected. The commercial material used for benchmarking rPP in direct comparison is labelled vPP(3dp) filament or pellets (if pelletized).

4.3.2 Pre-Extrusion Separation and Drying (rPP)

The experimentation begins with a simple method of separation in water by density. The main steps followed were: filling a pan with water and pouring rPP(bulk) flakes, stirring vigorously; take out the floating flakes slowly with a sieve into a glass tray to be dried; glass tray should have the flakes deposited uniformly and have less than 3 cm in height to achieve an homogeneous drying; given that PP has a density of 0.90 $g.cm^{-3}$ (Chanda and Roy 2007, 4–13) the group of flakes that floated was labelled rPP(mix) and the flakes with higher density were labelled unknown (UNK).

The glass tray, filter and plate are then placed in the lab oven for drying with parameter (T(ºC), t(h)) – oven temperature and time interval. Once the time period elapses the tray is taken from the oven to a scale and the weight is registered every 5 minutes until the material cools down to room temperature (or approximately 45 minutes). Date and time of start/stop of drying process was registered as well as weight before and after procedure. Subsequently, the weight variation is calculated (for before drying vs after cooling, after removing from oven vs after cooling). After that, flakes are transferred to a container with batch label *n* for reference. Afterwards, moisture analysis is performed on a sample from batch *n* in the thermal scale. For moisture analysis three runs were always carried out. For the first batches of rPP(mix) the drying parameters are adjusted until a satisfactory moisture content (%) is obtained. After that, the same setting is used for all the samples that follow. The parameters tested are presented in Table 13.

Table 13:Drying parameters tested – temperature and time interval. Final set values in dark grey.

[T, t(i)] (ºC, hh)	Batch
60, 18.50	S1
60, 63.50	S2
60, 21	S3
60, 43.37	S4
60, 24	S5-S7

The Toledo PB3002 was used for all these measures given that it was the only scale with the required sensitivity interval. Upon storing the dried flakes in container (one for each batch) the moisture analysis is performed in the thermal scale. The procedure was repeated 3 times. For each trial 20-30 g were used on an aluminium pan distributed uniformly. The parameters used are listed in Table 14 below:

Table 14: Parameters used in the thermal scale for moisture analysis.

Program Name	T(ºC) Max	Auto-Stop	Pre-Heating	Units
Standard, 80	80	0.1%/10s	Off	%M

The results were taken from the monitor connected to the thermal scale which also provided a curve of temperature vs time. The target moisture content was having average values inferior to 0.20%. These values were used to characterise the samples as well as to determine the final drying parameters. The same analysis was performed for vPP(3DP) later on.

4.3.3 Pre-Extrusion Characterisation

The first step in the characterisation prior to extrusion was to separate all the flakes in a sample according to the only visible property that differed: colours. To each set of flakes a code was attributed: colour name (e.g. BLUE, with abbreviation BL) and colour pitch number (0 to 3, from bright to dark; e.g. BL2 stands for medium blue). After all the colours were separated the following analyses were prepared: optical microscopy of every coloured flake, FTIR-ATR analysis for the most abundant colour flakes (half of the total number of flake colours approximately), TGA analysis to compare two flakes that had the same colour but different behaviour on separation (float vs non-float; white flake vs unknown white flake) and melt flow rate determination for samples of rPP(mix).

For the optical microscopy with digital probe all types of colour flakes were analysed. Two amplifications were used for all samples and the lighting was adapted case by case to produce sharp and detailed images. With the digital probe connected to a computer it was possible to take pictures and export in TIFF format.

For the MFR determination a detailed standard procedure was written for the equipment available in the lab. It is included in Annex A. The standard ASTM D1238-13 was used for MFR determination. The most relevant parts regarding procedure include: prior cleaning with PVC at low

temperature do decrease contamination; procedure A from ASTM D1238-13; perform at least 30 trials to allow for statistical analysis and the use of data cleaning with Python script (included in Annex C).

The FTIR spectra were achieved with a Perkin Elmer device equipped with a UATR Two accessory (ATR mode) at 4 cm^{-1} resolution. Eight scans were performed and accumulated. The 11 most abundant colours were analysed and their spectra were introduced in the Perkin Elmer database of FTIR-Spectra to find the best matches of materials. TGA was performed with the following parameters: temperature increase rate of 10 ºC.min^{-1} in the range 30-600 ºC and controlled nitrogen atmosphere with 200 ml/min constant flow. This allowed to analyse the thermal stability of the samples. The identification of peaks, graphing and curve overlapping was done with QtiPlot.

4.3.4 Extrusion Processing (rPP)

For the extrusion processing three types of variables were considered: independent variables, dependent variables and control variables. The extruder zone temperatures T(X) and the screw speed S(i) were chosen as the independent variables. Since the extruder has four zones (including die) it was defined that X represents a set of temperature values for each zone:

$$T(X) \equiv \{T(die), T(zone3), T(zone2), T(zone1)\}$$

The dependent variables were established as the filament cross sectional geometry (qualitative), the filament diameter (quantitative) and the overall quality. The latter is defined as a nominal composite variable with colours. It takes into consideration the previous two dependent variables as well as other factors that may be identified as relevant in particular cases: surface uniformity, existence of non-melted particles, etc. Lastly, the control variables identified were the cooling method, extruder feed rate, the conveyor belt speed, the distance from the conveyor belt to the die and the height of the conveyor belt relative to the extruder (all constant but adapted for each case; they were not the focus of the experiment and may be defined as extraneous variables).

The extrusion plan was defined based on the information provided in Giles (2014) as well as the results obtained in a thesis (Iunolainen 2017). Table 15 below shows the information provided by Giles regarding the best zone temperatures for extruding PP depending on the material MFR:

Table 15: Advised processing conditions for Polypropylene (adapted from Giles, 2014, p264). Melt Flow Rate for 230ºC with 2.16 Kg.

MFI 230ºC/2.16Kg	Die (ºC)	Zone 4 (ºC)	Zone 3 (ºC)	Zone 2 (ºC)	Zone 1 (ºC)	Melt Temperature (ºC)
0.2 - 10	227-260	227-260	227-243	210-232	171-193	232-288
12 - 35	**204-232**	**193-216**	**193-216**	**182-204**	**160-182**	**204-232**
50 - 300	177-193	177-193	177-193	171-182	149-168	177-193

Iunolainen (2017) studied the processing rPP. The optimal parameters found by the author are shown in Table 16. However, no information is provided regarding the type of extruder used (single or double screw).

Table 16: Optimal parameters determined by Iunolainen (2017).

MFI 230ºC/2.16Kg	Die (ºC)	Zone 4 (ºC)	Zone 3 (ºC)	Zone 2 (ºC)	Zone 1 (ºC)	Screw Speed (RPM)	Cooling Method
14.4	225	225	215	215	210	25	Water bath 50ºC

Parameters applicable to the material under analysis are highlighted in green colour. These were used to define the baseline of temperature ranges to be tested. A preliminary set of parameters with variations were tested in order to get familiar with the equipment and methods. These are shown in Table 17:

Table 17: Preliminary experiments to get familiar with equipment and gain sensitivity to material.

Screw Speed (RPM)	Die (ºC)	Zone 3 (ºC)	Zone 2 (ºC)	Zone 1 (ºC)
15	200	200	190	170
15	210	210	200	170
15	210	210	200	170
15	210	220	210	170
15	220	220	210	170
20	220	220	210	170

The main extrusion plan is shown in Table 18 in compact form for better readability. For each set of temperature all four values of screw speed are to be tested. The first set of temperatures was defined based on the values provided by Giles (2014). The next temperature sets are defined as the base level with constant 10 degree increments along the barrel.

Table 18:Main extrusion plan for experimentation with varying temperatures and screw speeds.

Screw Speed (RPM)				Die [ºC]	Zone 3 [ºC]	Zone 2 [ºC]	Zone 1 [ºC]
25	20	15	10	200	200	190	170
25	20	15	10	210	210	200	180
25	20	15	10	220	220	210	190
25	20	15	10	230	230	220	200
25	20	15	10	240	240	230	210

Pictures are taken to the resulting filaments for later comparison and evaluation of each set of parameters. A procedure was written for the twin-screw extruder and is included in Annex B.

4.3.5 Second Extrusion in Mini Extruder (rPP)

A simple test run was performed on the mini extruder 3devo with compounded pellets. The available amount of compounded pellets was insufficient to run another extrusion cycle in the twin-screw extruder due to its high material consumption. Only one set of parameters was tested. The mini extruder has a feedback loop: some parameters are adjusted given the diameter readings as the filament goes

through the laser sensor. The parameters used are shown in Table 19. Some of the parameters are dependent on the device itself, such as the screw speeds used.

Table 19: Parameters for single run of second extrusion in mini extruder.

Screw Speed (RPM)	Die (ºC)	Zone 3 (ºC)	Zone 2 (ºC)	Zone 1 (ºC)	Fan Speed
3.5	200	200	200	200	40%

The resulting filament was evaluated using the same method as for the previous extrusion experimentation.

4.3.6 Post-Extrusion Characterisation (rPP, vPP)

The characterisation of the filaments follows the same process an in section 4.3.3. After pelletization of rPP(CMP) and vPP(3DP) filaments several analyses are performed. Pellets from rPP with and without separation process are compared qualitatively by picture. Afterwards, MFR determination, FTIR and TGA are carried out with the same parameters as described in section 4.3.3. For filaments with reasonable quality, diameter control charts (length vs diameter) are plotted with measurements taken every 10 cm using a digital calliper. Moreover, attempts to print a benchy are performed with either or both materials.

4.3.7 Mechanical Testing (rPP, vPP)

This subsection is divided in 2 parts: first, producing tensile test specimens with rPP and vPP in hot press; second, performing the tensile testing with the specimens and analyse results in the Mechanical Technology Laboratory.

The filaments were pelletized in order to obtain small sized pellets. No processing parameters or method were initially available for the production of test specimens in hot press. As such, the process was optimized by trial and error until acceptable results were obtained. The following equipment were extensively used: measurement beakers, steel matrix mould, demoulding agent, blower, air gun and spatula. Matrix mould is used to produce type IV test specimens in accordance with ASTM D638. Several parameters were varied in order to obtain better results: hot press temperature and pressure, time in hot press, cooling time, number of moulds filled with pellets in the steel matrix, amount of demoulding agent (spray), time until starting to remove moulds, amount of PP pellets used (excess vs quantity to just fill gaps). Each of these parameters was found to have a considerable impact on the final results. The best test specimens were obtained using a 2-staged process at fixed temperature of 180-185ºC and varying pressure: first placing the mould at a pressure of 4 metric tons (constantly) and afterwards increase up to 6-8 metric tons. Finally, cooling was done using compressed air-gun.

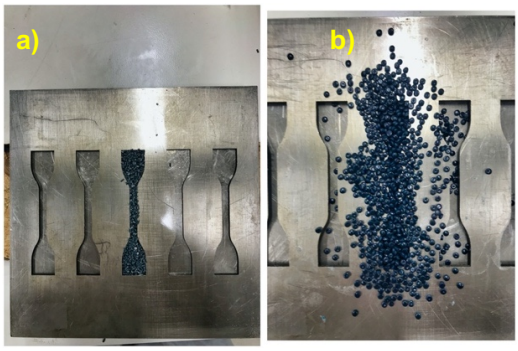

Figure 16: On the left (a) matrix mould with one groove filled with pellets before process was optimized for the material; on the right (b) matrix mould with one groove filled with pellets in excess around the groove profile after process was optimized for material.

In Figure 16 it is shown on the left how the test specimens were first being made (a). On the right the final method of filling the matrix mould is presented (b). Five and three specimens were produced with rPP and vPP, respectively. The latter were much more difficult to obtain due to the material properties. In section 5 the results before and after optimization are shown and discussed.

Mechanical tests were performed following the ASTM D638-14 standard – Standard Test Method for Tensile Properties of Plastics (ASTM D638 2015).The second part starts with measuring each specimen's relevant dimensions to obtain the cross-sectional area. Measures were taken from 3 different regions of each specimen in order to obtain an average value. For width and depth, a calliper (Mahr Type 16ER) and micrometre (Insize Digital Spherical Anil Tube Micrometre) were used. Tests were performed in the Mechanical Technology Lab. Pictures were taken during mechanical tests to visually register the behaviour of the specimens under load. Results were exported in csv format and analysed in excel. The stress-strain tests were performed with a grip displacement speed of 5 mm/min. Digital image correlation (DIC) was used as the extensometer. The output parameters used for analysis were Time (s), Extension (mm) and Load (N). Only engineering stress and strain are considered. The relevant equations for the determination of stress and strain are provided below. The stress is given by

$$\sigma = \frac{P}{A_0} \tag{3}$$

Where σ is the stress (MPa), P is the load (N) and A0 is the initial cross section area (mm^{-2}). The strain is determined with the equation

$$\varepsilon = \frac{L - L_0}{L_0} = \frac{\delta}{L_0} \tag{4}$$

Where ε is the strain (no dimension), L_0 is the initial test length (mm), L is the current length (mm) and δ is the displacement (mm). The yield strength σ_y is determined by visual inspection and by the 0.2% offset method. In order to determine Young's modulus (or modulus of elasticity) *E* (GPa) Hooke's Law was used:

$$\sigma = E\varepsilon \tag{5}$$

The modulus of elasticity is determined by finding the linear region of the stress-strain curve and doing a linear regression on that set of points. Several sets are tested for the selection of the best-fit interval.

The criteria comprise the statistical parameters R^2, P-value and significance-F. For curves that are not linear in the initial portion the appropriate toe compensation is employed following ASTM D638. From the linear regression, only the slope of the equation is used. The excel package *Data Analysis* was used for such. The moduli of resilience (U_r, MJm^{-3}) and toughness (U_t, MJm^{-3}) are determined by numerical integration and their formula is given by

$$U_r = \int_0^{\varepsilon_y} \sigma \, d\varepsilon \tag{6}$$

$$U_t = \int_0^{\varepsilon_f} \sigma \, d\varepsilon \tag{7}$$

Where the modulus of resilience corresponds to the area of the stress-strain curve from the origin to the yield point and the modulus of toughness corresponds to the entire area of the curve (up to the fracture). The numerical integrations were performed in QtiPlot.

4.3.8 Changes to Initial Methodology

Given the pandemic context and the resulting constraints several changes had to be made regarding the initially planned research boundaries and methodology. Other circumstances also contributed for this. Some experimentations were not possible to carry out due to the inability to obtain more rPP material from the company (Lipor). This coupled with the fact that only the double screw extruder was available (the single-screw extruder which was the main equipment to be used initially was not functioning), the material was consumed faster than expected and a couple experiments were therefore eliminated. These included the following: doing a second and third complete cycle of extrusion after obtaining the optimal parameters, testing different cooling methods as independent variable (a panel of blowers and water bath with proper equipment) and visiting the supplier company to better understand the upstream processes. A small experimentation for second cycle extrusion was performed in the 3Devo mini extruder. Moreover, it was not possible to receive training for FTIR and TGA analyses due to the limiting number of people allowed in each room. As such, the methodology became more limited than initially planned. The study of the cooling methods was central to the initial objectives. Two water bath apparatus were tested. The first did not work correctly and the second was validated upon testing. The first apparatus was comprised of a long and thin water tank coupled with a heater with recirculating capabilities with the water flowing in a closed loop (Figure 17a).

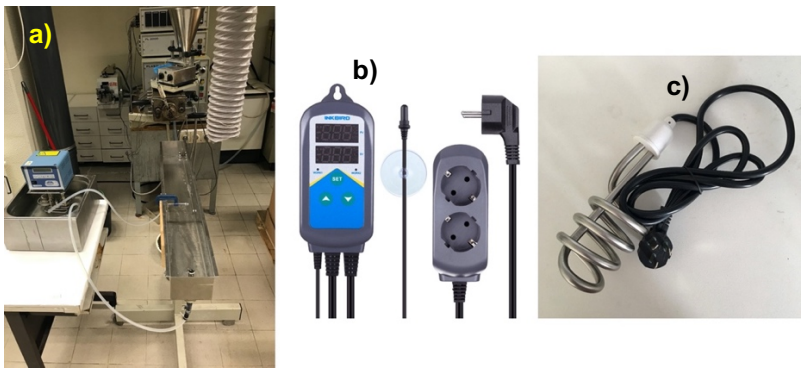

Figure 17: First water bath apparatus (a). Inkbird temperature controller (b) and heating element (c) of second water apparatus.

The second apparatus tested was made with the same water tank but without water circulation: the tank was filled with water and an Inkbird water-proof temperature controller with probe was connected to heating elements placed along the tank (Figure 17b, 17c). Gel permeation chromatography (GPC) was also in the initial planning but it was verified that for polypropylene the available equipment was not appropriate (PP requires high temperatures and stronger solvents to dissolve, only high-temperature chromatographer would allow it – HT-GPC). A *Do-it-Yourself* (DIY) tool for automated diameter measurement was built according to instructions found online using 3D printing, electronics and Arduino programmed with C language (EN 2020). Some parts were adapted to accommodate for the filament variations. Due to high diameter variability the device was barely used. Tool pictures are included in Annex D.

5 - Results and Discussion

5.1 – Overview

In this section the results are presented along with its discussion for better readability. Each subsection follows the same numbering as the methodology section for ease of reference. Only the more relevant data from experimentation is shown.

5.2 – Pre-Extrusion Separation and Drying

The rPP flakes were received as shown in Figure 14A of section 4. The mixture was provided as being polypropylene. It is observable that the material is extremely heterogenous. It is possible that after the processing, the resulting material is composed by various different polymers, or/and different formulations. As such, the composition of rPP(bulk) is assumed unknown. The density of PP is approximately 0.90 $g.cm^{-3}$. The density of water at 25 ºC and 1 atm is 0.997 $g.cm^{-3}$. The difference in density was used as a simple method of separation. Upon placing the flakes in water, the separation was relatively fast. An example is shown in Figure 20.

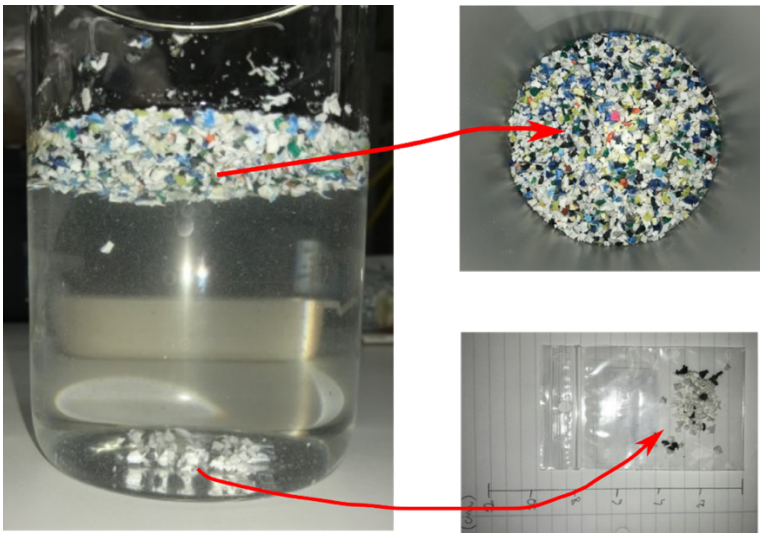

Figure 20: Separation of rPP(bulk) flakes in water. First batch of rPP(mix) flakes after separation and drying. The high heterogeneity of the material is noteworthy.

For all separations there were white and black flakes deposited at the bottom, thus, with higher density. The majority were white flakes indistinguishable from the white flakes with lower density. The hypotheses regarding the mixture composition was the following:

- Lower density flakes: PE (LDPE, LLDPE, HDPE), PP (possibly with low-molecular weight additives in the formulations)
- Higher density flakes: PP (copolymers or/and formulated with additives/fillers, e.g. titanium dioxide, talc, carbon black, etc.), ABS, PET

The typical density values for these polymers is presented in Table 20 in ascending order, however it should be noted that the received flakes, rPP(bulk) resulted from varied polymeric formulations.

Table 20: Typical density values of polymers that might be present in the mixture (data from Harper 2002, p7).

Polymer	**Density ($g.cm^{-3}$)**
PP	0.90
LDPE	0.92
HDPE	0.95
Water (25ºC, 1 atm)	0.997
ABS	1.18
PVC	1.40

The drying was always performed at 60 ºC. The target value for the moisture content was established as being at most 0.20% although no reference was found specifying the best interval for extrusion. In Table 21 the percentage weight variation is shown along with the average value of moisture content after measuring in thermal scale. The total weight variation (Δm Total) refers to the difference between weight before drying and immediately after drying in oven. The cooling weight variation (Δm Cooling, %) refers to the difference between weight immediately after taking flakes from oven and weight after cooling to room temperature (approximately 45-50 minutes after). Moreover, the average percentage

moisture content (based on 3 trial runs) and the corresponding standard deviation for each batch is also shown.

Table 21: Drying parameters, weight variations and average moisture content of each batch of material dried in oven.

Batch	**Drying Time t(i) (hh)**	**∆m Total (%)**	**∆m Cooling (%)**	**Avg Moisture (%)**	**Stdev Moisture (%)**
S1	18.50	4.87	N.A	0.28	0.03
S2	63.50	25.31	0.16	N.A	N.A
S3	21	7.72	-0.01	0.18	0.07
S4	43.37	7.13	0.00	0.16	0.05
S5	24	8.84	0.00	0.17	0.04
S6	24	9.48	-0.01	0.17	0.04
S7	24	5.21	-0.02	0.12	0.09

The target moisture content was achieved with drying time of at least 21h. For batches S1-S2 a glass beaker was used instead of a large tray. The S1 batch underwent 18.50h of drying and presented a higher moisture content. This could be due to using a glass beaker instead of the larger glass tray that was used for the remaining batches. The difference in moisture content from the later established 24h drying interval to the maximum value used (43.37h) is negligible for the quantities used (0.12%-0.17% vs 0.16%). Regarding weight variation after taking the sample from the oven and cooling until room temperature, the only noticeable difference occurred with S2. The remaining batches S3-S7 had either zero change or at most a 0.02% decrease in weight when cooling from 60ºC to room temperature. The weight variation during cooling is shown for batches S2-S7. The weight remains mostly constant with negligible changes. This confirms the material is not prone to absorb moisture. In fact, this is a characteristic of PP. However, given that the exact composition of rPP(mix) is unknown, the negligible moisture absorption hypothesis was tested and confirmed. Moreover, according to literature PP does not require drying prior to extrusion since it does not absorb moisture (Giles, Wagner, and Mount 2014, 263). The low water absorption can be explained by the nonpolar nature of polymer PP (Harper 2002, 53).

5.3 – Pre-Extrusion Characterisation

The pre-extrusion characterisation is composed of two blocks: the manual separation of flakes by colour and the characterisation processes. Moreover, the characterisation processes include the following:

1. MFR determination – rPP(mix) material
2. Optical microscopy – all flake types (flake[i])
3. FTIR-ATR – flake types of higher quantity (10 colour flakes)
4. TGA – flakes of same colour but with different behaviour upon separation

For manual separation a large sample was chosen after agitating the container in which the batch was stored. Afterwards 17 different flakes were found and labelled from the rPP(mix) sample. Two Flakes excluded during separation were also labelled with UNK (unknown) and their colour and pitch. Thus, a total number of 19 flakes were identified. Table 22 includes all flakes and their colour code (colour + approximate colour pitch). The same code scheme is used for FTIR-ATR and optical microscopy.

Table 22: Colour codes of all identified flakes in the rPP(mix) sample as well as the flakes that remained after separation (#18 and #19).

#	Code	Colour	Colour Pitch	#	Code	Colour	Colour Pitch
1	BL1	BLUE 1	LIGHT	11	GR1	GREY 1	LIGHT
2	BL2	BLUE 2	MID	12	GR2	GREY 2	MID
3	BL3	BLUE 3	DARK	13	GR3	GREY 3	DARK
4	G0	GREEN 0	BRIGHT	14	B1	BLACK 1	-
5	G1	GREEN 1	LIGHT	15	Y1	YELLOW 1	LIGHT
6	G2	GREEN 2	MID	16	R	RED	-
7	G3	GREEN 3	DARK	17	MG	MAGENTA	-
8	W1	WHITE 1	LIGHT	18	UNKW1	WHITE 1	LIGHT
9	W2	WHITE 2	BEIGE	19	UNKB	BLACK 1	-
10	W3	WHITE 3	DARK				

The results of MFR tests are presented in Table 23 below. Results with modified test parameters (200ºC, 2.16 Kg – N = 48 test runs) and a small sample with standard parameters (230ºC, 2.16 Kg – N = 8 test runs) are shown. The latter were included only to test the difference in MFR values when using the recommended parameters from ASTM D1238 standard. In literature, most the MFR tests found used standard parameters. Moreover, for the modified parameters 2 values were excluded since they had Z > 2. Average and standard deviation are included as well as the MFR control interval (which is used for graphing purposes). The interval is given by

$$MFR\ Control = [Average - Stdev, Average + Stdev] \quad (8)$$

Table 23: Melt flow rate tests results for rPP(mix) at 200ºC and 230ºC with 2.16 Kg standard weight using ASTM D1238.

N	Threshold (Z Score)	Excl.	T (ºC)	Avg (g/10min)	Stdev (g/10min)	Stdev/Avg (%)	MFR Interval
48	2	2	200	11.58	1.94	16.8	[9.64, 13.52]
48	1	15	200	11.71	1.31	11.2	[10.41, 13.02]
8	N.A	0	230	20.54	4.42	21.5	[16.12, 24.96]

The distribution of values across the sample for the modified parameters is shown in Figure 18 below. The control interval is included (red lines; blue line for average value):

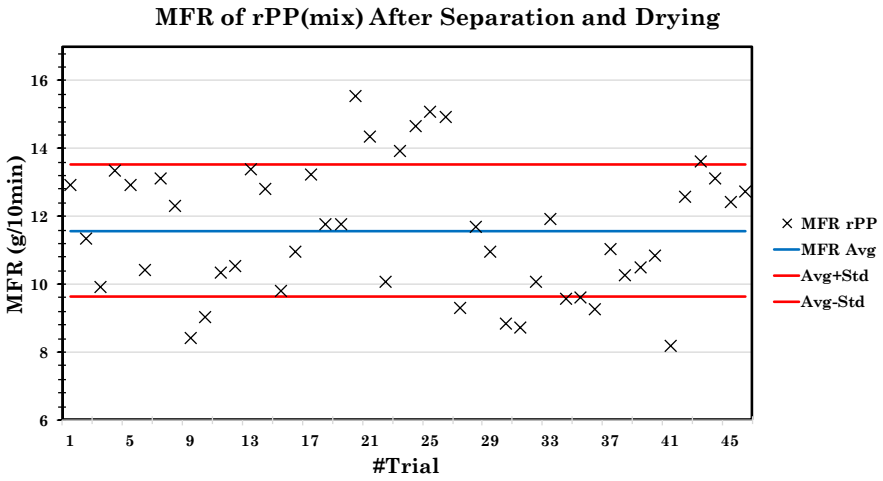

Figure 18: Control chart for MFR of rPP(mix) using modified parameters for 46 trial run.

Specific optimal values of MFR for extrusion and injection moulding were not found (particularly, two polymers with the same MFR value can have very different extrusion behaviour). However, it is common assumption that for extrusion low MFR values are more appropriate whereas for injection moulding higher values are preferable (because a lower melt viscosity allows a better flow through the runners and a better filling of the mould). On the website of Exxon Mobile Chemical, one of the biggest producers of polymers (Exxon Mobile Chemical 2021), an extensive list of polypropylene polymer products is available with data sheets. Of all listed products, only the polymers with MFR in the interval 1.8 to 5.5 g/10min are categorized for extrusion processing. From that value onwards, all products' data sheets attribute mostly injection moulding for processing method. Based on table 23 rPP(mix) melt behaviour seems to be relatively sensitive to temperature (MFR 11.58 vs 20.54 with 200ºC and 230ºC, respectively). The melt flow rate is characteristic of injection mould PP grades. As such, the rPP tested could be originated from a mixture of items mostly produced by injection moulding. In this case, reprocessing in extrusion might not provide the best results without appropriate conditions (fillers and water cooling). In the graph from Figure 18 it can be seen that the process of MFR determination is not under control given that 24 test run values fall outside of the control interval. This could be explained by the fact that the process is entirely manual and the polymer has a relatively high fluidity. However, if much longer time intervals were used maybe this issue could have been somewhat mitigated.

FTIR spectroscopy allows to obtain information regarding the presence of certain functional groups in a sample. By irradiating it with infrared light certain chemical bonds will vibrate to specific wavelengths. These changes in vibration are detected and translated from an interferogram to spectrum by Fourier series. The FTIR spectra obtained span across the range 4000 - 400 cm^{-1}. The most important region is located across 4000 – 1500 cm^{-1} since most bond stretching frequencies appear here. The region 400 – 1500 cm^{-1} is often called the fingerprint region and provides finer details on the material. Usually it is much more complex and includes more bands, sometimes overlapping. Thus it is more difficult to analyse reliably (Cortes 2010). Given the number and complexity of the flakes' spectra, FTIR device supplier extensive databases were used to match the curves to specific components. For such, the lab device software provides a table with a default number of best matches and a search score with scale 0 – 1 for each spectrum provided.

Table 24: FTIR spectra 3 best matches of flakes Blue 2, Blue 3 and Green 1 using PerkinElmer lab software and available spectra databases.

#	Colour	Search List	Search Score	Search Reference Spectrum Description
2	BLUE 2	1	0.9229	(PP) White bottle cap outside surface (top)
		2	0.9128	Polypropylene Isotactic
		3	0.9126	Polypropylene Isotactic
3	BLUE 3	1	0.9679	BBP24-1, PROF, IRS, BACK
		2	0.9615	BBP33-2, CORO KH500, IRS, BACK
		3	0.9593	BBP33-4, CORO 1056PE, IRS, BACK
		4	0.9508	Polyethylene High Density
5	GREEN 1	1	0.9223	(PP) White bottle cap outside surface (top)
		2	0.9169	Polypropylene Isotactic
		3	0.9137	N.A

Table 25: FTIR spectra 3 best matches of flakes Green 2, White 1 and White 2 using PerkinElmer lab software and available spectra databases.

#	Colour	Search List	Search Score	Search Reference Spectrum Description
6	GREEN 2	1	0.9009	N.A
		2	0.8965	Terpolymer EPDM polysar EPDM 585
		3	0.8963	Poly(1-Butene) Isotactic
8	WHITE 1	1	0.9016	(PP) White bottle cap outside surface (top)
		2	0.8990	Polypropylene Isotactic
		3	0.8802	Polypropylene Isotactic
9	WHITE 2	1	0.9071	N.A
		2	0.9050	(PP) White bottle cap outside surface (top)
		3	0.8953	Polypropylene Isotactic

Table 26: FTIR spectra 3 best matches of flakes Grey 1, Black 1, Yellow 1 and Unknown White using PerkinElmer lab software and available spectra databases.

#	Colour	Search List	Search Score	Search Reference Spectrum Description
11	GREY 1	1	0.8900	Terpolymer EPDM polysar EPDM 585
		2	0.8848	N.A
		3	0.8829	Poly(1-Butene) Isotactic
14	BLACK 1	1	0.8051	Calcium Carbonate
		2	0.8044	Polyethylene, Oxidized Acid Number 15 mg
		3	0.7951	Polyamide Resin Melting PT 95DEG C
15	YELLOW 1	1	0.9877	Polyethylene High Density
		2	0.9767	Polyethylene High Density

		3	0.9727	Polyethylene, Oxidized Acid Number 15 mg KOH/G
18	UNK WHITE	1	0.8983	Polypropylene Isotactic
		2	0.8976	(Polypropylene) White bottle cap outside surface (top)
		3	0.8757	Polypropylene Isotactic

Under the assumption that search scores > 0.90 would provide a relatively robust material match several conclusions can be derived from tables 24-26. The following flakes can be assumed to be polypropylene (varying colours can be explained by the use of pigments): Blue 2, Green 1, White 1, White 2 and Unknown White. Blue 3 flake has high search scores but the matching materials are trade names and not immediately recognised. Scores for the top four matches (an extra was included since it corresponds to one of the initial hypotheses – HDPE) are very similar in the range 0.95-0.97. The first results include at least 2 categories of materials: BBPxx and CORO. Upon looking for combinations of these reference descriptions on internet searches a few possible products came up. The acronym BBP might refer to professional label printers from Brady company that use high-performance labels and signs for industrial use (BRADY 2021). The labels are made of materials such as PP, HDPE, vinyl, polyamide, among others. The acronym CORO most probably refers to the Coroplast brand of corrosion protection tapes. According to the company's data sheets the KH500 and 1056PE tapes are commonly used together for double-tape system solutions. They are based on PE and include synthetic rubber (Coroplast(1) 2021, Coroplast(2) 2021). As such, it can be assumed that Blue 3 and Yellow 1 (due to high score) are both PE (possibly HDPE). The remaining flakes are Black 1, Grey 1 and Green 2. The first has a low search score but could be a mixture of PE and calcium carbonate (a commonly used additive with polyolefins PE and PP). Grey 1 and Green 2 have high scores and according to the search reference spectrum database they are similar in composition. The flakes may include EPDM (ethylene propylene diene monomer – synthetic rubber) and poly(1-butene) which are frequently added to PE and PP in order to obtain specific material characteristics. All in all, from the 10 flakes analysed the composition could be approximately summarised as follows in Table 27:

Table 27: Summary of flakes analysis by FTIR and spectra database reference.

Material	Percentage of Flakes	Composition	Flakes
PP N=5	50%	Polypropylene (Isotatic)	Blue2, Green1, White1, White2, UnkW
PE N=2	20%	Polyethylene	Blue3, Yellow1
Mixture N=3	30%	Polyethylene and Calcium Carbonate	Black1
		EPDM and Poly(1-Butene)	Grey1, Green2

Even though some flakes had higher density and were deposited in the bottom of the beakers they were identified as also being polypropylene. However, they might have a higher percentage of specific additives or fillers with bigger contribution to density. The two identified types of flakes that were

deposited at the bottom of the beaker could have traces of additives such as the following: talc, titanium dioxide, carbon black, cobalt blue among others. Plastic additives can be categorised (PolymerDatabase 2021) in the following way: (1) plasticizers (flexibility and durability improvement, e.g. phthalatic and benzoic acids), (2) impact modifiers (improvement of shock absorption capabilities, e.g. EPDM and other elastomers; the former was identified in the FTIR matching database), (3) lubricants (reduction of friction during processing, better processability, e.g. fatty acids, EVA waxes, silicones and oxidised PE), (4) fillers (one of the most important class of additives and mostly inorganic components that include calcium carbonate, talc, silica, carbon black among others), (5) flame retardants (to control flammability of polymers, can either be organic or inorganic compounds), (6) antioxidants (aiming to increase resistance to degradation of polymers, e.g. phenols and hindered amine light stabilizers), (7) thickeners (provide the desirable viscosity to the material, e.g. polymers that have hydrophilic groups) and (8) tackifier resins (usually low molecular weight additives for mobility enhancement and promote adhesion, e.g. hydrocarbon resins and rosin esters). From these additives described the following were clearly identified on the matching list using PerkinElmer software: EPDM (impact modifier) and calcium carbonate (fillers). There is strong evidence for the presence of talc and carbon black on the higher density flakes. In some cases, the additive's content is usually so low that it is hardly detected by FTIR spectroscopy. Figure 19 shows the stacked plots of all spectra of the analysed flakes. The data from the graph was the same data used in the FTIR equipment database matching software.

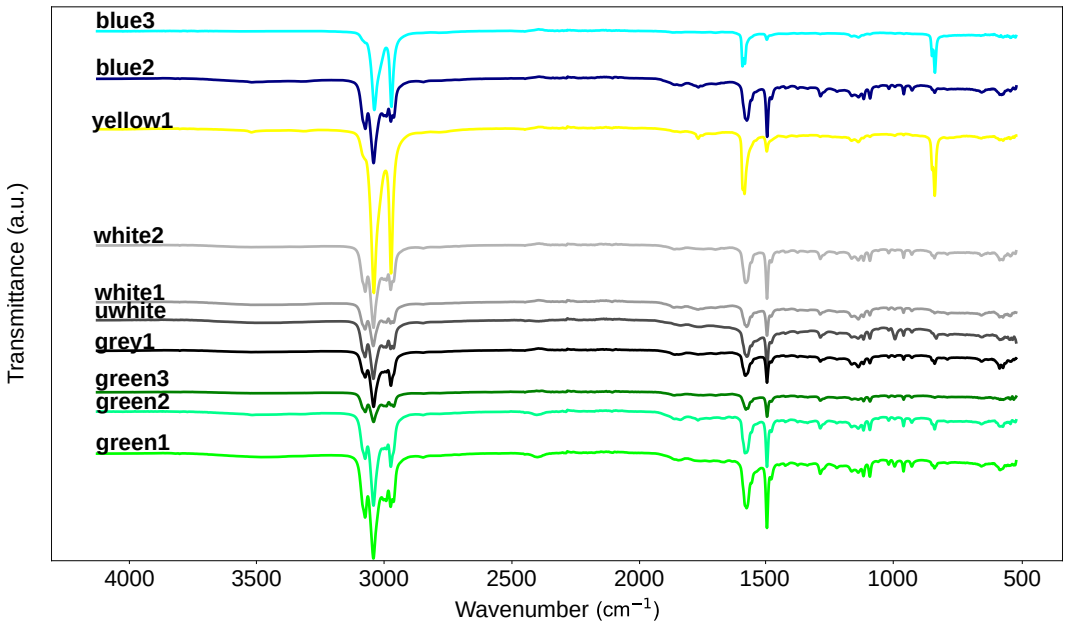

Figure 19: FTIR spectra of all tested flake samples, stacked, with custom offset to avoid overlapping.

It is important to note that when FTIR is performed using ATR the IR beam is reflected on the surface of the sample and as such only a few micrometres of material depth are analysed. It is not necessarily IR data of the major or entire component of a given flake. As such, the method analyses unspecified areas of the sample. Precise information could be obtainable using Micro-FTIR which allows to do a complete IR mapping of the entire area of the sample, analysing distinct regions. Thus, the FTIR-ATR method can cause some spectrum data to relate to surface impurities or melted impurities on the surface level. This was found in the microscopy analysis that is presented further on. Moreover, it is important

to emphasize that each coloured flake is not necessarily representative of other flakes that present the same colour and aspect.

To better understand the difference between lower and higher density flakes (floating vs depositing at the bottom) thermogravimetric analysis was performed for White 1 and Unknown White flakes. In Figure 20 the residual weight percentage (%) and first derivate of residual weight (%/min) curves are shown for the samples. The final residual mass values and maximum degradation rate points are labeled in the thermograms.

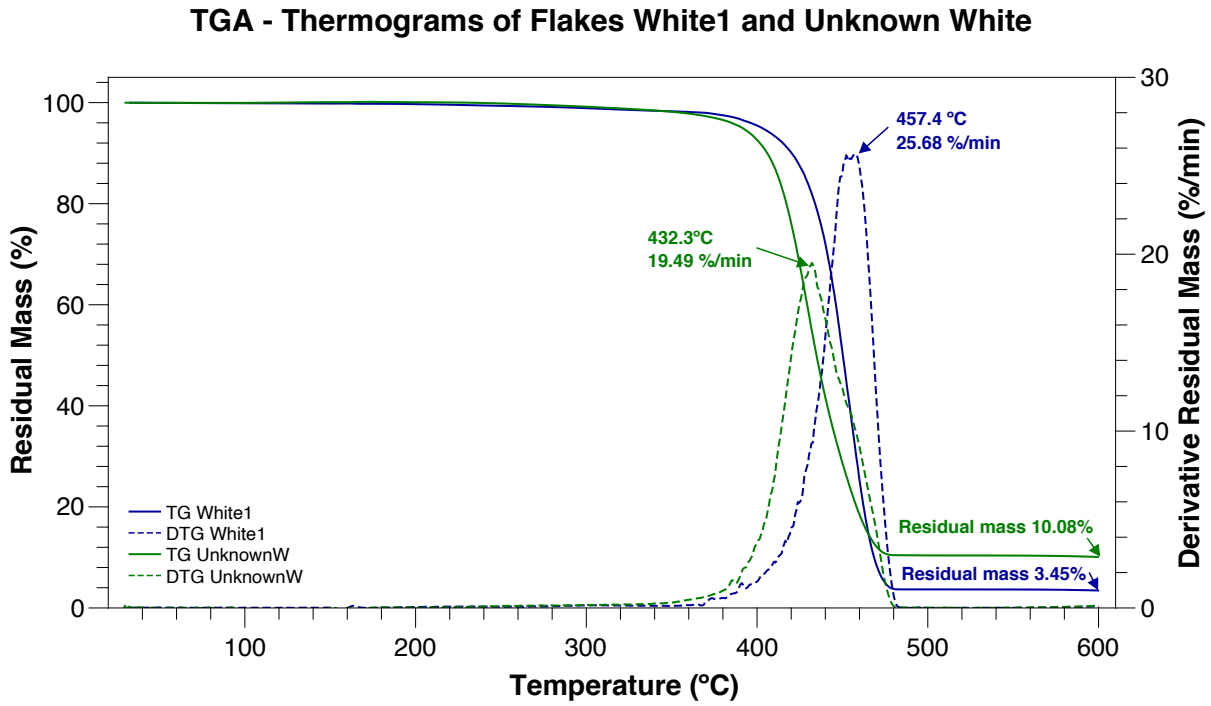

Figure 20: TGA graph of flakes White1 and Unknown White. Full lines represent residual mass (TG - thermogram) and dashed lines represent derivative residual mass (derivative thermogram – DTG).

The global maximum of the first derivative of residual mass (differential thermogram – DTG) represents the moment of highest degradation rate due to heating in the device chamber. From Figure 20 it can be seen that White1 has slightly higher degradation until approximately 250ºC. However, around 360ºC UnkW starts losing more weight at faster rate. The degradation temperature of White1 (maximum value of first derivative) is 457.4ºC with a maximum rate of degradation of 25.68%/min. The degradation temperature of UnknownWhite is 432.3ºC with a maximum rate of degradation of 19.49%/min. The peak of degradation occurs earlier (at a lower temperature) for UnkW but at a lower rate when compared to White 1 flake. The most notable difference, however, is the final residual mass of each flake. Flake UnkW is denser (would sink in water) and it could possibly be due to the presence of much higher quantity of fillers and additives. Given that at 600ºC the residual mass of UnkW is 10% this shows that the flake has a high composition of inorganic material (mixed with char from the degradation). The flake White1 had a final residual mass of 3.45%, almost 3 times lower. Thus, UnkW main difference might either be in the inorganic content or polymer composition. The derivative curve of flake White1 shows two local maxima points that show two extremely close steps of degradation. For White1 flake the rate of degradation increases past 1%/min at 370ºC where residual mass is 97.97% (a

weight loss of 2.03%) and degradation ends approximately at 479ºC at a residual weight of 3.93%. For flake UnkW degradation starts approximately at 380ºC at a residual weight of 97.35% (a weight loss of 2.65%). The flake only shows 1 step of degradation by looking at residual weight curve and first derivative of residual weight. The degradation finishes at approximately 476ºC with a residual mass of 10.75%.

Optical Microscopy was performed to all flake colours including the previously separated flake labeled as unknown white (for consistency it will continue to have the same label although it likely consists of PP with large percentage of fillers and additives). Based on the images captured with the digital sensor on the two-way microscope three categories were then devised based on the visual characteristics: (1) homogeneous material, rough surface and very clean or few specks of impurities at surface level; (2) homogeneous material, smooth surface and few to many impurities' specks or stains/smudges at surface level; (3) heterogeneous material (bonded/melted mixtures but clearly identifiable). Table 28 below shows a summary of the categories, flakes and known compositions from the previous FTIR analysis.

Table 28: Overview of the optical microscopy analysis – categorisation of flakes according to major characteristics and comparison with known compositions.

Category	Characteristics	Flakes	Compositions
1	Homogeneous, rough surface, clean or few impurities	Blue2	PP
		Green2	EPDM & Poly(1-Butene)
		Black1	PE & Calcium Carbonate
		Green0, Red	Unknown
2	Homogeneous, smooth surface, few to many impurities	Green1, UnkW, White1	PP
		Blue3, Yellow1	PE
		Grey1	EPDM & Poly(1-Butene)
		Blue1, Grey2, Magenta	Unknown
3	Heterogeneous (bonded/melted mixtures)	White2	PP
		Green3, Grey3, White3	Unknown

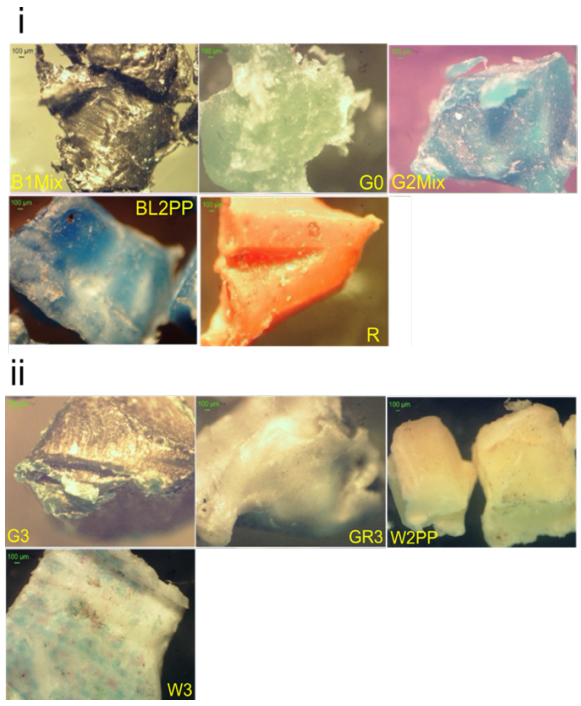

Figure 21: Optical microscopy of flakes. (i) Category 1 flakes: Black1, Green0, Green2, Blue2 and Red; (ii) Category 3 flakes: Green3, Grey3, White2 and White3

Figure 22: Optical microscopy of flakes, category 2 flakes: Flakes Blue1, Green1, Grey1, Grey2, Magenta, Yellow1, Blue3, Unknown White and White1.

In Figure 21i category 1 of flakes is shown. Flakes belonging to this category include Black1, Green0, Green2, Blue2 and Red. They all present very similar characteristics: they all appear to be homogeneous on the outside and have a relatively rough surface but none or small visible impurities, specks or smudges on the surface. Figure 22 shows the flakes belonging to category 2. It includes flakes Blue1, Green1, Grey1, Grey2, Magenta, Yellow1, Blue3, UnknownWhite and White1. Common characteristics are material homogeneity, relatively smooth surface and having few to many specks or stains of impurities. Lastly, Figure 21ii, category 3 comprises flakes Green3, Grey3, White2 and White3. Material heterogeneity is the common characteristic among them. Green3 appears to be a mixture of 2 materials melted together but with easily identifiable borders and no impurities are visible at surface level. Grey3 presents some small blisters ingrained or melted in the flake although difficult to identify. It also shows impurities over the surface. White2 shows small regions less homogeneous and several

specks scattered and smudges over the surface. Finally, flake White3 is the least homogeneous material. It shows 3 different colours of materials melted together or at least superficially: white, blue and pink regions (not necessarily the real colours given that the microscope light causes the perceived colours to differ from those visible with naked eye). It should be noted that the optical microscopy analysis performed only accounts for an extremely limited sample. From the entire batch of material received from LIPOR facilities other colours could exist. Moreover, seemingly identical flakes could be quite different upon inspecting with optical magnification. A flake with a given colour does not necessarily match other flakes of same colour in terms of composition and properties (as well as FTIR, microscopy, degradation behaviour on TGA, filler and additives, etc).

5.4 – Extrusion Processing

Initial experiments were performed in order to gain sensitivity to the material characteristics and to the twin-screw extruder. A base temperature level with 10ºC variations on different barrel zones were used. According to the colour scheme established in the methodology the results are presented in Table 29 below. Material batches S3 and S4 were used.

Table 29: Extrusion parameters and results (colour code) from initial and main extrusion plan.

Filament Code	Screw (RPM)	Die (ºC)	Zone3 (ºC)	Zone2 (ºC)	Zone1 (ºC)	Belt Speed (a.u.)
A1	15	200	200	190	170	-
A2	15	210	210	200	170	-
A3	15	210	210	200	170	-
A4	15	210	220	210	170	-
A5	15	220	220	210	170	-
A6	20	220	220	210	170	-
B1	10	200	200	190	170	20-30
B2	10	210	210	200	180	20-35
B3	10	220	220	210	190	30-35
B4	10	230	230	220	200	25-35
B5	10	240	240	230	210	25-35
C1	20	200	200	190	170	30-45
D1	15	200	200	190	170	-
D2	15	210	210	200	180	-
D3	15	220	220	210	190	-
D4	15	230	230	220	200	-
D5	15	240	240	230	210	-
D1_2	15	200	200	190	170	30
X1	15	170-180	200	190	170	35

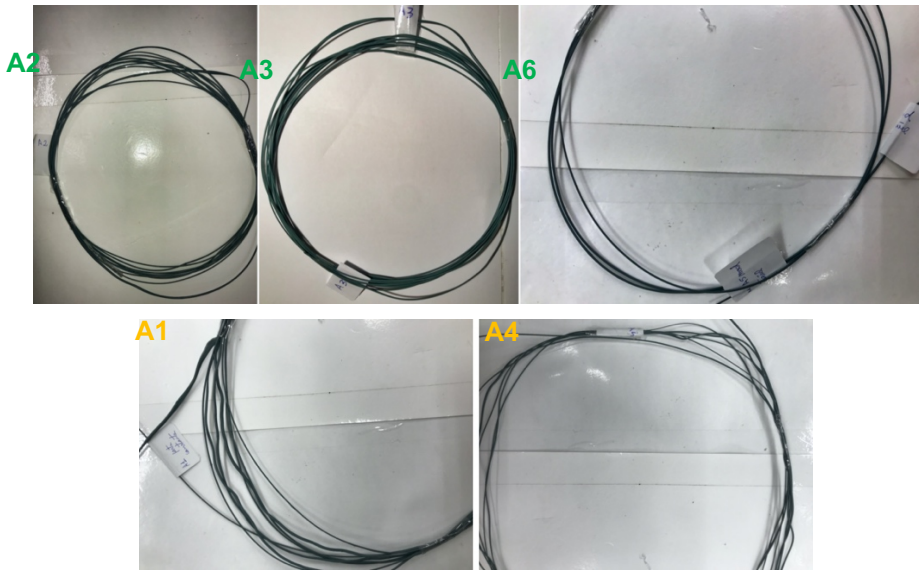

Figure 23: Filament samples from initial experimentation. Colour indicates overall quality.

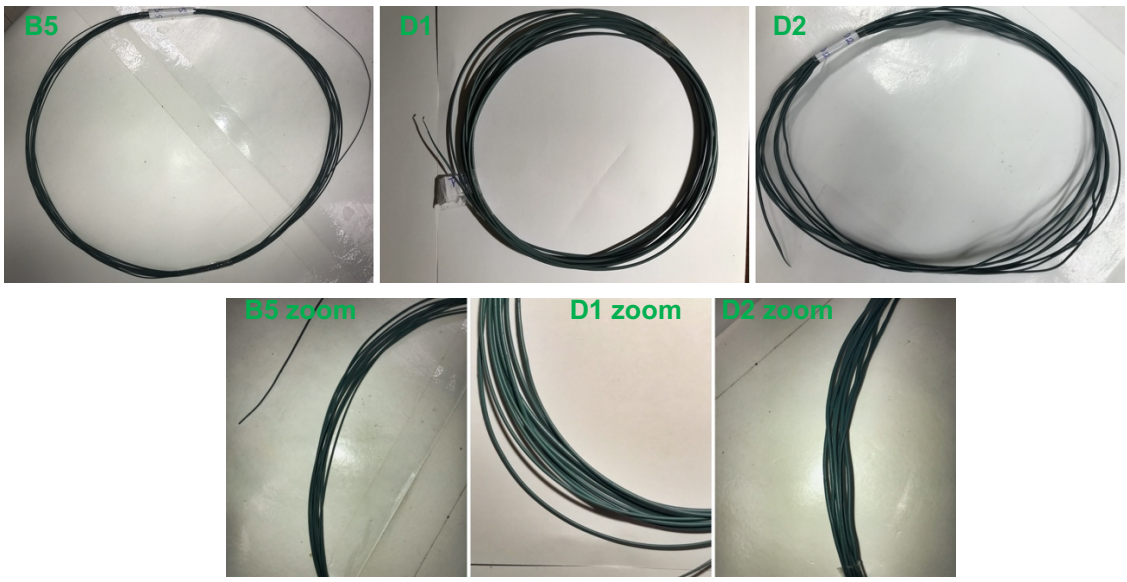

Figure 24: Filament samples of the best results obtained from main extrusion plan (overall view and zoom).

i

ii

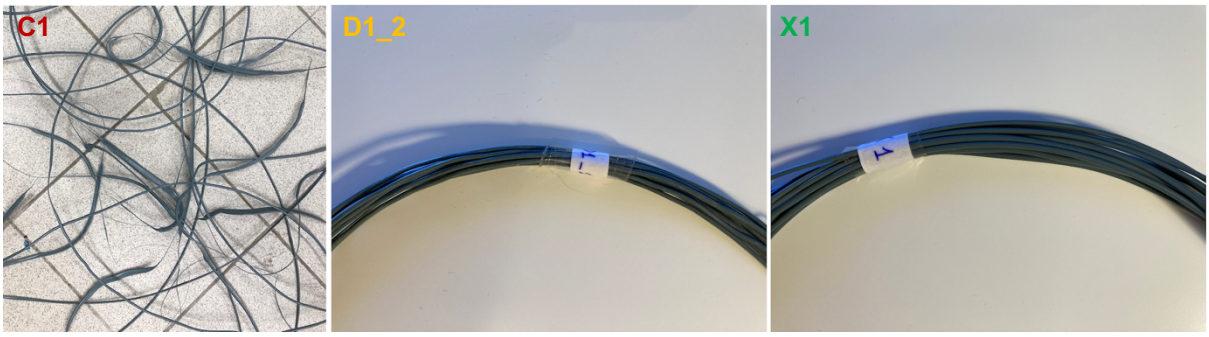

Figure 25: (i) Filament samples of poor (B1, B3, B5) results obtained from main extrusion plan. (ii) Sample of unfeasible (C1) result from main plan and samples from last extrusion attempt using D1 parameter (sample D1_2, poor) and X1 parameter tested by chance (good quality).

The green colour stands for satisfactory or good quality. A filament is obtained with good surface quality and no entanglements or twists. However, it can include considerable diameter variations or small diameters well below the required 3D printers (1.75±0.05 mm depending on printer tubes, bearings, motor and extruder). Good quality label is not related to printability of said filament nor does it imply any possibility to do so. Yellow colour means a filament is obtained but it is of poor quality but still accepted as result. It can have bad surface texture, be more brittle, difficult to wind it on a spool, having twists and characterised by difficult handling. A priori, deemed impossible for printing. The red colour that will show on other trials means the result is unacceptable/unfeasible and could barely be labelled as a filament. Either shapeless or, in most cases, mostly flattened (caused by cylinder) due to the combination of temperature and screw speed used. One noteworthy issue that occurred throughout every extrusion trial run is that the die temperature was extremely difficult to control given that the temperature controller unit attributed to the die sensor was giving erroneous readings. A workaround was employed for such: an extra temperature sensor was attached to the die ring and connected to a separate temperature reader unit. However, given that the barrel heating elements work in closed loop with the temperature control unit this led to having the die temperature constantly oscillating. Moreover, given the placement of the extra sensor, it is not certain if the reading gave the precise value inside the die. The temperature used for adjustments was that of the extra temperature reader attached to the new sensor. Contrary to single-screw extruders, double-screw extruders' residential time is non-linear. Although the residential time was not determined nor profiled this is an important aspect regarding filament quality. According to Harper (Harper 2002, 44) the heating times for the polypropylene should be minimized in order to reduce the chances of occurring oxidation, one of the main forms of degradation of this polymer. Given that the feedstock used for the filaments includes a considerable amount of PE as well other factors must be considered. The increased heating times inside the extruder barrel causes

degradation of the polymers. However, the degradation mechanisms of PE and PP in such conditions is different. On oxidation PE undergoes cross-linking whereas PP goes through chain scission. PP has decreased degradation resistance when compared to PE due to having a tertiary carbon. As a consequence, hydrogen abstraction occurs more easily compared to PE. One way of mitigating this is to add antioxidants to PP, which are likely present on the samples tested but not identified by FTIR-ATR spectroscopy (Harper 2002, 53).

For the main extrusion plan, only a subset of the devised experimentation was possible to carry out. The material batches used were S3, S4, S5 and S6 (all mixed evenly). As seen in Table 29 all subsets with S>15 RPM were unfeasible regardless of the temperature subset values. Filament would exit with high throughput and would flatten on the conveyor belt when passing by the cylinder (even when placing the cylinder as far as possible in the conveyor rail). Higher rate of cooling would be required to compensate. Moreover, only room temperature was used as cooling method. When using a blower or fan the filament would torsion and deviate from straight path on the belt. Two water bath apparatus were tested albeit only the second was functional with extra equipment brought to the lab but more polymer would be required. However, according to limited literature, optimal conditions include screw speeds of 20-25, puller and winder to control filament tension and warm water bath at the die exit (Iunolainen 2017). Accordingly, such conditions were not possible to be used for filament production. Only the validation of the second water apparatus was possible to perform. This would allow the use of water bath at approximately 40-50ºC which would be ideal. Moreover, such method would better control the brittleness and crystallinity of the filament upon cooling to avoid high crystal growth resulting in fragility. This would have to be confirmed with (DSC) to compare the several cooling methods (different cooling methods testing was excluded due to limitations described in section 4.3.8).

Table 30: Exclusion of variable sets constrained by high screw speed due to bad quality of the filament.

Screw Speed (RPM)				Die (ºC)	Zone 3 (ºC)	Zone 2 (ºC)	Zone 1 (ºC)
25	20	15	10	200	200	190	170
25	20	15	10	210	210	200	180
25	20	15	10	220	220	210	190
25	20	15	10	230	230	220	200
25	20	15	10	240	240	230	210

Sample images of the excluded subsets are presented further on. Figure 20A above presents the overall quality of the results obtained in the main extrusion plan (first introduced in subsection 4.3.4 and Table 18). The set of parameters D2 provided unfeasible results (red) with RT but compressed air gun allowed (handled manually) to obtain good results (i.e. green overall quality). However, the process was extremely manual. Constant adaptations were required while also controlling temperature, throughput, feeding, belt, etc., manually. Thus, impractical without a fixation or custom-built apparatus for practicality and consistency. Only 2 results were considered good and acceptable regarding overall quality. These best results (green) were obtained with the following conditions:

- Min screw speed and max temperature gradient - $S(1) = 10, T(5) = \{240, 240, 230, 210\}$

- Midpoint screw speed and min temperature gradient - $S(2) = 15, T(1) = \{200, 200, 190, 170\}$

The experimentation with screw speed S=20 with minimum temperature gradient T(1) produced unacceptable results (C1). As such, no other combinations of parameters were used beyond that point as previously mentioned. Figure 23 shows samples A1-A6. Samples A1 and A4 are labelled as poor (yellow in table). As it can be observed both filaments are twisted, with considerably high diameter variations and very difficult to wind in a circular form. It can be seen that the A2, A3 and A6 samples show more homogeneity, good surface quality and easily winded while maintaining their shape without uneven filament tensions. Figure 24 shows samples of good filaments from the main extrusion plan (B5, D1, D2) with their respective closeups. By visual inspection it is clear that D1 is better overall. Both B5 and D1 show good surface quality and tension, good handling and winding and they maintain their shape easily. Moreover, they do not seem to be fragile and no twisting was identified. Occasional blobs of irregularly melted material can be found but this issue is much more common in the poor-quality samples. Modified D2 sample was considered good but overall worse than B5 and D1. Figure 25 shows samples from poor results (B1, B3, B4) and unfeasible results (C1). It can be seen that filaments produced with parameters B1, B3 and B4 have a lot of twists and surface tensions. They were difficult to wind and handle. It was not possible to stretch the filaments straight and would easily become tangled. Unfeasible sets were all similar to C1: flattened, irregular, non-homogeneous, fragile.

Curiously, one of the best results (preliminarily labelled the best result before diameter process control charting) was obtained by mere chance. The main extrusion plan consumed most of the material available and a small batch S07 remained after extensive MFR tests. So far none of the filament samples seemed apt for use in 3D printing. With the last batch of material further extrusion was performed with the best set of parameters previously identified (D1) in an attempt to achieve a printable filament. The resulting filament sample was labelled D1_2 (parameter D1, second batch a few weeks apart). Despite using the same conditions for D1, the results obtained this time were worse. Thus, it was labelled as poor (yellow code) as seen in Figure 25ii. It is important to note that throughout all experiments, even with fixed parameters, great variations on results were seen with the extruder. As such, constant manual adaptations had to be made and from time to time a good filament would suddenly turn into a poor result during extrusion. In the specific case of D1_2 the only differences were carrying out the experiment a few weeks apart from the previous ones and the material batch used. For the main extrusion plan the flakes used were a mixture from batches S3-S6 (average moisture content of each batch was 0.16% to 1.18%) while for D1_2 batch S7 was used (average moisture content 0.12%). As previously mentioned, the die temperature was extremely difficult to maintain constant. Very often it would sharply increase (producing fumes) or rapidly decrease to levels well below the minimum advised for processing. It remains unknown whether the added sensor was correctly placed given that the original sensor (connected to main temperature controller and circuit) was malfunctioning. By mere chance, the double-screw extruder was left unattended for a very short period of time during which the die temperature lowered significantly and stabilised between 170ºC - 180ºC. For die exit this is considerably low and more adequate for the feeding zone. The resulting filament showed very good results upon visual inspection. This stresses the need for careful, customised adaptation and tuning of the extrusion parameters (temperature profile, screw speed, etc.) when processing recycled polymers of unknown

sources. Using parameters achieved from the literature provides no guarantee of success. The set of parameters is labelled X1 and it is included in Figure 25ii. Screw speed and temperatures are the same as for D1 except the die and slightly higher belt speed. Filament sample obtained with D1 parameters is slightly worse than one previously analysed. Although the shadows on the images make it difficult to observe in higher detail it was possible to see zoomed in that D1_2 sample is worse (more twisting and worse surface quality) and that X1 sample shows good surface quality, tension, handling and apparently ductile enough. It should be noted that when the die temperature drops to around 175ºC the filament quality is improved but the extrudate flow has constant interruptions and instability. Thereby, only some sections were good. With the die at 200 - 210ºC the extrudate has slightly lower quality but the throughput rate is more stable. Given the instability on the die temperature it was also possible to observe that around 210ºC and above the material has surface tension and starts to become twisted and does not remain in linear trajectory on the conveyor belt. A selection of filament samples was shown to a company that focuses on 3D printed solutions (3DWays) and it was pointed out that X1 sample, based on visual inspection, seemed the best candidate for printing test although the diameter was considerable higher than the standard dimension used in 3DP (1.75 mm). Only after were the control charts performed and as such the conclusions about the best filament can change further on in the subtopic *5.6 – Post Extrusion Characterisation*.

5.5 – Second Extrusion in Mini Extruder

After the extrusion experimentation was concluded the filament samples were collected and catalogued. Short filaments of poor and good quality were pelletized to allow for the production of test specimens for mechanical tests and MFR determination of the filaments. A considerable amount of compounded pellets was still available but would not be enough to perform a second extrusion cycle in the twin-screw extruder. As such, a small experimentation was performed with the 3Devo mini extruder which requires a much lower amount of material and wastes much less given that it operates with an electronic closed feedback-loop system. This means that after setting a material profile with the temperature values, screw speed and cooling parameters the equipment adjusts the throughput according to the readings of the diameter sensor. Although the screw barrel is short the extrusion process is automatic and adjusted in real-time according to the diameter measurements of the extruded filament. This provides advantages for well-behaved and good quality materials but the opposite is true for more irregular materials. The typical screw speeds used in such equipment are much lower than those of big extruders. Several tests were performed in an attempt to fine-tune the temperature profile for the rPP(cmp) pellets in order to perform good short tests with the low amount of material available. The best set of parameters after a few trial runs is the one in Table 31. Given that the temperatures (process value – PV vs setpoint value - SV) varied considerably several samples were taken and labelled P1, P2 and P3 (Profiles). For temperature zones the difference between SV and PV was approximately a 5ºC decrease in some cases and for the screw speed it was observed PV = SV ± 0.3 RPM of maximum difference.

Table 31: Overall quality of the experimentation of second cycle extrusion in the 3Devo mini extruder. One set of parameters and three different filament samples collected.

Filament Code	Screw Speed (RPM)	Die (ºC)	Zone 3 (ºC)	Zone 2 (ºC)	Zone 1 (ºC)	Fan Speed (%)
P1, P2, P3	3.5	200	200	200	200	40

In Figure 28 closeup pictures of samples P1-P3 are shown. It is possible to observe the varnished effect possibly due to PLA contamination (the most used material in that particular equipment) in P1. Some unevenly melted blobs are seen in P2 along the filament in closeup image but other than that the surface quality is good and homogeneous. P3 is seemingly better in quality. No melting defects are observable and overall and it seems better than both P1 and P2 albeit the fact the it is an extremely short filament (a good cut section from a longer poorer filament).

Figure 26: Closeups of filament samples P1, P2 and P3 (green, good results).

5.6 – Post-Extrusion Characterisation

The post-extrusion characterisation pertains mostly the material obtained from the extrusion on the twin-screw extruder. For such, bad quality filaments were excluded and good quality samples were pelletized – rPP(cmp) pellets. Afterwards, the following tests were performed with rPP(cmp) and vPP(3dp): MFR determination (using the same methods as before), FTIR-ATR and TGA. For rPP(cmp) visual comparison with non-separated extruded rPP pellets was also done. Finally, diameter process control was performed with the filament samples classified as good (green) both from the first extrusion (which was the equivalent to compounding) and second extrusion in the 3Devo.

For the MFR determination two analysis' scenarios were employed: elimination of data points using Z score with threshold t=1 and t=2. Table 32 summarises the results obtained in the MFR determination for rPP(cmp) and vPP(3dp). The results previously obtained for rPP(mix) are included for comparison.

Table 32: Melt flow rate tests results for rPP(cmp) pellets after first extrusion, and vPP(3dp) pellets and rPP(mix) at 200ºC with 2.16 Kg standard weight using ASTM D1238.

rPP(cmp)							
N	Threshold (Z Score)	Excl.	T (ºC)	Avg (g/10min)	Stdev (g/10min)	Stdev/Avg (%)	MFR Interval
38	2	1	200	11.05	1.50	13.5	[9.65, 12.55]
38	**1**	**13**	**200**	**11.06**	**0.81**	**7.4**	**[10.25, 11.88]**

vPP(3dp)							
N	Threshold (Z Score)	Excl.	T (ºC)	Avg (g/10min)	Stdev (g/10min)	Stdev/Avg (%)	MFR Interval
47	2	3	200	4.51	0.61	13.6	[3.90, 5.12]
47	**1**	**14**	**200**	**4.53**	**0.36**	**8.0**	**[4.17, 4.89]**
rPP(mix)							
N	**Threshold (Z Score)**	**Excl.**	**T (ºC)**	**Avg (g/10min)**	**Stdev (g/10min)**	**Stdev/Avg (%)**	**MFR Interval**
48	2	2	200	11.58	1.94	16.8	[9.64, 13.52]
48	**1**	**15**	**200**	**11.71**	**1.31**	**11.2**	**[10.41, 13.02]**

The MFR value at 200ºC of rPP(cmp) is 11.06 g/10min with a standard deviation of 0.81 g/10min (nearly 7% of the average value). After extrusion, the melt flow rate of the material decreased by 0.65 g/10min relative to rPP(mix) which corresponds to a decrease of 5.55%. This could possibly be due to some cross-linking occurring, which increases the melt viscosity. However, the relative standard deviation of rPP(cmp) is much lower compared to rPP(mix): 7.4% vs 11.2%. Thus, the measurements for rPP(cmp) appear to be more consistent after data was cleaned. The MFR control interval is much tighter for rPP(cmp) and as such, the process is more controlled. The most noteworthy feature on Table 32 is the difference in melt flow rate from rPP(cmp) and vPP(3dp): 11.06 g/10min vs 4.53 g/10min. This confirms the remark about MFR of the rPP material in the subsection of pre-extrusion characterisation: the rPP material under study seems more suitable for manufacturing processes other than extrusion due to the relatively high MFR. The filament vPP(3dp) is manufactured with the sole purpose of being extruded in 3D printers (printers using FDM/FFF). Typically, for extrusion processing lower MFR polymers are used. vPP(3dp) melt flow rate is reasonable for such type of material processing. After all, the MFR of rPP(cmp) is approximately 2.4 times higher than that of vPP(3dp). Moreover, as with rPP(cmp), the standard deviation of vPP(3dp) is also comparably much lower than with rPP(mix). This could be attributed to having more experience on the MFR determination process since chronologically, the first trials were those of rPP(mix). In this case, the human factor plays an important role with gaining more control over the manual processes. In Figure 27 the control charts for the MFR determination are showb. Top and bottom images refer to of rPP(cmp) and vPP(3dp), respectively. The blue dashed line represents the average value while the dark red and bright red represent the control interval. On both graphs it is possible to observe that, proportionately, a larger amount of data points in vPP(3dp) are concentrated around the average value line when compared to those of rPP(cmp).

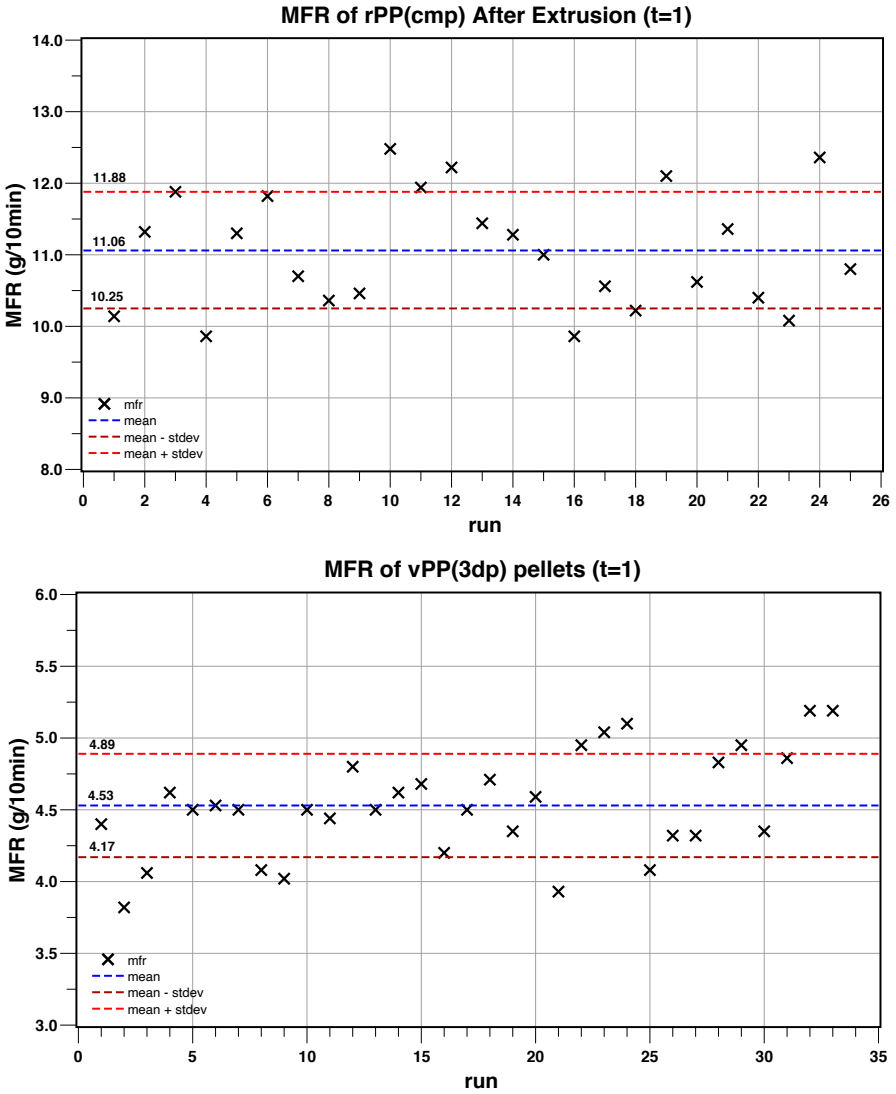

Figure 27: Control charts for MFR of rPP(cmp) pellets after first extrusion (top) and rPP(3dp) pellets (bottom).

The next comparative analysis between rPP(cmp) and vPP(3dp) pertains the FTIR spectra of one tested sample of each material. In Figure 28i the spectra of each material are plotted and stacked with fixed offset for better visibility. The peaks are identified in the graph by the label with the corresponding wavenumber. The blue line represents vPP(3dp) material and the green line represents the rPP(cmp) material.

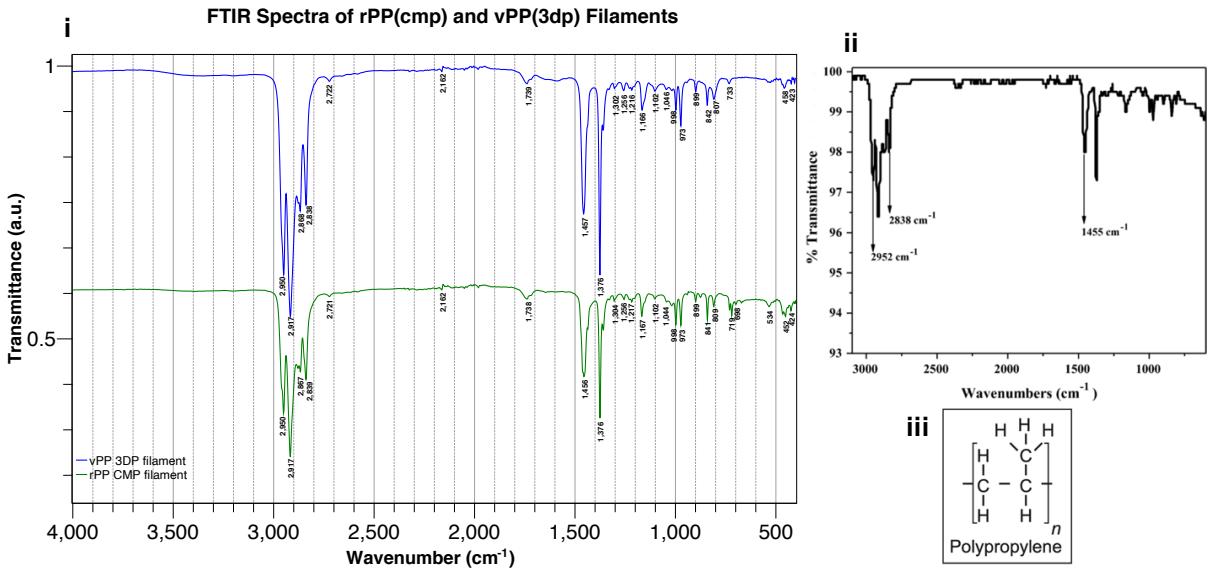

Figure 28: (i) FTIR spectra of rPP(cmp) filament pellets (D1 sample) and vPP(3dp) with stacked curves (fixed offset). (ii) Typical FTIR spectrum of PP (Gopanna et al. 2019). (iii) PP chemical structure (Giles, Wagner, and Mount 2014, 215).

The identified peaks of both materials are listed in Table 33-34 and classified according to shape, type of band and possible functional group associated. Table 33 refers to the main spectrum region while Table 34 refers to the fingerprint region. Moreover, green peak values are common to both spectra and dark yellow values are unique to the respective spectrum.

Table 33: Peak list from the rPP(cmp) and vPP(3dp) FTIR spectra with the following features: peak wavenumber, shape and amplitude. Main spectrum region interval]1500,4000] cm^{-1}.

rPP(cmp) Peaks			vPP(3dp) Peaks			IR Correlations
Wavenumber cm^{-1}	Shape	Band	Wavenumber cm^{-1}	Shape	Band	(Mistry 2009, 36–45)
2 950	sharp	Strong	**2 950**	sharp	Strong	-CH3
2 917	sharp	Strong	**2 917**	sharp	Strong	-CH2-
2 867	sharp	Strong	**2 868**	sharp	Strong	-CH3
2 839	sharp	Strong	**2 838**	sharp	Strong	-CH2-
2 721		Weak	**2 722**		Weak	Amino acids / Ethers / Charged amine derivatives
1 738	large	Mid	**1 739**		Mid	Alkenes (CR1R2=CH2) Overtone

Table 34: Peak list from the rPP(cmp) and vPP(3dp) FTIR spectra with the following features: peak wavenumber, shape and amplitude. Fingerprint region represented: [1500,400] cm^{-1}.

rPP(cmp) Peaks			vPP(3dp) Peaks			IR Correlations
Wavenumber cm^{-1}	Shape	Band	Wavenumber cm^{-1}	Shape	Band	(Mistry 2009, 36–45)
1 456	sharp	Strong	**1 457**	sharp	Strong	Nitrosamines (RNN=O), Alkanes CH2, CH3
1 376	sharp	Strong	**1 376**	sharp	Strong	Aliphatic Nitro Compounds NO2, Alkane CH3, Carbozylic acids, Halogen Compounds C-F stretch

1 304		weak	1 302		weak	Sulfur Compounds (S=O stretch), Alkene trans
1 256		weak	1 256		weak	Conj Ethers (ROR stretch)
1 217		weak	1 216		weak	Aromatic Phosphorus Compound (P-O stretch)
1 167	sharp	mid	1 166	sharp	mid	Sulfonyl chlorides (S=O), Sulfonamydes (S=O), Alkanes Gemynal Dimethyl (skeletal vib)
1 102		weak	1 102		weak	Aliphatic Ethers (R-O-R stretch)
1 044		weak	1 046		weak	Aliphatic Ethers (R-O-R stretch)
998	sharp	mid	998	sharp	mid	Phosphorus Comp (P-O), Monosubstituted alkenes (RCH=CH2)
973	sharp	mid	973	sharp	mid	Disubstituted Alkenes (RCH=CH2), C-H def)
899	sharp	mid	899	sharp	mid	Tetra- or penta-substituted benzene Containing 1 free H, Monosubstituted alkenes
841	sharp	mid	842	sharp	mid	Benzene ring with 2 adjacent H atoms, Pentasubstituted benzene, Trisubstituted Alkenes
809	sharp	mid	807	sharp	mid	Halides (C-Cl stretch), Benzene ring with 3 adjacent H atoms, Trisubstituted alkenes
-	-	-	733		weak	Benzene ring with 4 adjacent free H atoms
719	sharp	mid	-	-	-	Benzene ring with 5 adjacent free H atoms, Disubstituted Alkenes
698		weak	-	-	-	N.A
534		weak	-	-	-	N.A
452		weak	458		weak	N.A
424		weak	423		weak	N.A

Several key aspects can be taken from Tables 33-34. The total number of identified peaks are 25 and 23 for rPP(cmp) and vPP(3dp) respectively. There are 22 peaks in common for both materials. In the main region the 4 strong peaks are the same for both materials. The remaining peaks are weak and mid bands. In the fingerprint region the first 2 peaks common to both materials 1456/1457 cm^{-1} and 1376 cm^{-1} are strong bands. The remaining common peaks have the same band type in the two materials. Regarding unique peaks, 3 were found in rPP(cmp) and 1 was found in vPP(3dp). The unique peaks in rPP(cmp) are found at 719 cm^{-1} (mid band), 698 cm^{-1} and 534 cm^{-1} (both weak bands). Only 1 unique peak was found in vPP(3dp) spectrum: the weak band at 733 cm^{-1}. Possibly due to the extrusion process that much more resembles a compounding process the spectrum of rPP(cmp) is much simpler than those of the rPP(mix) flakes. This could be due to rPP(cmp) being a much more homogeneous material after the extrusion specifically with a twin-screw extruder in counter-rotating mode (which is usually more appropriate for compounding processes). In Figure 28iii the chemical structure of polypropylene is shown. It can be seen that it has the following bonds whose peaks are found in the above tables: -CH2, -CH3 and -CH. The FTIR spectra of both samples matches the typical spectrum of polypropylene. According to Gopanna et al. (2019) the characteristic IR peaks of PP are located at the following

wavenumbers: 2952 cm^{-1}, 2917 cm^{-1}, 2838 cm^{-1}, 1455 cm^{-1}, 1375 cm^{-1}, 1165 cm^{-1}, 997 cm^{-1}, 972 cm^{-1}, 840 cm^{-1}. All of these peaks were clearly identified in both filaments (Figure 28i, Tables 33-34).

With the TGA analysis of both filaments the intended objectives were the following: (1) quantification of the major constituents (through the number of degradation curves), (2) assess the decomposition and thermal stability and (3) quantify the inorganic filler content (through the residual weight at the end of the trial run) and the volatiles content (the weight loss until around 350ºC). A few limitations were found that will be discussed after the main analysis. The main TGA graph is shown in Figure 29Ci: stacked plot with residual weight (thermogram - line) and first derivative of residual weight (derivative thermogram – dashed line) of both materials. Filament sample rPP(cmp) is shown in green while vPP(3dp) is shown in blue.

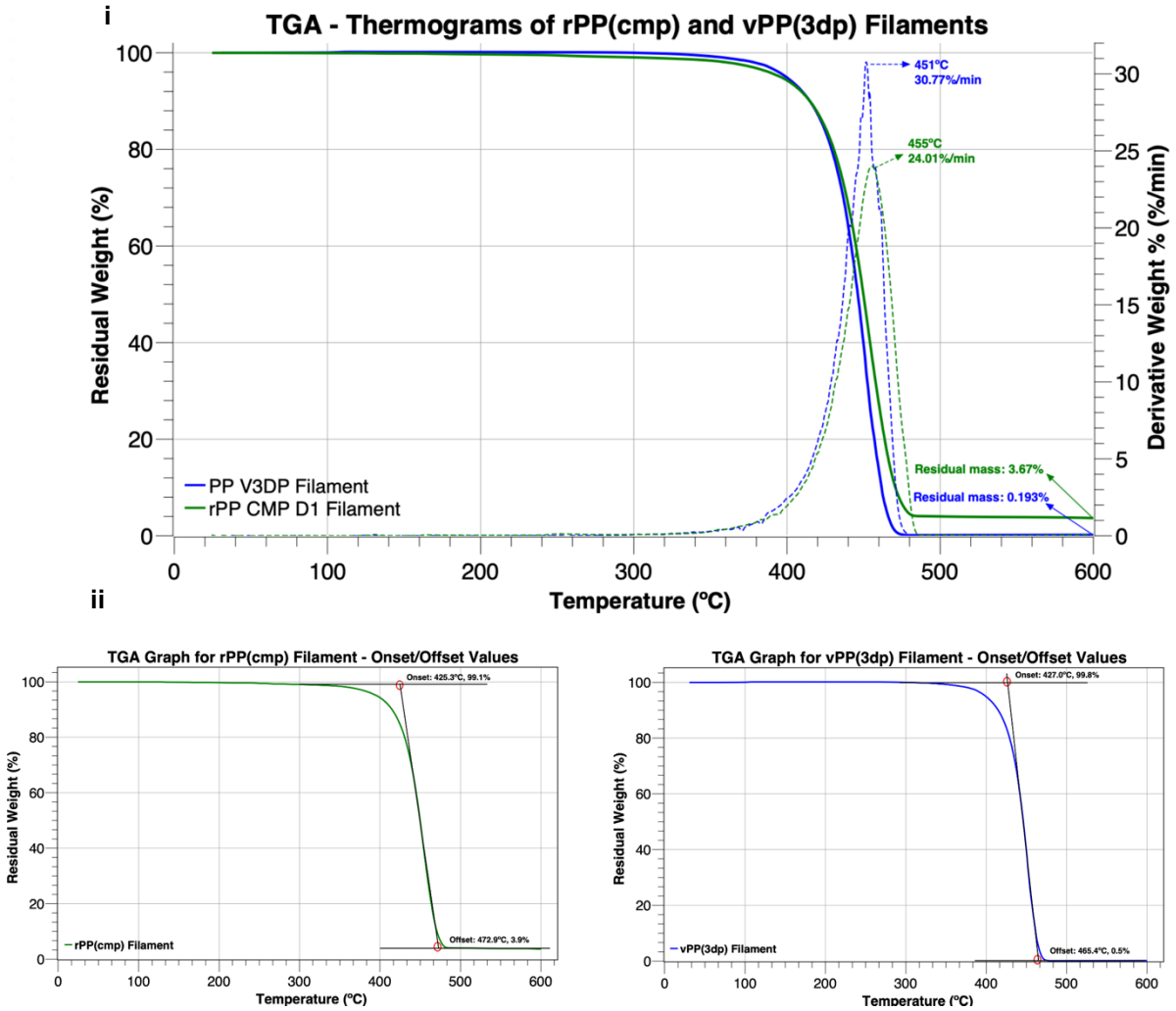

Figure 29: (i) Thermograms of rPP(cmp) and vPP(3dp) filament samples. (ii) Extrapolated onset and offset values for rPP(cmp) sample (left) and vPP(3dp) sample (right).

From Figure 29i and 29ii several points can be highlighted. There is a considerable difference in residual weight between the samples. The final residual weight of rPP(cmp) is 3.67%, much higher than that of vPP(3dp) which amounts to only 0.193%. The former is approximately 18 times higher than the latter. This can indicate that rPP, as expected, has a much higher content of inorganic fillers and additives in comparison to vPP. Moreover, based on the derivative curves (using DTG data) the polymer

temperature of degradation (i.e. the temperature value of the maximum of the first derivative) of both materials is approximately the same: 451ºC for rPP(cmp) and 455ºC for vPP(3dp). However, the maximum rate of degradation is considerably higher for rPP (30.77%/min) than vPP (24.01%/min). Based on the residual weight curve shape and given that for rPP and vPP the first derivative curves only have 1 global and local maxima it can be concluded that there is only 1 degradation step for both materials. Thus, it is likely that only 1 major constituent exists in each material tested. By visual inspection of the graph it can be seen that rPP starts losing weight earlier in the trial which is noticeable between 200ºC – 400ºC. At around 380ºC the rate of degradation of vPP intersects that of rPP and becomes higher. Approximately at 420ºC the degradation curves intersect and vPP starts to degrade faster and its degradation ends earlier and with a much lower residual weight as noted before. In Figure 22Cii the extrapolated onset and offset degradation values are presented. However, these are rough approximations due to limitations upon using the software functions and as such these are only auxiliary parameters. Tangent lines (A and B, respectively) are drawn to the initial portion of the residual weight curve and final portion of the residual weight curve. Another tangent (C) to the degradation step curve is drawn. The intersection between A and C provides de extrapolated onset temperature and the intersection between B and C provides the extrapolated offset temperature. For rPP(cmp) the extrapolated onset and offset values (T, %) are (425.3ºC, 99.1%) and (472.9ºC, 3.9%). For vPP(3dp) the corresponding values are (427.0ºC, 99.8%) and (465.4ºC, 0.5%) for onset and offset, respectively. Although not precise values, these are in accordance with the previous observations. Lastly, another relevant parameter that can be taken from the graphs or their source data is the percentage weight of volatile compounds for each material. This corresponds to the weight loss until 350ºC (if the interval up to 100ºC is counted than the weight loss also includes moisture content). For rPP(cmp) the volatiles content considering the ranges [24ºC, 350ºC] and [100ºC, 350ºC] are 1.609% and 1.538%, respectively. For vPP(3dp) the volatiles content considering the ranges [30ºC, 350ºC] and [100ºC, 350ºC] are 0.72% and 0.766%, respectively. Based on these values it can be concluded that rPP(cmp) sample has approximately twice the volatile compounds content compared to vPP(3dp). However, it should be noted that the residual weight for vPP actually increased upon heating up to a maximum of 100.173% at 116ºC which was not expected. This could be caused by a calibration issue or an unknown particularity of the material. Both TGA tests were performed under an inert atmosphere with a constant nitrogen stream. Thus, combustion of the sample is avoided. One implication of such method is that at the end of the trial run which finishes around 600ºC the residue can include a considerable amount of char which is not to be counted as inorganic additive/filler. To obtain a more accurate value and useful information regarding inorganic additives and fillers (final residual weight) the following testing method could be employed: heating up to 600ºC with nitrogen stream (inert atmosphere); afterwards cool the sample to around 500ºC under nitrogen stream; finally, heat the sample from 500ºC up to 800/850ºC with high air stream (oxygen rich) to degrade and exclude the remaining char from the previous heating cycle. This could also provide more information since other degradation curves could occur due to changes in atmosphere and related reactions. In the framework of this research work some laboratory classes were prepared for students of the Masters in Materials Engineering. During class extrusion of rPP was performed without prior separation of higher density flakes. As such, it is possible to compare the pellets obtained

from filaments of rPP extruded with and without prior separation and drying in Figure 30. The pellets on the left are much more homogeneous and with better surface quality.

Figure 30: Comparison of pellets obtained from rPP(cmp) with separation process (left) and without separation process (right).

The tables and graphs that follow provide the diameter control process of the best results obtained. Tables 35 and 36 provide both the extrusion and diameter control parameters obtained for samples A3, D1, X1, P1, P2 and P3. Figure 31 provides the graphical diameter control process for the overall best filament samples (D1, P1, P2 and P3).

Table 35: Extrusion processing parameters and diameter control measurements for A3, D1 and X1 filament samples (first extrusion/compounding).

Filament A3					
Screw Speed (RPM)	Cooling method	Die (˚C)	Zone3 (˚C)	Zone2 (˚C)	Zone1 (˚C)
15	RT	210	210	200	170
#Data Points	Filament Length (m)	Avg Diameter (mm)		Diameter Stdev (mm)	Stdev/Avg (%)
66	6.50	1.17		0.21	18.56
Filament D1					
Screw Speed (RPM)	Cooling method	Die (˚C)	Zone3 (˚C)	Zone2 (˚C)	Zone1 (˚C)
15	RT	200	200	190	170
#Data Points	Filament Length (m)	Avg Diameter (mm)		Diameter Stdev (mm)	Stdev/Avg (%)
46	4.50	1.75		0.23	13.35
Filament X1					
Screw Speed (RPM)	Cooling method	Die (˚C)	Zone3 (˚C)	Zone2 (˚C)	Zone1 (˚C)
15	RT	170-180	200	190	170
#Data Points	Filament Length (m)	Avg Diameter (mm)		Diameter Stdev (mm)	Stdev/Avg (%)
103	10.20	1.90		0.22	11.39

Table 36: Extrusion processing parameters and diameter control measurements for P1, P2 and P3 filament samples (second extrusion in mini extruder 3Devo).

Filament P1					
Screw Speed (RPM)	Cooling method	Die (˚C)	Zone3 (˚C)	Zone2 (˚C)	Zone1 (˚C)
3.5	Fan (40%)	200	200	200	200
#Data Points	Filament Length (m)	Avg Diameter (mm)		Diameter Stdev (mm)	Stdev/Avg (%)
40	3.90	1.72		0.12	6.86
Filament P2					
Screw Speed (RPM)	Cooling method	Die (˚C)	Zone3 (˚C)	Zone2 (˚C)	Zone1 (˚C)
3.5	Fan (40%)	200	200	200	200
#Data Points	Filament Length (m)	Avg Diameter (mm)		Diameter Stdev (mm)	Stdev/Avg (%)
160	15.90	1.74		0.19	10.71
Filament P3					
Screw Speed (RPM)	Cooling method	Die (˚C)	Zone3 (˚C)	Zone2 (˚C)	Zone1 (˚C)
3.5	Fan (40%)	200	200	200	200
#Data Points	Filament Length (m)	Avg Diameter (mm)		Diameter Stdev (mm)	Stdev/Avg (%)
16	1.50	1.82		0.09	5.07

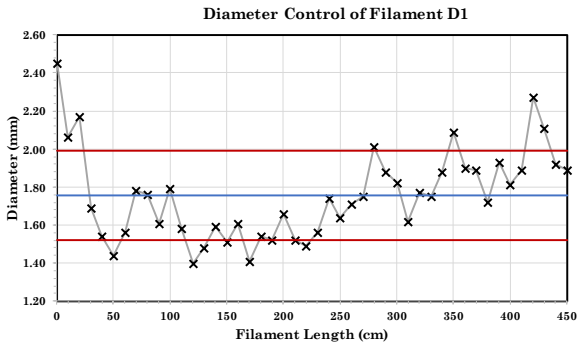

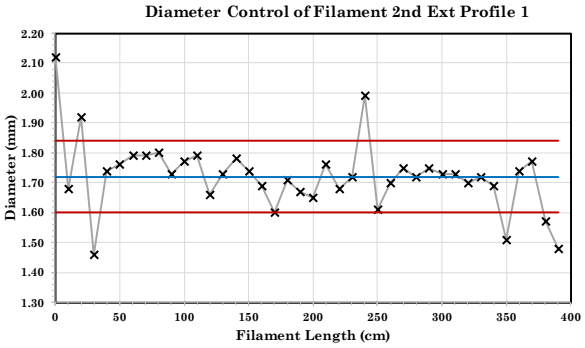

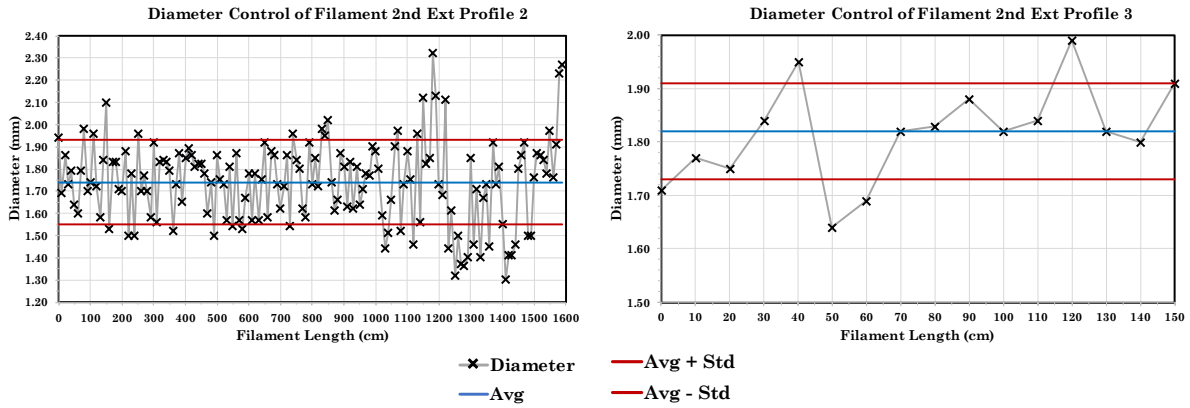

Figure 31: Diameter process control graph for filament samples D1, P1, P2 and P3.

Based on the previous tables and graphs it can be seen that this type of diameter control data is extremely useful to understand the full profile of the filaments. More fine-grained information is obtained on the quality control in order to better compare and assess differences. Overall, the best filament seems to be P1 which has an average diameter of 1.72 mm (close to the ideal 1.75 mm) and one of the lowest ratios of standard deviation-average value. However, the filament is rather short at 3.90 m. Given that much more data is available for P2, this filament sample also provides an interesting control graph. In the control diameter process the total data gathered with all analysed samples was the following: 431 measured data points covering 42.50 m of filament length.

No printing was possible with the rPP filament. It was possible, though, to print a small benchy with vPP(3dp) filament but it was a much more difficult task than expected (an Ender 3 V2 was used). Many attempts were required and several types of glues for the printer bed (set to maximum temperature) had to be tested, nearly damaging it (UHU spray provided the best result). It was crucial to glue an initial printed rafting bed to the printer bed and then print on top of the rafting. Although the process was difficult, complex and lengthy, the final quality of the benchy was extremely good. Both the benchy and rafting are shown in Figure 32 with the final benchy on the left and ongoing printing stage on the right.

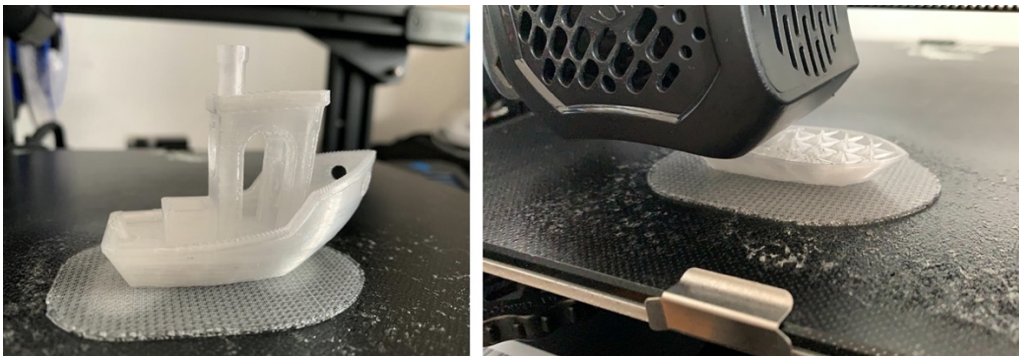

Figure 32: Benchy printing with vPP(3dp) filament on an Ender 3 V2 printer using rafting and strong glue. It is possible to see the glue heavily staining the printer bed (right).

5.7 – Mechanical Testing

The mechanical characterisation of rPP and vPP with tensile testing was the last part of the research methodology. For such, 5 test specimens of rPP(cmp) and 3 test specimens of vPP(3dp) were tested. These are shown in Figure 33(iii) below.

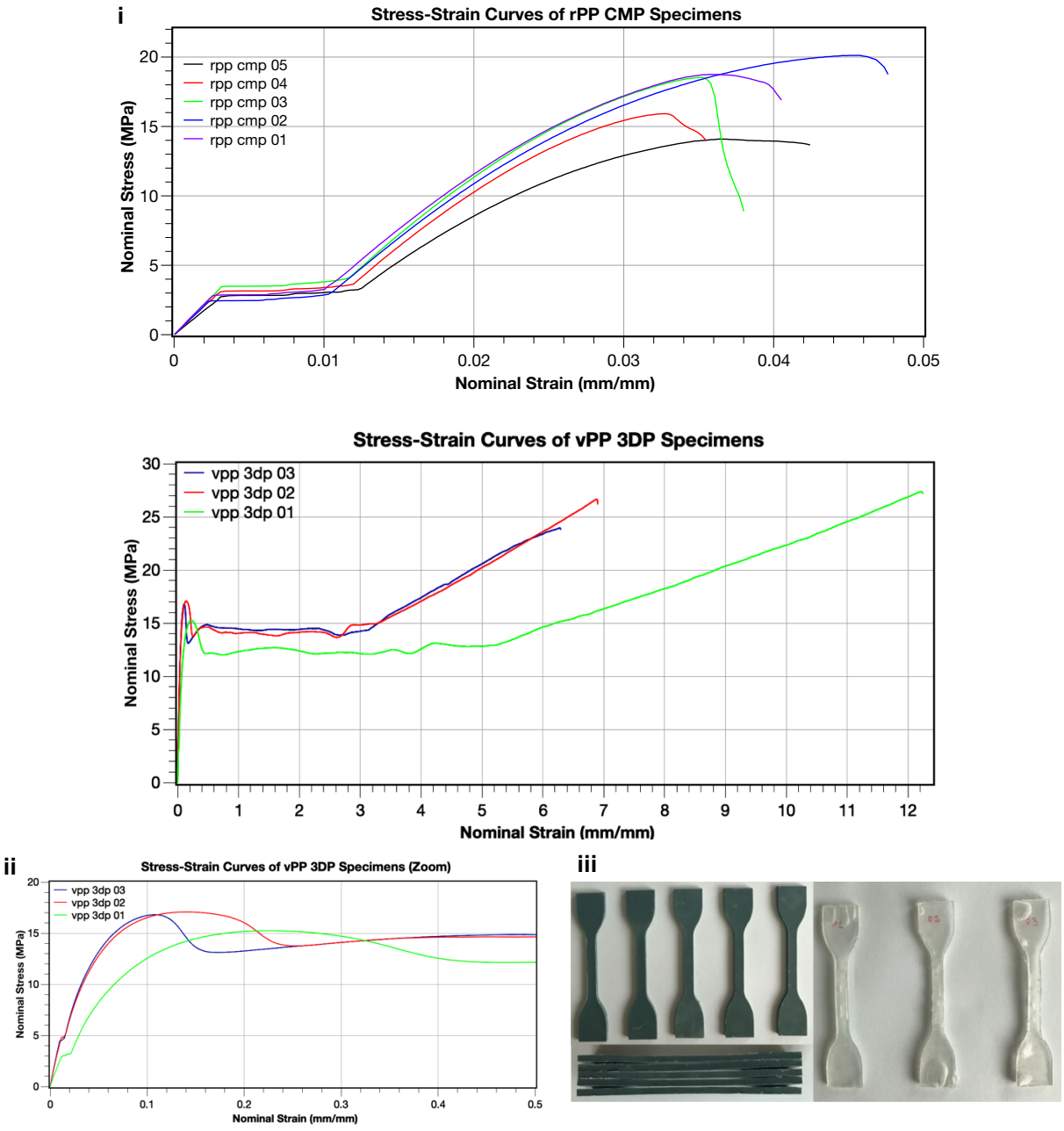

Figure 33: (i) Stress-Strain curves for rPP(cmp) and vPP(3dp). (ii) Stress-Strain curve of vPP(3dp) zoomed in. (iii) Specimens (rPP on the left, vPP on the right) by hot press moulding for use in tensile tests.

In this subtopic the results of the tensile tests and relevant discussion are described. The mechanical properties used to compare both materials through tensile tests are: the yield strength (σ_y,

value of stress after which the deformation is plastic and as such the material does not fully recover and a portion of deformation becomes permanent), the ultimate tensile strength (UTS, maximum stress the test specimen can take until failure), the yield strain (ϵ_y, strain corresponding to the yield point on the curve, after which full recovery of material length is not possible to due plastic or permanent deformation) the nominal strain at failure (ϵ_f), Young's Modulus (E, this property provides information about the tensile stiffness or rigidity of a given material) calculated using 0.002 offset method and toe compensation, modulus of resilience ($U_{r,}$, work energy absorbed by the material until the yield point), modulus of toughness (U_t, work energy absorbed by the material until it fails) and ductility (capacity to accommodate plastic deformations after the yielding point is reached, measured by the ratio $^{\epsilon_f}/_{\epsilon_y}$).

The difference in the stress-strain curves of rPP(cmp) and vPP(3dp) specimens is staggering. In Figures 33i this is easily observable looking at the abcissa of both graphs: scale difference of strain at failure between rPP(cmp) and vPP(3dp) is approximately 0.040 mm/mm vs 12.000 mm/mm, a ratio of 300. This is not exclusive of these 2 particular specimens. This extremely high gap occurred with all specimens. This shows that vPP(3dp) specimens have a capacity to accommodate deformation two orders of magnitude higher compared to the rPP(cmp) specimens. In Figures 34i and 34ii some of the tensile test results are presented in bar charts for comparison of both materials (Young's Moduli and strain at failure, respectively).

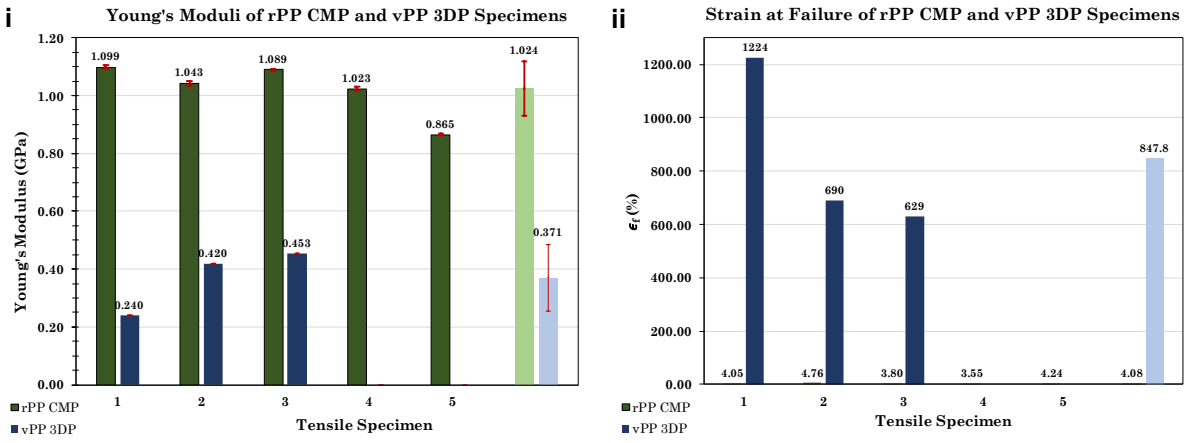

Figure 34: (i) Comparison of Young's Moduli of rPP(cmp) and vPP(3dp. (ii) Comparison of strain at failure of rPP(cmp) and vPP(3dp).

Table 37: Summary of the mechanical properties of rPP CMP and vPP 3DP filaments obtained from the tensile test perfomed to the 8 test specimens.

Filament	Young's Modulus *E*			U_r		U_t	
	Avg (GPa)	StDev (GPa)	Lin. Regr. R^2 Min (%)	Avg (MJm^{-3})	StDev (MJm^{-3})	Avg (MJm^{-3})	StDev (MJm^{-3})
rPP CMP	1.024	$2x10^{-3}$	99.96	$1.035\ x10^{-2}$	$1.74\ x10^{-3}$	$4.101\ x10^{-1}$	$9.85\ x10^{-2}$
vPP 3DP	0.371	$1\ x10^{-3}$	99.94	$3.012\ x10^{-2}$	$9.72\ x10^{-3}$	$1.443\ x10^{2}$	$5.30\ x10^{1}$

Filament	σ_y		ϵ_y		UTS		ϵ_f		ϵ_f/ϵ_y
	Avg (MPa)	StDev (MPa)	Avg (%)	StDev (%)	Avg (MPa)	StDev (MPa)	Avg (%)	StDev (%)	Avg (a.u.)
rPP CMP	2.96	0.39	0.489	0.042	17.48	2.43	4.08	0.46	8.4
vPP 3DP	4.102	1.02	1.264	0.082	26.02	1.81	847.8	327.3	675.2

Table 37 summarises the mechanical properties obtained for rPP(cmp) and vPP(3dp) filaments through tensile tests. One can notice that properties such as the Young's Modulus, modulus of resilience, the yield strength and strain, and ultimate tensile strength are not very different from one material to another, differing for a factor of 2 to 3 approximately; rPP(cmp) specimens showed to be around 3 times stiffer than vPP(3dp) ones, while vPP(3dp) filaments showed to have modulus of resilience 3 times higher than rPP(cmp). Regarding the modulus of toughness, the difference is much greater with vPP(3dp) having a value nearly 352 times higher than that of rPP(cmp). Both materials have relatively close yielding points, vPP(3dp) reached yielding later in the tensile test with a respective tensile strength around 2 times higher than rPP(cmp) and a tensile strain around 3 times higher. The abysmal difference between the two materials comes down to the failure point, not in terms of strength, but in terms of deformation. The nominal strain at failure is 2 orders of magnitude higher in vPP(3dp) specimens, indicating this material's much better capacity to accommodate plastic deformations after yielding before reaching failure point when compared to rPP(cmp). This evidence is also reflected in properties like ductility and toughness, vPP(3dp) showed much better capacity than rPP(cmp) in these two mechanical properties. A few possible aspects regarding rPP(cmp) that might explain some of the differences include: higher degree of crystallinity, cross-linking based polymer degradation phenomenon and/or the presence of specific additives with impact on rigidity (shown by Young's Modulus) and reducing resilience and toughness.

The stacked stress-strain curves are shown in Figures 34i (overview for rPP(cmp) andvPP(3dp)) and 33ii (zoom-in for vPP(3dp)). Photographs of the test specimens are provided in Figure 24A. It is important to note that after the tensile tests it was verified that some of the rPP(cmp) specimen had material gaps in the interior which certainly contributed to the results.

For 3DP one critical property of the materials used for filaments based on the mechanical tests performed appear to be the capacity to accommodate deformation. It has been shown that up to the yield point the two materials do not show a significant difference in the deformation capacity. The commercial 3DP filament is more elastic and reaches the yield point at a later stage. Regarding the capacity to accommodate plastic deformation the vPP(3dp) material shows a staggering difference to rPP(cmp) with the former having a much higher capacity (and thus it is possible to observe necking behaviour after yield point). This mechanical analysis possibly shows the fitting properties of a suitable filament for 3DP such as vPP(3dp). When the vPP(3dp) test specimens were inspected to assess the quality prior to the tensile tests it was possible to notice that they felt somewhat rubbery, very flexible and malleable. A non-tested hypothesis is that the vPP(3dp) material contains elastomeric additives that

provide these characteristics, or simply some additives, acting as plasticizers. Such information was not available from the vPP(3dp) supplier.

Figure 35 shows images taken during the tensile test performed for one of the vPP(3dp) specimen. No record of the rPP(cmp) tensile test was registered since every specimen reached failure just after a minute the test had started (vs 1h length tests for each vPP(3dp) specimen) and no extension was noticeable at naked eye.

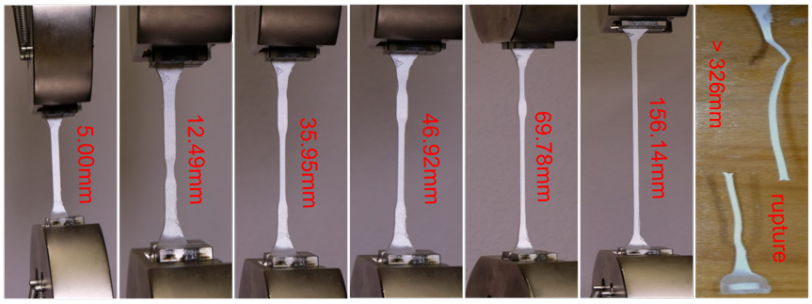

Figure 35: Sample of vPP(3dp) specimen under traction with strain extensions of 5.00 mm to approximately 326 mm (failure point).

5.8 – Limitations of the Experimental Work and Data Analysis

Throughout the research project several important limitations were identified regarding both the experimental work and data analysis. Some are related to the equipment as well as the impact of the COVID situation. The identified limitations can be grouped according the structure of the experimental work.

Regarding the initial steps of separation and drying, the upstream processes that lead to the material being tested are a black box. More information would be useful to better characterize and understand the limitations and characteristics of the initial state of the material. This highlights the well-known complexity of plastic recycling activities: namely the steps of sorting, polymer identification, washing and processing parameter tuning/compounding to deliver a good quality plastic product, which might explain the reason for the yet inadequate recycling numbers. The separation process of PE/PP from other polymers or PE/PP with high filler content was extremely simple since it was based only in density differences. Given that PE and PP have similar density values this would only allow for separation of particles with a much higher value. Different types of washing could have been performed but due to the volume of material being processed no efficient method was found (e.g. magnetic stirring with added detergent would only allow for very small portions of material to be processed simultaneously). Only 1 temperature value was used for drying but others could improve the moisture content. However, testing a wider range would require more material which would turn the scope of experimentation too broad.

In the domain of the pre-extrusion characterisation a few noteworthy limitations were identified. Melt flow rate was determined using an extremely manual process that is prone to errors and considerable variations. This resulted in high standard deviations and disperse data points. To counter this issue a high number of tests were performed. Another possibility to mitigate the issue could have been testing much larger time intervals than those used. Due to the manual nature of the equipment and the

mentioned implications, it was not possible to obtain robust results at the advised parameters from the ASTM standard which was 230ºC in order to compare with literature results and for future reference. As such, the temperature was decreased to 200ºC to allow for better control. Regarding TGA it could have been interesting to perform a multi-stage degradation analysis as described in subtopic 5.6: inert gas stream with heating up to 600ºC, followed by cooling to 500ºC and change of stream to compressed air (oxygen rich atmosphere) and heating up to 800/850ºC to exclude the char from residual weight and better understand the nature of additives and fillers present with combustion degradation as opposed to inert degradation. This would possibly add at least another degradation curve and the final residual weight would exclude the char weight. A residual weight would be obtained for each stage with different characteristics and implications associated. Alternatively, using only inert gas stream but with a much higher maximum temperature value of testing could provide more insights on the nature of materials being tested. Regarding the FTIR spectroscopy, it would be interesting to obtain higher rate scans and their individual spectra would allow for statistical analysis of the spectra and the use of PCA and both classification and clustering algorithms (mostly supervised machine learning) to better analyse the differences between rPP and vPP filament samples. Given how similar the spectra of both materials are and how different they are in terms of handling and mechanical characteristics it could provide useful information. Scripts were already obtained in order to perform this processing.

Regarding the extrusion processing the limitations relate to the type of equipment used, the optimal conditions for PP processing and inability to obtain more material. The extruder used is very manual in operation thus making the diameter control of the filament much more difficult (as opposed to the mini extruder that provided much more consistent diameters across the filament due to the control feedback loop). The optimal conditions were not possible to test: warm water bath (equipment acquired too late and no material was possible to order again) and automatic puller and winding device. Moreover, there was no possible way to assure the straight path of the extruded filament that would too often be snaking until the end of the conveyor belt.

For the second extrusion using the 3Devo mini extruder, although the device is more limited in terms of heating system and barrel length than a full-fledged extruder, the great advantage was the complete automatization of the equipment with controlled close feedback loop system and this was the likely cause for the much better results in terms of diameter consistency with the integrated laser measurement device. Nonetheless, given the material limitations, it was not possible to test MFR of 2nd extruded pellets to assess differences from the 1st extruded ones (as to not destroy important filament samples by pelletizing them).

For the post-extrusion characterisation some of the limitations are the same as previously identified in the pre-extrusion characterisation. The most noticeable limitation is related to the diameter control process employed. Even though a large number of data was obtained (a very time-consuming procedure) the measurements were performed only in one cross-sectional dimension. This means that even if the standard deviation was zero with a fully constant diameter value, the filament could have been elliptical shaped or have any other symmetrical shape (although by visual inspection this would be easily identified). To counter this, 2 measurements would be required in orthogonal directions to assess the geometry of the cross section of the filament. However, this was not feasible to perform. Even though

a device for automatic measurements was built and tested it had the limitation of not being able to measure filaments that had single points with diameter higher than 1.95 due to limitations of the PTFE tube and printed parts. In the context of the mechanical testing two limitations were identified. The first pertains the supplier of the commercial 3DP filament used as benchmark and the second related to the process of fabrication of the tensile test specimens. The company from which vPP(3dp) spool was bought did not provide sufficient information regarding mechanical properties of the material, nor composition/formulation. No technical data sheet was available and upon request they informed the only mechanical property available was the flexural modulus (often identified as G) which was not relevant. Thus, no information was provided regarding the Young's modulus, yield strength, UTS or nominal strain at failure to compare with those obtained in the mechanical tests performed (it would allow to determine, for instance, the impact of the method of fabrication). More importantly, the method of test specimen production was not adequate (but initially there was none available and having one is due to the persistence of Prof Ana Marques that managed to arrange all the necessary equipment) and this had an impact on the tensile tests. The most appropriate method (having into account the high MFR values of the rPP obtained from LIPOR) would be injection moulding but it was not available (and the moulds are extremely expensive to produce). The method used entailed long processing times and very long cooling times (high nucleation and crystallinity) thus leading to extremely brittle test specimens for rPP (they would easily snap at the slightest tension by hand and they would fail during testing after around a minute). As such, the tensile tests showed much poorer results than what was expected (except for vPP which were completely unexpected and that shows how distinct a 3DP optimized filament is from the rPP urban waste recycled filament obtained). Nevertheless, it should be stressed that the method to process rPP, reported at the present dissertation, deals with urban plastic waste, thus contributing to the sustainability goal of plastic waste reduction and reutilization.

The scope of the research could be even broader (as initially planned) if more material had been supplied to enable the testing of different cooling methods (including the optimal method of warm water bath). Also, a single-screw extruder (linear residence time and less material consumption) might have been tested but it was not functioning at the time (it is not clear if this was a relevant limitation or not).

All in all, the major weaknesses of the research could be summed up as: (1) inability to obtain more material, (2) not being able to test warm water bath that could have helped to obtain a printable filament, (3) the test specimen production method with strong implications in the tensile tests (crucial to assess properties) and (4) the author's inability for timely communication, feedback and delivery of information and reports. Nonetheless, valuable information was obtained regarding PP sourced directly from urban waste management facilities and its comparison with optimized PP for 3DP.

6 - Conclusions

Throughout the research the main results can be grouped according to (1) characterization of materials (sorted plastic waste), (2) best extrusion parameters, (3) the best filament samples obtained, (4) the printability of the 2 materials under study and the (4) main distinguishing features between the rPP and vPP materials. Regarding (1) it was found that rPP(bulk) is mostly made of PP, PE and high-density PP (with high content of inorganic components according to TGA) which were separated in water. Commonly used additives were identified such as EPDM, calcium carbonate and poly(1-butene) through FTIR analysis. Existence of other impactful additives was hypothesised such as talc, titanium dioxide and carbon black. The best first extrusion cycle results (with fixed cooling method RT) on the twin-screw extruder were achieved with the following parameters: $S(2) = 15\,RPM$, $T(1) = \{200, 200, 190, 170\}$, $S(2) = 15\,RPM$, $T(1modified) = \{170 - 180, 200, 190, 170\}$. However, the best filaments were obtained after a second cycle of extrusion was performed with a mini-extruder that had a closed-loop feedback control unit for diameter consistency. The parameters used for such were $S = 3.5\,RPM$, $T = \{200, 200, 200, 200\}$, with blower cooling (at 40%). According to diameter control process of all good filaments, the best ones were always obtained after extruding in the mini-extruder. Overall, the best filament is P1 which presents an average diameter of 1.72 mm with a standard deviation of 0.12 mm (ratio of deviation by average of 6.86%) and 3.90 m length. This is very close to commercial filament dimensions and tolerance (1.75 ± 0.05 mm). It was not possible to obtain a rPP filament good enough (diameter consistency respecting 3D printers' admissible tolerances) for printing tests. To print a benchy an estimated 6 m filament with no significant diameter variations would be required. A benchy with vPP (commercial PP formulation optimized for 3DP, vPP(3dp)) was successfully printed but after many attempts and combinations of parameters, glues and raft types (the material was difficult to work with in printing). There were major differences when comparing rPP(cmp) and VPP(3dp) materials. rPP(cmp) had a MFR value of 11.1 g/10min while vPP(3dp) had 4.5 g/10min (at 200ºC). With TGA data it was shown that rPP(cmp) had a final residual weight 18 times higher than that of vPP(3dp) at 600ºC (3.67% vs 0.193%) which may indicate the former has considerable content of inorganic additives. Moreover, considering the interval 100ºC - 350ºC the volatiles content of rPP(cmp) was also higher (1.54% vs 0.77%). Finally, regarding the mechanical characteristics of the tensile specimens rPP(cmp) showed a much higher rigidity (Young's modulus nearly 3 times higher, 1.02 GPa vs 0.37 GPa). The yield stress and strain were higher for vPP(3dp) (especially the yield strain). The ultimate tensile strength (maximum stress) for rPP(cmp) was 17.5 MPa while vPP exhibited a value of 26.0 MPa. The most noteworthy difference was the strain at failure (ϵ_f) and the ductility ratio (ϵ_f/ϵ_y): an abysmal difference of 4.08% and 8.4 for rPP(cmp) and 847.8% and 675.2 for vPP(3dp). The handling (rubbery test specimens on hands) and properties of vPP(3dp) are somewhat elastomeric, thus, it appears to suggest the presence of elastomer content (unconfirmed hypothesis) or plasticizers, which could be crucial for printability. Despite the challenges arisen, the present dissertation deals with the recycling of PP waste, contributing to the urgent sustainability goal of plastic waste reduction. Hopefully, it will provide relevant data for the implementation and optimization of PP recycling industrial processes.

All the work carried out allows to fill some gaps identified on the literature: complete data (MFR graphical distribution, TGA, FTIR) on the processing and characterisation of PP obtained directly from waste treatment/separation facilities with little optimization on the upstream processes (no other work was found with this scope). Moreover, a thorough comparison was performed between the rPP filament material and a virgin PP fully optimized for 3DP which allows, for future works, to better optimize rPP. Finally, no similar fine-grained diameter control processing was found in the literature and it may provide a transparent way of benchmarking, doing material profiles and comparing future works in the same domain. Thus, research question (1) introduced in the Research Scope (4.1) is answered (regarding main characteristics of PP flakes sourced from waste treatment facilities, filaments produced with it and similarities/differences with those of 3DP PP filament). One literature gap failed to be solved. No successful 3D printing was achieved with rPP. As such, research question (2) was not answered (process improvement to attain printability with rPP filaments). Secondly, given that the research was performed in the context of a Pedagogical Innovation Project (*PIP* - aimed to use exclusively reused/recycled material) it was out of the scope of the research (and would become too broad) the use of other mixtures. This leads to a myriad of possibilities for future research to improve rPP printability. PP is one of plastics with higher waste percentage but with low usage on the realm of 3DP. Some specific ideas seem interesting to explore in order to close the identified gaps and further promote a much easier framework for environmentally conscious industry. These include mixtures of rPP with different virgin PP grades with desired extrusion characteristics (for instance, from ExxonMobil), with low percentage vPP(3dp), compatibilizers (e.g. Maleic anhydride) and additives (elastomers for higher flexibility such as the saturated rubbers EPDM or ethylene-vinyl acetate to mimic the vPP(3dp) behaviour). Lastly, two other possibly impactful ideas could be interesting. In the same way open-source (OS) software is changing corporate and business environments (e.g. Chromium, Mozilla Firefox, Blender, Linux that drives the majority of supercomputers and internet servers, Python, Wordpress, 7-Zip, Docker containers) the same could be applied to materials, both those for 3DP filaments (after all, the well-known 3DP company Prusa started as open-source model) as well as those used for mass production in all other domains (which originate the plastic waste used for this research). This would allow a much more efficient recycling (by fully knowing the composition) and much more efficient transformation for other purposes (in this domain, repurposing plastic waste for 3DP). This could even be achieved with mini QR codes containing the IUPAC references and percentages of the components. There has been a boom on OS hardware in 3DP world with good results on extruders, printers and accessories such as automatic winders (based on frugal innovation). Some OS extruders achieve filaments as precise as 1.75 mm ± 0.05 mm diameters. All files are freely available, anyone can build them and a worldwide community provides continuous contributions. Such frugal innovations bring down the costs to as low as 500€-1 000€ with easily obtainable components (compared to tens of thousands for commercial extruders). Some prominent examples with exclusive focus on producing 3DP filaments include RepRapable Recyclebot, Filament Factory and Lyman/Mulier Extruder (*see generally* Woern et al. 2018; Capotexl 2014; Lyman and Mulier 2014).

References

[1] ACC. 2019. 'Lifecycle of a Plastic Product'. 2019. https://plastics.americanchemistry.com/Lifecycle-of-a-Plastic-Product/.

[2] AIMPLAS. 2019. 'Classification and Identification of Plastics'. *Plastics Technology Centre* (blog). 20 March 2019. https://www.aimplas.net/blog/plastics-identification-and-classification/.

[3] AM Terminology. 2015. 'ISO/ASTM 52900(En), Additive Manufacturing — General Principles — Terminology'. International Standard ISO/ASTM 52900:2015. ISO/ASTM. https://www.iso.org/obp/ui/#iso:std:iso-astm:52900:dis:ed-2:v1:en.

[4] Angatkina, Kateryna. 2018. 'Recycling of HDPE from MSW Waste to 3D Printing Filaments'. Fi=AMK-opinnäytetyö|sv=YH-examensarbete|en=Bachelor's thesis|. 2018. http://www.theseus.fi/handle/10024/146732.

[5] ASTM D638. 2015. 'Test Method for Tensile Properties of Plastics'. ASTM International. https://doi.org/10.1520/D0638-14.

[6] Attaran, Mohsen. 2017. 'The Rise of 3-D Printing: The Advantages of Additive Manufacturing over Traditional Manufacturing'. *Business Horizons* 60 (5): 677–88. https://doi.org/10.1016/j.bushor.2017.05.011.

[7] Baechler, Christian, Matthew DeVuono, and Joshua M. Pearce. 2013. 'Distributed Recycling of Waste Polymer into RepRap Feedstock'. *Rapid Prototyping Journal* 19 (2): 118–25. https://doi.org/10.1108/13552541311302978.

[8] Barnes, David K. A., Francois Galgani, Richard C. Thompson, and Morton Barlaz. 2009. 'Accumulation and Fragmentation of Plastic Debris in Global Environments'. *Philosophical Transactions of the Royal Society B: Biological Sciences* 364 (1526): 1985–98. https://doi.org/10.1098/rstb.2008.0205.

[9] Ben-Ner, Avner, and Enno Siemsen. 2017. 'Decentralization and Localization of Production: The Organizational and Economic Consequences of Additive Manufacturing (3D Printing)'. *California Management Review* 59 (2): 5–23. https://doi.org/10.1177/0008125617695284.

[10] Bogue, Robert. 2013. '3D Printing: The Dawn of a New Era in Manufacturing?' *Assembly Automation* 33 (4): 307–11. https://doi.org/10.1108/AA-06-2013-055.

[11] BRADY. 2021. 'BBP33 Labels'. 2021. https://www.bradyid.com/labels/bbp33.

[12] Capotexl. 2014. 'Filament Factory – A 3D Printer Filament Extruder'. Capotexl. 31 May 2014. https://capotexl.de/diy-filament-extruder/.

[13] Chanda, Manas, and Salil K. Roy. 2007. *Plastics Technology Handbook*. 4th ed. Plastics Engineering Series 72. Boca Raton, FL: CRC Press/Taylor & Francis Group.

[14] Chong, Siewhui, Guan-Ting Pan, Mohammad Khalid, Thomas C.-K. Yang, Shuo-Ting Hung, and Chao-Ming Huang. 2017. 'Physical Characterization and Pre-Assessment of Recycled High-

Density Polyethylene as 3D Printing Material'. *Journal of Polymers and the Environment* 25 (2): 136–45. https://doi.org/10.1007/s10924-016-0793-4.

[15] CIEL. 2019. 'Sweeping New Report on Global Environmental Impact of Plastics Reveals Severe Damage to Climate'. *Center for International Environmental Law* (blog). 2019. https://www.ciel.org/news/plasticandclimate/.

[16] Coroplast(1). 2021. 'Coroplast 1056 PE - Anti-Corrosion Tape'. 2021. https://www.coroplast-tape.com/en-us/corrosion-protection-tapes/coroplast-1056-pe.

[17] Coroplast(2). 2021. 'Technical Adhesive Tapes'. http://epvs.ru/images/katalogi/COROPLAST.pdf.

[18] Cortes, Sergio. 2010. 'INFRARED SPECTROSCOPY (IR) Theory and Interpretation of IR Spectra'. Lecture Notes. https://personal.utdallas.edu/~scortes/ochem/OChem_Lab1/recit_notes/ir_presentation.pdf.

[19] Creative Mechanisms Staff. 2016. 'Additive Manufacturing vs Subtractive Manufacturing'. Creative Mechanisms. 4 January 2016. https://www.creativemechanisms.com/blog/additive-manufacturing-vs-subtractive-manufacturing.

[20] Crump, S. Scott. 1992. Apparatus and method for creating three-dimensional objects. United States US5121329A, filed 30 October 1989, and issued 9 June 1992. https://patents.google.com/patent/US5121329A/en.

[21] D20 Committee. 2019. 'Practice for Coding Plastic Manufactured Articles for Resin Identification'. ASTM International. http://www.astm.org/cgi-bin/resolver.cgi?D7611D7611M-19.

[22] Denoncourt, Justine Mathieu, Sarah J. Wallace, Shane R. de Solla, and Valerie S. Langlois. 2015. 'Plasticizer Endocrine Disruption: Highlighting Developmental and Reproductive Effects in Mammals and Non-Mammalian Aquatic Species'. *General and Comparative Endocrinology*, Disruption of the thyroid and sex steroid hormone systems and their crosstalk in aquatic wildlife, 219 (August): 74–88. https://doi.org/10.1016/j.ygcen.2014.11.003.

[23] Dizon, John Ryan C., Alejandro H. Espera, Qiyi Chen, and Rigoberto C. Advincula. 2018. 'Mechanical Characterization of 3D-Printed Polymers'. *Additive Manufacturing* 20 (March): 44–67. https://doi.org/10.1016/j.addma.2017.12.002.

[24] Domingues, J., T. Marques, A. Mateus, P. Carreira, and C. Malça. 2017. 'An Additive Manufacturing Solution to Produce Big Green Parts from Tires and Recycled Plastics'. *Procedia Manufacturing*, International Conference on Sustainable and Intelligent Manufacturing, RESIM 2016, 14-17 December 2016, Leiria, Portugal, 12 (January): 242–48. https://doi.org/10.1016/j.promfg.2017.08.028.

[25] EN. 2020. '3D Filament Meter Caliper Arduino I2c Tutorial'. 2020. http://www.electronoobs.com/eng_arduino_tut93.php.

[26] Exxon Mobile Chemical. 2021. 'Polypropylene Product Data Sheets | ExxonMobil Chemical'. 2021. https://www.exxonmobilchemical.com/en/resources/product-data-sheets/polypropylene.

[27] GB 18455-2001. 2001. ‘Packaging Recycling Marks’. 2001. https://www.cedm.be/system/files/public/rohs-service/GB18455-2001.pdf.

[28] Geyer, Roland, Jenna R. Jambeck, and Kara Lavender Law. 2017. ‘Production, Use, and Fate of All Plastics Ever Made’. *Science Advances* 3 (7): e1700782. https://doi.org/10.1126/sciadv.1700782.

[29] Giles, Harold F., John R. Wagner, and Eldridge M. Mount. 2014. *Extrusion: The Definitive Processing Guide and Handbook*. PDL Handbook Series. Amsterdam: William Andrew, an imprint of Elsevier.

[30] Gopanna, Aravinthan, Ramesh N. Mandapati, Selvin P. Thomas, Krishnaprasad Rajan, and Murthy Chavali. 2019. ‘Fourier Transform Infrared Spectroscopy (FTIR), Raman Spectroscopy and Wide-Angle X-Ray Scattering (WAXS) of Polypropylene (PP)/Cyclic Olefin Copolymer (COC) Blends for Qualitative and Quantitative Analysis’. *Polymer Bulletin* 76 (8): 4259–74. https://doi.org/10.1007/s00289-018-2599-0.

[31] Groover, Mikell P. 2013. *Fundamentals of Modern Manufacturing: Materials, Processes, and Systems*. 5th ed. Hoboken, NJ: John Wiley & Sons, Inc.

[32] Hammer, Jort, Michiel H. S. Kraak, and John R. Parsons. 2012. ‘Plastics in the Marine Environment: The Dark Side of a Modern Gift’. In *Reviews of Environmental Contamination and Toxicology*, edited by David M. Whitacre, 1–44. Reviews of Environmental Contamination and Toxicology. New York, NY: Springer. https://doi.org/10.1007/978-1-4614-3414-6_1.

[33] Hamod, Haruna. 2015. ‘Suitability of Recycled HDPE for 3D Printing Filament’. Fi=AMK-opinnäytetyö|sv=YH-examensarbete|en=Bachelor’s thesis|. http://www.theseus.fi/handle/10024/86198.

[34] Harper, Charles A., ed. 2002. *Handbook of Plastics, Elastomers, and Composites*. 4th ed. McGraw-Hill Handbooks. New York: McGraw-Hill.

[35] How2Recycle. 2020. ‘How2Recycle - A Cleaner World Starts With Us’. 2020. https://how2recycle.info/.

[36] IAPD M2. 2015. ‘IAPD Plastics Primer, Module 2’. The International Association of Plastics Distributors. 2015. https://www.iapd.org/IAPD/Training_Education/Performance_Plastics/IAPD/Training/Training___Education_Main.aspx?New_ContentCollectionOrganizerCommon=1&hkey=8230a10c-9292-4779-8c70-41de149b1b64.

[37] Iñiguez, Maria E., Juan A. Conesa, and Andres Fullana. 2017. ‘Microplastics in Spanish Table Salt’. *Scientific Reports* 7 (1): 8620. https://doi.org/10.1038/s41598-017-09128-x.

[38] ISO. 2016. ‘The Plastic Industry’. 2016. https://committee.iso.org/files/live/sites/tc61/files/The%20Plastic%20Industry%20Berlin%20Aug%202016%20-%20Copy.pdf.

[39] ISO Committee. 2016. ‘The Plastic Industry’. https://committee.iso.org/files/live/sites/tc61/files/The%20Plastic%20Industry%20Berlin%20Aug%202016%20-%20Copy.pdf.

[40] Iunolainen, Elina. 2017. ‘Suitability of Recycled PP for 3D Printing Filament’, 48.

[41] Jambeck, J. R., R. Geyer, C. Wilcox, T. R. Siegler, M. Perryman, A. Andrady, R. Narayan, and K. L. Law. 2015. ‘Plastic Waste Inputs from Land into the Ocean’. *Science* 347 (6223): 768–71. https://doi.org/10.1126/science.1260352.

[42] Kosuth, Mason, and Tyree. 2017. ‘Synthetic Polymer Contamination in Global Drinking Water’. 2017. http://orbmedia.org/stories/Invisibles_final_report.

[43] Lafleur, Pierre G., and Bruno Vergnes. 2014. *Polymer Extrusion*. Materials Science Series. London : Hoboken, NJ: ISTE ; Wiley.

[44] Law, Kara Lavender. 2017. ‘Plastics in the Marine Environment’. *Annual Review of Marine Science* 9 (1): 205–29. https://doi.org/10.1146/annurev-marine-010816-060409.

[45] Le Guern. 2020. ‘When The Mermaids Cry: The Great Plastic Tide’. 2020. https://coastalcare.org/2009/11/plastic-pollution/.

[46] Lebreton, L., B. Slat, F. Ferrari, B. Sainte-Rose, J. Aitken, R. Marthouse, S. Hajbane, et al. 2018. ‘Evidence That the Great Pacific Garbage Patch Is Rapidly Accumulating Plastic’. *Scientific Reports* 8 (1): 4666. https://doi.org/10.1038/s41598-018-22939-w.

[47] Lehrer, Jason, and Marietta R. Scanlon. 2017. ‘The Development of a Sustainable Technology for 3D Printing Using Recycled Materials’. In . https://peer.asee.org/the-development-of-a-sustainable-technology-for-3d-printing-using-recycled-materials.

[48] Lyman and Mulier. 2014. ‘Lyman / Mulier Filament Extruder V5 by Hlyman’. Thingiverse.Com. 2014. https://www.thingiverse.com/thing:380987.

[49] Machado, Anderson Abel Souza, Werner Kloas, Christiane Zarfl, Stefan Hempel, and Matthias C. Rillig. 2018. ‘Microplastics as an Emerging Threat to Terrestrial Ecosystems’. *Global Change Biology* 24 (4): 1405–16. https://doi.org/10.1111/gcb.14020.

[50] Metal AM. 2020. ‘Boeing 777X Takes Flight with Reported 300 Additively Manufactured Parts in Each GE9X Engine’. Metal Additive Manufacturing. 31 January 2020. https://www.metal-am.com/boeing-777x-takes-flight-with-reported-300-additively-manufactured-parts-in-each-ge9x-engine/.

[51] Mistry, B. D. 2009. *A Handbook of Spectroscopic Data Chemistry (UV, IR, PMR, CNMR and Mass Spectroscopy)*. Jaipur: Oxford Book Co.

[52] Mutiva, Bande Leonard, Jean Bosco Byiringiro, and Peter Ng’ang’a Muchiri. 2018. ‘A Study on Suitability of Recycled Polyethylene Terephthalate for 3D Printing Filament’, 6.

[53] OC. 2015. ‘Stemming the Tide: Land-Based Strategies for a Plastic-Free Ocean’. Ocean Conservancy. 2015. https://oceanconservancy.org/wp-content/uploads/2017/04/full-report-stemming-the.pdf.

[54] Ophardt, Charles, and Layne A. Morsch. 2015. ‘26.1 Introduction to Synthetic Polymers’. Chemistry LibreTexts. 27 April 2015. https://chem.libretexts.org/Courses/University_of_Illinois%2C_Springfield/UIS%3A_CHE_269_(Morsch_and_Andrews)/Chapters/Chapter_26%3A_Synthetic_Polymers/26.1_Introduction_to_Synthetic_Polymers.

[55] Pechter, David. 2019. ‘3D Printing and Additive Manufacturing – What’s the Difference?’ All3DP. 24 January 2019. https://all3dp.com/2/3d-printing-and-additive-manufacturing-what-s-the-difference/.

[56] Plastics Europe. 2019. ‘Plastics – the Facts 2019’.

[57] Plastics Europe (2). 2019. ‘Thermoplastics’. PlasticsEurope. 2019. https://www.plasticseurope.org/en/about-plastics/what-are-plastics/large-family/thermoplastics.

[58] Plastics Europe (3). 2019. ‘Plastics - The Facts 2019 An Analysis of European Plastics Production, Demand and Waste Data’. 2019. https://www.plasticseurope.org/application/files/9715/7129/9584/FINAL_web_version_Plastics_the_facts2019_14102019.pdf.

[59] PolymerDatabase. 2021. ‘Plastic Additives’. 2021. https://polymerdatabase.com/Additives/Polymer%20Additives.html.

[60] Rauwendaal, Chris. 2014. *Polymer Extrusion*. 5th edition. Munich : Cincinnati: Hanser Publications ; Hanser Publication.

[61] RepRap PT. 2021. ‘RepRap 3D Printer Shop | Filamento, Peças e Impressoras 3D - Filamento, Peças e Impressoras 3D’. 2021. https://reprap.pt/.

[62] Ritchie, Hannah, and Max Roser. 2018. ‘Plastic Pollution’. *Our World in Data*, September. https://ourworldindata.org/plastic-pollution.

[63] Rochman, Chelsea M., Eunha Hoh, Tomofumi Kurobe, and Swee J. Teh. 2013. ‘Ingested Plastic Transfers Hazardous Chemicals to Fish and Induces Hepatic Stress’. *Scientific Reports* 3 (1): 3263. https://doi.org/10.1038/srep03263.

[64] SAC GB16288-2008. 2008. ‘Marking of Plastics Products, National Standard Of The People’s Republic of China, The Standardization Administration of the People’s Republic of China (SAC)’. http://www.gbstandards.org/GB_standard_english.asp?code=GB/T%2016288-2008&word=Marking%20of%20plastics%20products.

[65] Sheoran, Ankita Jaisingh, and Harish Kumar. 2020. ‘Fused Deposition Modeling Process Parameters Optimization and Effect on Mechanical Properties and Part Quality: Review and

Reflection on Present Research'. *Materials Today: Proceedings* 21: 1659–72. https://doi.org/10.1016/j.matpr.2019.11.296.

[66] Terner, Mathieu. 2015. 'The Current State, Outcome and Vision of Additive Manufacturing'. *Journal of Welding and Joining* 33 (6): 1–5. https://doi.org/10.5781/JWJ.2015.33.6.1.

[67] The Guardian. 2018. 'Whale Dies from Eating More than 80 Plastic Bags'. *The Guardian*, 3 June 2018, sec. Environment. https://www.theguardian.com/environment/2018/jun/03/whale-dies-from-eating-more-than-80-plastic-bags.

[68] Turbide, Dave. 2015. '3-D Printing Evolves, Finds Unique Place in Manufacturing'. SearchERP. 26 February 2015. https://searcherp.techtarget.com/tip/3-D-printing-evolves-finds-unique-place-in-manufacturing.

[69] UNEP. 2018. 'Plastic Planet: How Tiny Plastic Particles Are Polluting Our Soil'. UN Environment. 4 April 2018. http://www.unenvironment.org/news-and-stories/story/plastic-planet-how-tiny-plastic-particles-are-polluting-our-soil.

[70] Woern, Aubrey L., Joseph R. McCaslin, Adam M. Pringle, and Joshua M. Pearce. 2018. 'RepRapable Recyclebot: Open Source 3-D Printable Extruder for Converting Plastic to 3-D Printing Filament'. *HardwareX* 4 (October): e00026. https://doi.org/10.1016/j.ohx.2018.e00026.

[71] Zander, Nicole E., Margaret Gillan, Zachary Burckhard, and Frank Gardea. 2019. 'Recycled Polypropylene Blends as Novel 3D Printing Materials'. *Additive Manufacturing* 25 (January): 122–30. https://doi.org/10.1016/j.addma.2018.11.009.

[72] Zander, Nicole E., Margaret Gillan, and Robert H. Lambeth. 2018. 'Recycled Polyethylene Terephthalate as a New FFF Feedstock Material'. *Additive Manufacturing* 21 (May): 174–82. https://doi.org/10.1016/j.addma.2018.03.007.

[73] Zelinski, Peter. 2017. 'Additive Manufacturing and 3D Printing Are Two Different Things'. Additive Manufacturing. 8 April 2017. https://www.additivemanufacturing.media/blog/post/additive-manufacturing-and-3d-printing-are-two-different-things.

Annex A

MFR Determination Procedure

(In Portuguese)

Plastómetro (Medição de MFR)

Material relevante: base de plástico para colocar na base do equipamento para proteger superfície; copo graduado, balança, luva térmica, tesoura metálica (ou alicote de corte pequeno), ferramenta de compactação piston (gaveta equip), escova metálica, pinça, norma ASTM, cronómetro;

Limpeza equipamento

- Começar com procedimento de limpeza com PVC e definir temperatura de ~175ºC no equipamento após ligar módulo de aquecimento. Não ultrapassar 180ºC com este polímero uma vez que o PVC liberta gases tóxicos a altas temperaturas;
- Após o aquecimento, introduzir o PVC de limpeza e usar a ferramenta de compactação que se encontra na gaveta do equipamento para encher cilindro de forma homogénea;
- Colocar os pesos maiores e exercer pressão;
- Puxar o manípulo preto que prende a fieira (*die*) e continuar a exercer pressão no piston; a fieira começará a sair aos poucos;
- Cuidado: após calçar luva térmica, meter a mão por baixo para apanhar a fieira com luva para não sair da bancada;
- Exercer pressão no piston, começará a sair um compactado de PVC amolecido que agarrará polímeros e detritos acumulados no cilindro;
- Com a ferramenta branca de espigão desobstruir a saída da fieira;
- Após saída completa do compactado de PVC, empurrar o manípulo preto e colocar a fieira no topo do cilindro, direita, com auxílio de pinça se necessário ou outro acessório para o efeito; garantir que fica presa e direita na base do cilindro;
- Repetir o processo (total de 2x pelo menos).
- Com as escovas metálicas limpar o piston se tiver resíduos de polímeros acumulados;

Nota: se o manípulo preto que prende a fieira oferecer resistência e não estiver solto ao puxar, não forçar; antes de qualquer procedimento usar óleo lubrificante (e.g. wd40 que existe no laboratório contíguo) até ser possível mexer o manípulo sem fazer força;

Ensaio MFR

- Consultar a norma do procedimento de medição de MFR e ler as secções mais importantes (nomeadamente procedimento A, tabelas de tempos standard e tabela em

anexo com valores padrão para cada tipo de polímero); anotar temperatura de valor padrão do peso a utilizar (e.g. 230ºC/2.16Kg, 230ºC/5Kg, etc);

- Ligar o instrumento no manípulo preto;
- Ligar o módulo de aquecimento no botão vermelho e definir a temperatura padrão;
- Colocar recipiente (e.g. cilindro graduado na gaveta por baixo do equipamento) na balança e medir quantidade fixa de pellets do polímero a testar (e.g. 5g, próximo do volume do cilindro interno) de forma a manter o processo controlado e com a menor variabilidade possível;
- Encher o cilindro do equipamento e empurrar com uma das ferramentas que se encontram na gaveta da base do equipamento; convém ser relativamente rápido para evitar degradação do polímero, etc;
- Colocar piston (que deve ser pousado sempre em cima do equipamento quando é retirado), preparar cronómetro e meter o peso padrão no topo;
- A cada intervalo padrão cortar o extrudido com tesoura (a partir do topo ou outro ponto de referência, desde que seja sempre o mesmo e fácil de marcar), sucessivamente, até o piston chegar à base (consiste numa série completa);
- Usar balança de precisão para medir os vários filamentos extrudidos;
- Repetir processo;
- Obter, no mínimo, 30 medições para se fazer análise estatística e controlo de processo posteriormente; se possível, obter 40-50 amostras (análise de distribuição, análise de erro, eliminação de outliers com base no z-score, análise SPC etc);
- No fim do ensaio: retirar peso do piston; retirar piston e caso esteja sujo de polímero, limpar com escova metálica (conjunto de gavetas brancas da bancada) e voltar a introduzi-lo; desligar módulo de aquecimento; assim que a temperatura baixar a um patamar seguro, desligar equipamento no manípiulo preto;

Nota 1: Deixar nota escrita sobre último polímero usado no equipamento para facilitar o trabalho de quem vá usar o equipamento posteriormente;

Annex B

Twin-Screw Extruder Procedures

Brabender Single-Screw Extruder Procedures

Start-up procedure

1. Start the cooling system – turn on the water supply;
2. Switch on the heating module – the yellow and red switch in the left side of the extruder;
3. Increase the temperature in intervals of no more than 40ºC and ensure that the heating light is on (blinking or stable) and that the temperature is increasing. If the temperature does not change, decrease the programmed temperature (lower interval of input) and ensure it starts blinking;
4. Ensure that the heaters have reached the processing temperature of the polymer in the barrel (you must know the polymer that was processed before and its processing temperatures; if you don't know then ask David, the person responsible for the extruder) or the processing temperature of the polymer you intend to study (choose the highest temperature for first runs to get acquaintance with material properties);
5. Turn on the motor by turning on the yellow and red switch in the lower module (right side of the extruder). Afterwards ensure that the RPM switch is set to 0 and press the green button. The display of the RPMs and Amps turns on;
6. Turn the rpm button and set the rpm value that you intend to study and ensure that the screw inside the barrel starts to turn;
7. If the screw is turning, feed the material in the hopper and turn on the hopper vibration (white switch in a white plug in the back of the lower module);
8. If the material that was inside the barrel is the same that you intend to study then you are ready to go;
9. Let the extruder stabilize before proceeding with the experiment (10/15min at least); one of the indicators is the heaters temperatures stabilizing;
10. If the material you intend to study is different and has the same processing temperature, ensure that the time it took to stabilize is enough for the changeover to occur, if so, continue with the tests;

11. If the material you intend to study is different and it has a higher processing temperature ensure that the time it took to stabilize at higher value T is enough for the changeover to occur, if so, continue with the tests;
12. If the material you intend to study is different and has a lower processing temperature, let the extruder work for 10-15 minutes and then decrease the set temperatures accordingly. Let it stabilize for 10-15 minutes and proceed with the tests;
13. Ensure that you let the extruder stabilize for 10-15 minutes every time you change the set temperatures and RPM values;

Shutdown procedure

1. The last material to be used on the extruder must be virgin pellets of the polymer used in the last test run – if you are studying recycled material, please do a changeover to the virgin polymer of the same type and continue extruding (until, as much as possible, only extrudate of virgin material comes out);
2. When you have step 1 assured you need to remove the polymer material as much as possible from the extruder (barrel & die), i.e., ensure that the hopper is empty and that no stream is leaving the die anymore;
3. After the material stops to come out from the die, turn the RPM to zero, after that, turn off the motor (red switch in front of the extruder) and turn off the power switch in the right side of the extruder;
4. Decrease the heaters set temperatures to zero;
5. Wait until all the heaters temperatures reach 50ºC (or lower near room temperature?) to turn off the heating module – switch in left side of the extruder;
6. Turn off the water supply of the cooling system (turn off the tap in the wall);

NB: if there is someone in the lab you might ask them if they can turn off the water supply of the cooling system and the heating module. In that case proceed until step 4 of the **shutdown procedure**.

Annex C

Python Script for Data Cleaning of MFR Experimentations

```
#!/usr/bin/env python3
# -*- coding: utf-8 -*-
"""
Created on Mon Sep 14 15:31:55 2020

@author: ant
"""

import numpy as np
import pandas as pd
from scipy import stats
import matplotlib.pyplot as plt

outliers = []

#Open csv file and import to dataframe df
df = pd.read_csv(r'mfr_vpp_3dp_filament_raw_data.csv')

#show dataframe df in console
#print(df)

#calculate the z-score of every row in column MFR
z = np.abs(stats.zscore(df['MFR [g/10min]']))

#introduce threshold variable which will be the z-score limit to consider
threshold = 1

#fill outliers list with the elements whose z-score are outside of the threshold
interval
outliers = np.where(z>threshold)

#create new dataframe df_new which has the values of MFR after excluding outliers
whose z-zcore>threshold
df_new = df[z<threshold]

times =list(set(df_new['t [s]']))
colours = ['r', 'b']
plt.figure(figsize=(12,12/1.618))

new_avg = df_new['MFR [g/10min]'].mean()
plt.hlines(new_avg, 0, 49, ls = '--', color='k', label='MFR Average')
```

```
for time, colour in zip(times, colours):
    index = time == df_new['t [s]']
    plt.plot(df_new['run'][index], df_new['MFR [g/10min]'][index], 'o', label = str
(time) + 's', color=colour)
    plt.xlabel('run')
    plt.ylabel('MFR (g/10min)')
    plt.xlim(0,50)
    plt.ylim(0,20)



plt.legend(loc='best')
plt.show()

print(df_new)

print(new_avg)

df_new.to_csv('mfr_vpp_3dp_data_clean.csv')
```

Annex D

DIY Diameter Measurement Tool

Open sourced tool

Source: http://electronoobs.com/eng_arduino_tut93.php

Components, STL files for 3DP and C program openly available at website.

Figure D.1: (a) Front and rear view of measurement tool for filament diameters. (b) Electronic schematics for connecting digital caliper to Arduino (EN 2020).

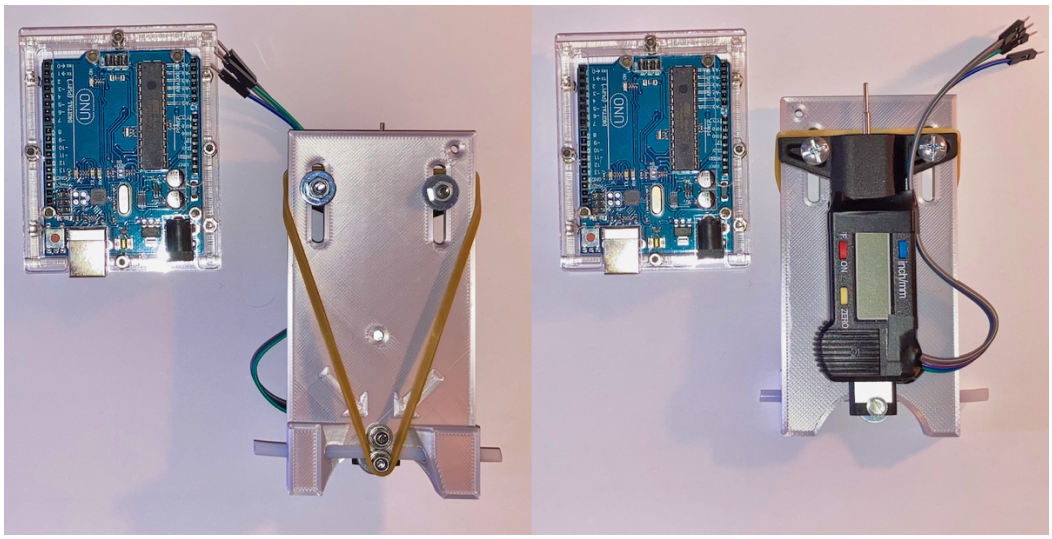

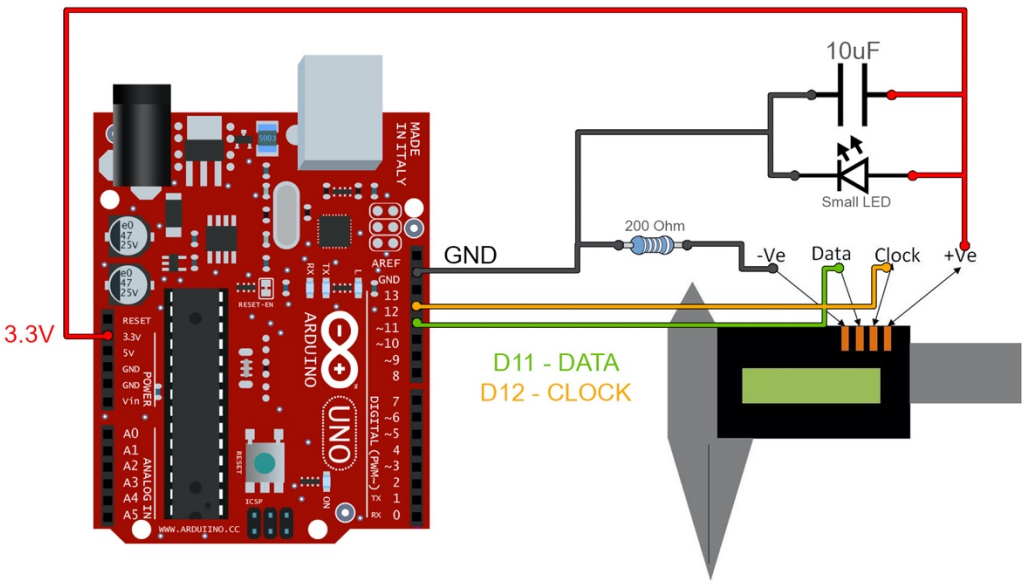

Printed part adapted to allow for larger diameters (using the STL file provided in source). Source code for basic functionality provided below (as published on website):

```
/* Read the caliper data with Arduino and display mm or inch on serial monitor
and LCD
 * Tutorial on: https://www.electronoobs.com/eng_arduino_tut93.php
 * Schematic: https://www.electronoobs.com/eng_arduino_tut93_sch1.php
 *
Caliper         |       Arduino
GND (black)             GND + 200 ohm
DAT (brown)             D11
CLK (blue)              D12
VCC 3.3V (red)          3.3V
 */

#define CLOCK_PIN 12
#define DATA_PIN  11


void setup()
{
  Serial.begin(9600);
  pinMode(CLOCK_PIN, INPUT);
  pinMode(DATA_PIN, INPUT);

}

char buf[20];
unsigned long tmpTime;
int sign;
int inches;
long value;
float result;
bool mm = true; //define mm to false if you want inces values

void loop()
{
  while(digitalRead(CLOCK_PIN)==LOW) {}
  tmpTime=micros();
  while(digitalRead(CLOCK_PIN)==HIGH) {}
  if((micros()-tmpTime)<500) return;
  readCaliper();
  buf[0]=' ';
  dtostrf(result,6,3,buf+1); strcat(buf," in ");
  dtostrf(result*2.54,6,3,buf+1); strcat(buf," cm ");
```

```
  if(mm)
  {
    Serial.print(result); Serial.println(" mm");
    delay(100);
  }
  else
  {
    Serial.print(result); Serial.println(" in");
    delay(100);
  }
}
void readCaliper()
{
  sign=1;
  value=0;
  inches=0;
  for(int i=0;i<24;i++) {
    while(digitalRead(CLOCK_PIN)==LOW) {}
    while(digitalRead(CLOCK_PIN)==HIGH) {}
    if(digitalRead(DATA_PIN)==HIGH) {
      if(i<20) value|=(1<<i);
      if(i==20) sign=-1;
      if(i==23) inches=1;
    }
  }
  if(mm)
  {
    result=(value*sign)/100.0;
  }
  else
  {
  result=(value*sign)/(inches?2000.0:100.0); //We map the values for inches,
define mm to false if you want inces values
  }

}
```